LOW CYCLE RESPONSE OF

DENTED PIPELINES

SUBJECT TO CYCLIC AXIAL AND BENDING LOADS

By

Mohamad Azadeh

Submitted in partial fulfillment of the requirements

for the degree of Doctor of Philosophy

Dalhousie University

Halifax, Nova Scotia

November 2017

Table of Contents

List of Tables

List of Figures

Abstract

In the present thesis, the ratcheting and low cycle fatigue responses of dented pipes undergoing quasi-static cyclic loads are investigated through a series of experiments conducted on small-scale pipe samples, and performing detailed nonlinear FE analysis. The investigation addresses the response, and in-service life estimation of dented pipes undergoing inelastic cycles of axial and bending loads.

Development of ratcheting strain in small-scale dented steel pipes subject to cyclic axial loads is investigated experimentally. It is observed that regardless of the nature of the applied loads, collapse of pipes loaded monotonically or cyclically would essentially occur at the same average strain level. The experimental results reveal that larger dent depths significantly affect the total number of cycles to failure; the number of cycles prior to collapse dramatically decreases by as much as 75% when the dent depth was increased by 2%.

Moreover, a nonlinear FEA framework is developed as an alternative and feasible approach for testing load-bearing capacity of dented pipes under cyclic axial loads. A set of parametric FE analyses is performed to investigate the influence of mean stress, stress amplitude, loading regime and hardening-related parameters. It is concluded that the application of larger stress amplitudes (while maintaining the same maximum stress) contributed to pipes earlier failure in comparison to the condition when pipes were subjected to a higher mean stress. It is also observed that the combined non-linear kinematic/isotropic hardening model is extremely sensitive to the material parameters used in describing the model.

Finally, the influence of dent depth on the evolution of pipe cross-section ovalization under a low number of curvature-controlled symmetric bending loads is investigated. Two empirical equations are proposed to estimate the remaining in-service life of dented pipes. The first equation estimates the number of cycles causing the local instability of pipe's cross-section and consequently, initiation of fatigue cracks. The second equation predicts the variation of ovalization as a function of the applied loading cycles.

List of Abbreviations and Symbols Used

Abbreviations

AF	Armstrong Frederick
AGA	American Gas Association
API	American Petroleum Institute
ASME	American Society of Mechanical Engineers
BS	British Standards
BKH	bilinear kinematic hardening
CANMET	Canada Centre for Mineral and Energy Technology
CL	cyclically loaded
CSA	Canadian Standards Association
DAQ	data acquisition
DNA	Det Norske Veritas
EPRG	European Pipeline Research Group
FE	finite element
FEA	finite element analysis
LVDT	linear variable differential transformer
MKIN	multi-linear kinematic hardening
ML	monotonically loaded
PDAM	Pipeline Defect Assessment Manual
PRCI	Pipeline Research Council International
SMYS	specified minimum yield strength
UTS	ultimate tensile strength

Romans

$\mathbf{a}$	back-stress tensor
b	isotropic hardening material property
C	initial kinematic hardening modulus
d$\mathbf{a}$	incremental back-stress tensor
d	dent depth
D, D_o	pipe outside diameter
ΔD_o	change in pipe outside diameter
$\Delta D_{o,initial}$	permanent change of pipe outside diameter after indentation
E	modulus of elasticity
f	yield function for time independent plasticity in Equation (4.8)
F_{max}	maximum indentation force
H	plastic modulus
h	hardening modulus
J_2	von Mises distance in the deviatoric stress space
k	initial size of yield surface
L	axial pipe gauge length
M	applied bending load to pipe
M_0	reference bending load of pipe
$M_{P0.2}$	0.2% curvature offset plastic bending load
N	number of loading cycles
N_f	number of loading cycles at failure
$\mathbf{n}$	normal matrix to yield surface

Q	isotropic hardening material property
R_o	radius of curvature of intact pipe surface subject to bending
R_1	external surface radii of curvature in the transverse planes through the dent (see Figure 2.3)
R_2	external surface radii of curvature in the longitudinal planes through the dent (see Figure 2.3)
S_m	minimum of 2/3 of yield strength or 1/3 of ultimate strength of material
t	pipe wall thickness
$\mathbf{X}$	back-stress tensor
$\mathbf{X}'$	deviatoric back-stress tensor
X_0	initial value back stress
Y	radius of yield surface

Greeks

ε_1	bending strain in circumferential direction
ε_2	bending strain in longitudinal direction
ε_3	membrane strain in longitudinal direction
ε_i	critical strain acting on the inside pipe surfaces
ε_o	critical strain acting on the outside pipe surfaces
$\bar{\varepsilon}_C$	average critical axial strain
$\bar{\varepsilon}_L$	average limit axial strain
$\bar{\varepsilon}_{x,initial}$	applied initial average limit axial strain
ε_{p_0}	initial value of the plastic strain

σ_o	0.2% strain offset yield stress
$\sigma_{x.max}$	maximum axial stress
σ_m	mean axial stress
σ_a	axial stress amplitude
σ_y	yield stress
$\boldsymbol{\sigma}$	Stress tensor
$\boldsymbol{\sigma^{dev}}$, $\boldsymbol{\sigma'}$	deviatoric stress tensor
δ	initial dent depth
$\delta_{residual}$	dent depth after rebound
δ_x	average axial strain
δ_x^p	average peak axial strain
δ_{ij}	Kronecker's delta
ρ	radius of curvature
κ_o	reference curvature of pipe
κ_c	applied curvature to pipe
$d\boldsymbol{\epsilon^e}$	incremental elastic strain tensor
$d\boldsymbol{\epsilon^p}$	incremental plastic strain tensor
$d\varepsilon_{ij}^e$	elastic strain incremental component
$d\boldsymbol{\sigma_{dev}}$	incremental deviatoric stress tensor
λ, μ	Lamè constants
γ	rate of kinematic hardening decrease

Acknowledgements

First of all, I would like to thank my parents and my beloved brother. I cannot imagine having been able to finish my studies, without their unreserved love and encouragement.

I would also like to express my deepest gratitude to Dr. Farid Taheri. His wise, professional, and patient supervision enabled me to liberally pursue my research interests. Without his guidance and constant support in every aspect, attainment of this degree would have been impossible. I also like to thank my committee members, Dr. Gordon Fenton and Dr. Shawn Kenny.

My thanks also go to all my friends and colleagues at Dalhousie University, especially Nikzad Nourpanah, Morteza Mehrzadi, Shiva Eslami, Babak Ahamadi, Zohreh Asaee and David De Cicco. I cherish all the good times and beautiful memories.

I am very thankful to the skillful technicians of our department, Misters Brian Kennedy, Blair Nickerson and Jesse Keane for their assistance and technical support throughout my experimental works.

Last but not least, my sincere gratitude goes to all the people who shared parts of their life story with me that helped to shape, hopefully, a more realistic view of our human nature.

Chapter 1

Introduction

1.1 Background

Oil and gas transmission pipelines have had a reasonably good safety record (Hill, 1991). This is due to a combination of good design practice, use of more refined materials, and controlled operating practices. However, like any engineering structure, pipelines do occasionally fail. The most common causes of damage causing failure in onshore and offshore oil and gas transmission pipelines in the Western Europe and North America are mechanical damage and corrosion.

1.2 Dent as a Form of Mechanical Damage

Damage in the form of dents is of one the most common forms of pipeline mechanical damage (Cosham and Hopkins, 2002), which in turn may lead to loss of integrity, affect the load-bearing capacity and operating life of the pipeline. Mechanical damage can also cause changes to the geometry of the pipeline's cross section, and wall thickness, and causes local changes in material properties. Dents in pipelines are usually defined as a change in pipe curvature, but without reduction in wall thickness. This type of mechanical damage causes gross distortion of pipe's cross-section, and can occur due to impact by excavation equipment, or by any other heavy objects hitting them during their transportation, installation and trenching, and in service.

During operation, oil and gas pipelines undergo cyclic loadings caused by repetitive start-up/shutdown, fluid pressure fluctuation, temperature changes, seismic loads and in

the case of offshore pipelines, by the action of currents. Due to the common exposure of oil and gas pipelines to the mentioned operational loads, cyclic response of pipeline becomes an important concern, especially in dented pipelines. The life assessment of dented pipelines under cyclic loads can avoid overly conservative assessments and unnecessary maintenance. The increased knowledge with respect to performance of dented pipes would prevent unnecessary replacement costs, thus saving money without causing catastrophic failure and environmental damage.

1.3 Research Motivations

The experimental and numerical background to the effect of dent undergoing monotonic and cyclic pressure is well understood and documented. The current codes, such as CSA Z662 (CSA, 2015) and ASME B31.4 (ASME, 2012) recognize the work undertaken to date, in that dents are allowed to remain in service, provided they satisfy certain criteria. However, the same does not hold true for pipelines undergoing low cycles of axial and bending loads. Life assessment of dented pipelines under such cyclic loads is still a young and evolving subject, with several unexplained issues and unanswered questions.

1.4 Objectives of the Present Work

The main objective of the thesis is to understand and analyze the performance of pipelines containing dents, subjected to cyclic axial and bending loads via experimental and numerical investigations. The research also examines the remaining life of oil and gas dented pipelines subjected to repeated loading by investigating the number of cycles to failure. When applicable (i.e. under cyclic bending loads), the thesis will also discuss the development of ovalization in the dented region during the loading and provide the details

of an empirical relationship developed to relate the number of applied loadings cycles causing failure, as a function of dent depths.

Moreover, a FEA framework is presented as an alternative and feasible approach for testing load-bearing capacity of dented pipes under cyclic axial loads. Throughout the thesis, all the finite element analyses (FEA) are performed using ABAQUS software package.

1.5 Layout of Thesis

This thesis is structured within six chapters, including the present one. Three of the chapters (Chapters 3 to 5) are the main body of original research articles that resulted from the work carried out, and are published in peer-reviewed journals (Azadeh and Taheri, 2014, 2015, 2016).

The second chapter of the thesis presents a thorough literature review of the subject, structured in two sections. The effect of a dent on load-bearing capacity of pipelines is introduced in the first part of the literature review. Subsequently, the relevant experimental and numerical investigations related to straight pipes, subjected to cyclic axial and bending loads are reviewed.

In chapter 3, development of the ratcheting strain in a small-scale dented steel pipe subject to cyclic axial loads is investigated experimentally, and its life cycle is traced. In this part of the investigation, the pipes' dents were formed by a cylindrical indenter. The work also investigates the effect of applied mean stress and stress amplitude on ratcheting.

Chapter 4 builds on the FEA framework of the previous chapter and presents a comprehensive parametric study on various features of a dented pipeline. In this chapter, a nonlinear finite element framework is developed to simulate the low cycle fatigue response

of dented pipes undergoing monotonic and cyclic axial loads. A combined non-linear isotropic/kinematic hardening material model is utilized to capture the cyclic response of the dented pipes.

In chapter 5, the influence of dent depth on the evolution of pipe cross-section ovalization under a low number of curvature-controlled symmetric bending is investigated. Moreover, two empirical formulas are proposed to estimate the remaining in-service life of dented pipes. The first formula estimates the number of cycles causing the local instability of pipe's cross-section and consequently, initiation of fatigue cracks. The second equation predicts the growth of ovalization as a function of the applied loading cycles.

The main conclusions drawn from the present research are summarized and outlined in chapter 6 of this thesis, along with some recommendations for future research in this field.

Chapter 2

Literature Review

2.1 Summary

In this chapter, a review of the literature is conducted to study how the current guidelines and previous research works address the significance of a dent in pipelines performance. It is found that the dent depth (measured as a percentage of outer diameter of the pipe) is most commonly used by different codes, standards, and manuals for determining the severity of a dent. A majority of the research works on the subject of pipeline containing a dent has been conducted to establish the pipeline's burst strength and fatigue life. However, investigation of fatigue life of the dent was limited to studies that considered cycles of internal pressure. To maintain and improve safety record of pipelines, emphasis is being placed on the significance of a dent and its influence on fatigue life of pipes that are subjected to low cycles of axial and bending loads.

Over the past 50 years, research associated with dents in pipelines have included full-scale pipe testing programs, laboratory testing of pipe ring samples containing dents, and finite element analysis based studies. The goal of the efforts has been to provide the necessary knowledge and background to allow for the development of guidelines for determining what dents levels could be left in service, and which ones should be removed to ensure the continued safe operation of the pipeline.

The works cited in the following review are organized in two sections. The first section introduces the fundamentals of dents as a mechanical damage. Then, state-of-the-art methodologies of indentation simulation and also recommendations in code of practices

are reviewed. A brief review of the historical dented pipeline research is also presented. This section, finally addresses literature related to the effect of dents on pipes response in terms of both the burst pressure and the fatigue life of the pipeline.

In the second section, the fatigue ratcheting phenomenon is introduced and a brief literature review on the evolution of material models that have been developed for plastic strain accumulation is presented. Available literature covering the subject of straight pipelines undergoing cyclic axial and bending loads is also reviewed. The chapter will be concluded with review of the works that describe methodologies that have been developed for finite element simulation of straight pipes under such loading scenarios and discussion of their results.

2.2 Dent Characteristics, Simulation and Fatigue Life

The following section summarizes a variety of articles, which examine the effect of a dent on pipeline integrity. The terminologies that are commonly used to characterize a dent are noted, followed by the main body of works regarding FEA simulation of indentation. The focus of this section is on reporting studies that investigate the fatigue life of dented pipelines. It should be noted that in such studies, the pipes would be subjected to cyclic pressures, which would ultimately cause pipe's failure.

2.2.1 Dent Terminology in Pipelines

A dent in pipes is identified as a gross disturbance of the cross-section of the pipe, caused by the impact or forcing of a foreign body, resulting in plastic deformation of the pipe wall. A dent can be categorized as:

- Smooth or Plain Dent: A dent, which causes a smooth change in the cross-section of the pipe, does not contain a stress concentrator or wall thinning, and does not change the curvature of an adjacent girth or seam welds.
- Unconstrained Dent: A dent that is free to rebound elastically (spring- back) when the indenter is removed, and is free to re-bound as the internal pressure varies.
- Constrained Dent: A dent that is not free to re-bound, because the indenter is not removed. A rock induced dent is an example of a constrained dent.
- Complex Dent: Any dent with a gouge, groove, scratch, stress riser, or other secondary defect, or a dent that affects the curvature of a nearby weld.

The depth of a dent is defined by the depth which results in the maximum reduction of pipe diameter, as identified by "H" in Figure 2.1.

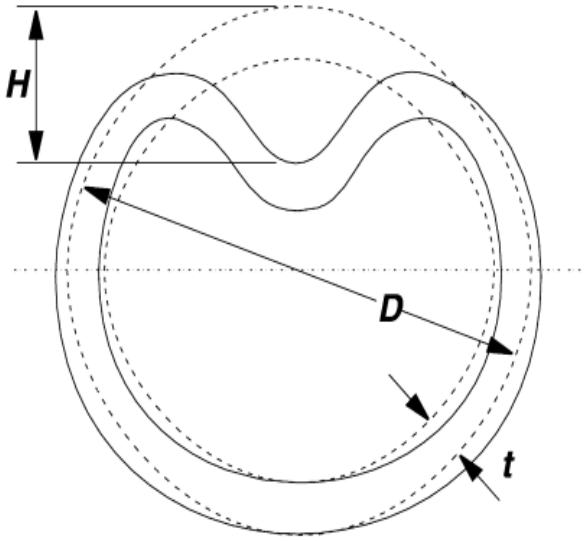

Figure 2.1 Dimensions of a dent (Hopkins and Leis, 2003)

The depth of a dent depends on the force caused by the indenting object, the diameter and wall thickness of the pipe, internal pressure, material properties, and any constraint in pipe's deformation. Pipes of larger diameter and lower wall thickness deform more elastically under an applied force. However, if the pipeline is constrained by stiff soil, then the damage may be greater.

Clearly, a pipe with lower yield strength will plastically deform sooner under an applied force. If a pipeline is internally pressurized during the damage process, then the effective stiffening will act against the applied force and possibly reduce dent depth. These parameters affect the resulting depth of indent and, thus affecting, the pipeline's structural integrity.

2.2.2 Load-Deflection Curve for Pipe Indentation

Figure 2.2 shows a typical load-deflection curve during and after denting an unpressurized pipe by an excavator. The deformation can be characterized by six phases, as follows:

Phase I. When the radial load is first applied, pipe deforms linearly up to the point of first yield. Yielding initially occurs under the corners of the excavator tooth, in location of contact with pipe wall surface only.

Phase II. As indentation continues, yielding extends through wall thickness of the pipe. As it might be expected, there would be no great deal of variation between this region and the fully elastic region that precedes it. At the end of this phase, the pipe wall would have reached its plastic capacity in the longitudinal direction.

Phase III. The onset of plastic straining in the circumferential direction marks a major reduction in the stiffness of the pipe. The plastic capacity is consumed

rapidly in the circumferential direction, resulting in a plateau type region in the load deflection curve.

Phase IV. As the deflection of the pipe becomes larger, membrane straining starts to dominate the response, resulting in an apparent increase in stiffness. Plastic membrane yielding occurs in a broad region, extending in the longitudinal direction only. Strain hardening begins to have an effect during this phase.

Phase V. Unloading of the excavator tooth results initially in elastic recovery of the dent. The slope of the load-deflection curve in this region matches that of phase I.

Phase VI. When the indenter load is lowered, the dented region tends to re-round elastically. The reversal of plastic straining occurs principally in the circumferential direction.

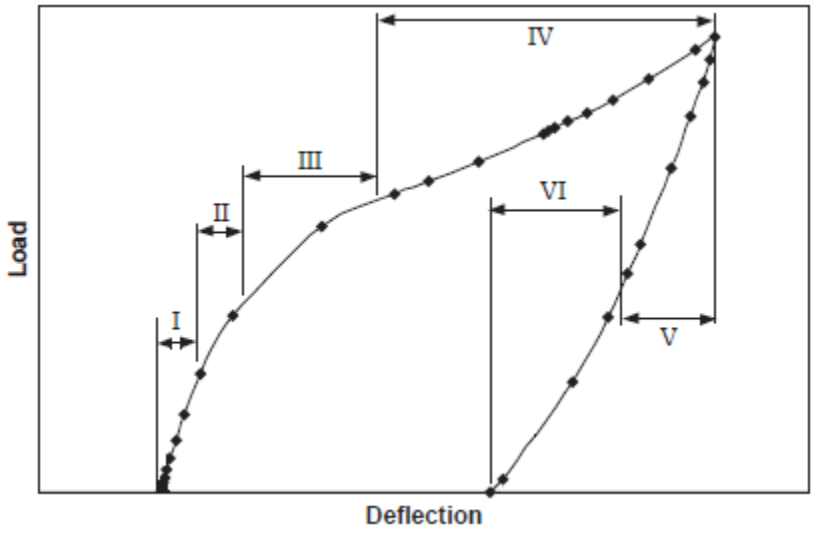

Figure 2.2 Variation of the denting force versus depth of a dent (Brooker, 2004)

2.2.3 Industry Guidance and Recommendations

Three levels of analysis can be identified in the current industry guidelines and recommendations, categorized based on the level of analytical complexity and the amount of supporting information necessary for the assessment:

- Level 1: This level is an acceptance/rejection criterion that is linked to characterization of the damage and a simple severity parameter such as damage depth. It is based on linear elastic fracture mechanics.
- Level 2: This level is a screening assessment that ranks damage severity; for example, those based on estimated strains calculated from local radii of curvature and those incorporating geometric parameters (D and t), material parameters (SMYS, UTS) and/or operational parameters (pressure, load cycling duty). This level is based on the R-curve and is used when failure is likely to occur. This level considers the effect of plasticity.
- Level 3: This level is a fitness-for-purpose engineering critical assessment that uses specified or actual material properties, finite element modeling, and fracture mechanics to predict pressure and/or remaining life of the damaged pipe. It is based on the J-integral, which accounts for crack arrest.

2.2.3.1 Level 1 Method (Depth Only)

The work reviewed by Fowler et al. (1994) and that undertaken by Rosenfeld et al. (2002) forms the basis of many of the recommendations and guidelines adopted by ASME B31.8 (ASME, 2012) and API 1156 (2000). The guidance is based on allowable dent depth, or an estimated dent strain that takes into account the dent profile and wall thickness. Plain dents or dents with metal-loss corrosion are characterized by a six percent depth or strain safety

threshold below which they are not considered to be at risk of bursting or delayed failure, providing that the pipeline does not experience unusually severe pressure cycling. The depth threshold for dents on girth or the weld in not compromised. The depth threshold for dents that have undergone grind repairs (to remove shallow gouges and/or surface cracking), is four percent.

The Canadian Standard CSA-Z662 (CSA, 2015) states that "the following dents are considered to be defects that impact pipeline integrity unless determined by an engineering assessment to be acceptable:

- Dents that contain stress concentrators (gouges, grooves, arc burns, or cracks).
- Dents that are located on the pipe body and exceed a depth of 6 mm and 101.6 mm in D_o or smaller than 6% of the outside diameter in pipes that are larger than 101.6 mm D_o.
- Dents that are located on a mill or field weld and exceed a depth of 6 mm in pipe 323.9 mm D_o or smaller or 2% of the outside diameter in pipe larger than 323.9 mm D_o.
- Dents that contain corroded areas with a depth greater than 40% of the nominal wall thickness of the pipe.
- Dents that contain corroded areas having depth of greater than 10 percent and up 40% of the nominal wall thickness of the pipe corrosion, and a depth and length that exceed the maximum allowable longitudinal extent determined in accordance with ASME B31G.

The European Pipeline Research Group (EPRG) (Bood et al., 1999) has developed a series of rule-of-thumb methods for determining the burst and fatigue failure of various

types of damage. EPRG concludes that plain and smooth dents up to seven percent depth (measured in pressurized pipe) will not fail at pressures up to 72% of SMYS. The guidance is applicable to pipes with 168-190 mm (6 to 7.5 inches) diameter and 5.6-12.7 mm (0.22 to 0.50 inches) wall thickness.

2.2.3.2 Level 2 Method

Recent editions of ASME B31.8 contain guidelines on assessing strain fields around dents. Acceptance is established by comparing an estimated strain with a suitable strain criterion (Equations 2.1 to 2.5). ASME has adopted six percent depth ratio as the acceptance criterion for plain dents, and four percent for dents at welds. The approach allows a more meaningful estimation of dent severity than dent depth alone.

According to the ASME B31.8 the estimation of the total critical strain in a dent requires the following strain components.

- Bending strain in circumferential direction, ε_1.
- Bending strain in longitudinal direction, ε_2.
- Membrane strain in longitudinal direction, ε_3.

The strain components are then combined by assuming that each of the components occurs coincidently at the dent apex (Noronha et al., 2010). The equations for calculation of different strain components are as follows.

$$\varepsilon_1 = \left(\frac{t}{2}\right)\left(\frac{1}{R_o} - \frac{1}{R_1}\right) \tag{2.1}$$

$$\varepsilon_2 = -\left(\frac{t}{2}\right)\left(\frac{1}{R_2}\right) \tag{2.2}$$

$$\varepsilon_3 = \frac{1}{2}\left(\frac{d}{L}\right)^2 \tag{2.3}$$

where, R_o is the radius of curvature of intact pipe surface (half the nominal pipe outside diameter) and t, d, L correspond to the wall thickness, dent depth and dent length in longitudinal direction, respectively. R_1 and R_2 are the external surface radii of curvature in the transverse and longitudinal planes through the dent, respectively (Figure 2.3).

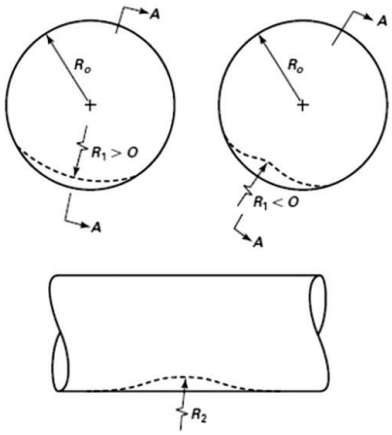

Figure 2.3 Geometric parameter of a dent (ASME B31-8, 2012)

All the strain components are combined according to the following equations to calculate the critical strain acting on the inside and outside pipe surfaces. These are ε_i and ε_o, respectively.

$$\varepsilon_i = \sqrt{\varepsilon_1^2 - \varepsilon_1(\varepsilon_2 + \varepsilon_3) + (\varepsilon_2 + \varepsilon_3)^2} \tag{2.4}$$

$$\varepsilon_o = \sqrt{\varepsilon_1^2 + \varepsilon_1(-\varepsilon_2 + \varepsilon_3) + (-\varepsilon_2 + \varepsilon_3)^2} \tag{2.5}$$

The dent is considered acceptable when the larger of the values ε_i and ε_o is lower than the allowable strain limits, which is taken as 6%. It should be noted that ASME B31-8 assumes that the membrane strain in the circumferential direction is negligible. It is,

presuming that this 6% limit is recommended to ensure safety of a dent under static and cyclic fatigue loads.

To determine the burst pressure of dents and gouges, the European Pipeline Research Group (EPRG) (Bood et al., 1999) has developed a best-correlation model that equates the failure pressure of a pipe to a function that includes the pipe material strength and toughness and geometry, and its dent or gouge depth. To overcome the complexity of the model, a series of diagrammatic methods has been developed linking defect depth, wall thickness, and operating pressure.

EPRG has also developed a set of guidelines that incorporates an additional factor of safety to simplify application of the equation. The approach is applicable to dents and gouges up to 10% deep in pipes with 168-1220 mm (6 to 48 inches) diameter and 3-18.6 mm (0.11 to 0.73 inches) wall thickness.

In the early 2000s, a need for "usable guidelines" for the assessment of damaged pipes persuaded 15 oil and gas companies to sponsor a project to produce the pipeline defect assessment manual. In this manual, Cosham and Hopkins (2002) performed a comprehensive study on the Pipeline Defect Assessment Manual (PDAM) to provide guidance to pipeline operators as to the best methods available to assess failure of pipeline defects that included corrosion, gouges, dents, cracks, weld defects, and combinations of these. In this manual, they compared the various ASME, API, BS and EPRG recommendations and selected what they consider to be the best Level 1 and Level 2 methods for assessing pipe burst conditions. To analyze plain dents (Level 1), they recommended simple empirical thresholds proposed by Rosenfeld et al. (2002), EPRG (Bood et al., 1999) and Fowler et al. (1994). However, it should be noted that Cosham and

Hopkins (2002) allowed a higher depth threshold (i.e., 10%), irrespective of whether the depth is measured with or without internal pressure. In summary, however, they conclude that there are no reliable methods for predicting the burst strength of dents at welds or at kinks. Moreover, to assess the influence of combined dents and gouges, they recommend using the Dent Fracture Model, but with incorporation of an appropriate correction factor, so that model's uncertainty could be accounted for.

The Pipeline Defect Assessment Manual (PDAM) also contains recommendations for assessing the fatigue life of dents and gouges. To analyze plain dents, Cosham and Hopkins (2002) recommend use of the original EPRG plain dent fatigue model, but including a modification that would account for uncertainty. Moreover, they suggested use of the most applicable EPRG dent-gouge fatigue models to evaluate combined dents and gouges. They also acknowledged that the results revealed considerable scatter, and that a correction factor must be applied to account for the significant influence of uncertainty.

According to DNV-OS-F101 (DNV-OS-F101, 2013), for dents without notches and sharp bottom gouges, the length in any direction should be less than or equal to 0.5D, where D is the nominal diameter of the pipe. The depth shall not exceed 6.4 mm.

2.2.3.3 Level 3 Methods

Engineering critical analysis, or fitness-for-purpose assessments, are explicitly included in the Canadian Standard CSA-Z662 (CSA, 2015) as an alternative to Level 1 or Level 2 assessment methods. Other standards and guidance are less explicit, but in several instances, they recommend seeking expert advice if such an approach is contemplated.

Engineering critical analysis of mechanical damage usually includes as much detail as is available concerning the geometry of the pipe, the character and geometry of the damage,

the relevant material properties, and pipeline operating conditions. The analysis likely will also be based on the most-recent versions of the Level 2 methods, customized if necessary to suit the specific situation.

There are no formal standards for conducting an engineering critical analysis. Regulatory authorities require the operator to demonstrate that satisfactory analysis has been undertaken in accordance with the prevailing best engineering practice.

2.2.4 Finite Element Simulation of a Dent

Numerical studies of deformation and re-rounding behavior of dent in pipes commenced in the 1980s. The nonlinear deformation model predictions were compared against experimental data, showing generally good agreement (Lancaster and Palmer, 1996). The results were used to model the relationship between the initial and residual dent depths and to study residual strains near the dent. Similar analyses indicated that strains and deformation characteristics are determined by the shape of the indenter, the way the indenter is applied, and the material properties of the pipe (Cosham et al., 2004). The resulting strain distribution also depends on the strain hardening of the pipe and on the friction forces between the pipe and the indenter.

Fowler et al. (1992) undertook finite element analyses to study the fatigue response of offshore pipelines, hosting plain dents, under cyclic pressure. They used an elastic-plastic material model, discretizing half-symmetry of the geometry with 3-D shell elements, and rigid element was used for modeling the indenter. A longitudinal wedge-shaped denting tool was used to create a dent on 12″ diameter steel pipes, with dent depths ranging between 5% - 20% of the pipe's diameter. The models were loaded using the same sequence as the

experimental tests and then fatigued to failure. These results were used to develop dent stress concentration factors that could later be used to predict the life of a dented pipe.

Leis et al. (1998) investigated the effect of dents on a pressurized pipe with a quarter model using 8-noded shell elements. The indenter and pipe supports were modelled as rigid bodies. Additional analysis using a shell-to-solid approach was also conducted. This analysis involved 20-node solid brick elements, which were used to model the indented region, while shell elements were used to model the region away from the dented area. The results obtained from the FE analysis in terms of a load displacement curve were reasonable when compared against experimental data.

The investigation of the effect of localized geometric imperfections on the stress response of pipelines was carried out by Rinehart (2004). The work covers a wide range of topics including 3D finite element analysis and 2D elastic semi-analytical analysis of dented cylindrical shells for a wide variety of dent shapes, with the aim of estimating stress concentration factors associated with dent shapes.

An experimental and numerical study on pipes having dents and gouges was carried out by Błachut and Iflefel (2008). A set of experiments were carefully designed to stablish a reliable reference for further numerical investigations. They reported the best practice available in the literature regarding FE simulation of indentation. They investigated the main factors dominating the response of pressurized dented pipes subjected to monotonic bending, including the change in length, width and shape of the dent, and contact mechanisms related issues between the indenter and pipe's surface and that between the pipe and its supports. The developed FE model accurately simulated the experimental load-deflection curve. However, due to the large strains developed in simulation of bending

effect, the accuracy of the results was not comparable with the results obtained from indentation simulation.

Hyde et al. (2009) investigated long radial indenting of pressurized pipes by finite element analysis and analytical methods. Several scenarios were considered such as different pressure levels, different support conditions, different material properties and different geometry of the pipes.

2.2.5 Fatigue Life of Pipelines containing Plain Dent

One of the earlier papers on dented pipelines was presented by Kiefner (1969) at the 4th American Gas Association Symposium on Pipeline Research. This paper summarized the results from the Fracture Initiation phase of the NG-18 research committee. It goes through a general description of how defects resulted in leaks and/or rupture, and presents a relationship between flaw size and failure stress. Strain gauge readings during pressurization indicated that "the principal effect of plain dents is to introduce highly localized longitudinal and circumferential bending stresses in the pipe wall". It is also mentioned that "without a sharp stress concentrator in the dent, yielding occurs over large enough areas that no high stress gradients are present".

In a paper summarizing pipeline failures spanning a period of 20 years, Eiber (1979) noted that failures in the base metal of pipelines were usually associated with a gouge or a dent. It was noted that there was typically a cold worked region at the base of the dent that had shallow surface cracks in the gouge and dent features examined. The internal pressure would attempt to re-round the pipe to its original shape, but this in turn resulted in cyclic bending stresses in the deformed region. The presence of a crack and cyclic stresses could lead to fatigue crack growth and failure of the pipeline. Eiber suggested that it was

impossible to estimate the severity of mechanical damage defects on the appearance alone. The author noted that dents often contained some levels of mechanical damage from which a failure would be initiated.

In the early 1980s, CANMET began a systematic series of studies to examine the behavior of dents under typical pipeline loading conditions. The first report included eight tests, where four different round indenters were used to hydraulically form plain dents to a depth of 6% of the pipe D_o (Wang and Smith, 1982). In the experiments, the dents either simulated construction damage (i.e. dented and then hydrostatically tested), or in-service damage (i.e. formed after the hydrotest and then fatigue tested up to 12000 cycles at pressures corresponding to the hoop stress as high as 80% SMYS). Cracks were observed in only one specimen, near the ends of a long dent, where re-rounding was restricted; a repeat of the test failed to produce cracks. No cracking was observed in any of the other tests, either.

CSA conducted a study on experimental works and Nova's operational experience to review the current guidelines regarding plain dents and dents with gouges. The data included dents with welds and dents with gouges, using some of the work completed at the British Gas (Jones, 1982). It was determined that plain dents up to 10% of the D_o in depth could remain in service without an adverse effect on pipeline integrity, and it was recommended that the 6% criterion be adopted for plain dents in gas pipelines.

A study sponsored by the United States Department of Transportation by Keating and Hoffman (1997) involved experimental investigation and finite element modeling of dents in pipelines. Damage included dents due to rocks, dents formed with backhoe teeth, and short longitudinal dents with gouges. The investigation included the effect of dent restraints

and their rebound behavior. Their review of existing data included a study by Urednicek (1986) on a pipe that was statically pressurized to failure. The author concluded that:

- The fatigue behavior of long, plain dents had been adequately studied experimentally by AGA.
- Short dents and dents that were restrained against elastic rebound needed to be further studied.
- Dent residual stresses were influenced by the denting process and the elastic-plastic dent rebound.
- Dent stiffness, which influences the denting process and rebound behavior, was a three-dimensional phenomenon, and 2-D modeling could not accurately represent dent's behavior.

In the early 1990s, Stress Engineering Services undertook several studies of dented pipes for the American Gas Association (Fowler et al., 1994). The results showed that neither the dent type, nor the dent length was important in terms of reducing the fatigue life, but the dent depth, D/t ratio, and weld type were influencing factors. In order to produce a dent with a given final depth, it was necessary to indent the pipes to about twice the desired depth. Their studies indicated that smooth dents less than 5% of the pipe D_o should not pose a significant threat to the integrity of a pipeline, unless it is subjected to severe pressure cycling.

Rosenfeld (1997) and Rosenfeld et al. (1997) completed studies for the American Gas Association to develop a theoretical model to describe the re-rounding of a dent in pressurized pipes. The dent was assumed to be long, so that only the cross-sectional shape needed to be considered, and the analysis used a cyclic flow strength to account for the

Baushinger effect and strain hardening. The mechanics of dent re-rounding were described to show that it takes several cycles of pressure for the dent to become completely re-rounded. Other equations were presented to calculate the rebounded dent depth using the pipe dimensions, initial dent depth, width of the dent at half of the maximum dent depth, and pressure in the pipe. Formulas for calculating the bending strains at the apex of the dent and the re-rounded dent width were provided and were used to determine the fatigue life of the dents, based on the number of cycles for fatigue crack initiation. One of the primary reasons for undertaking this study was the general feeling that fatigue life may be a more rational basis for rating the severity of a dent than the existing criteria that rely solely on dent depths with a maximum depth of 6% of the pipe diameter. It has been suggested by Rosenfeld that in some cases, deeper dents might be permitted to remain in service, while in other cases, shallower dents should be repaired.

A study, examining the effects of dents and mechanical damage on pipeline integrity, was carried out by Stress Engineering Services under the API sponsorship (Alexander and Kiefner, 1997). The first of the two reports summarizes the results of tests completed on NPS 12 pipes, with a few tests using NPS 24 and NPS 32 pipes. The results are comprehensive in that they include the indented shapes of the pipe, the total number of cycles to failure in fatigue tests, and details of any cracks in each of the tests. Overall, API 1156 looked at several variables, which included dent depth, indenter type, pipe diameter, pipe wall thickness, smooth and sharp dents, both constrained and unconstrained, stress concentrations (corrosion, weld seams, and girth welds), and the effect of hydrostatic testing. Most dents were made without the pipe being pressurized; some tests were made

with pressurized pipe, others were tested straight to failure by puncturing, and the remainder were fatigue tested. The main findings included the following:

- The pressure carrying capacity of the pipe was not affected by smooth dents without stress concentrators.
- The dents re-rounded elastically up to 67% of the maximum depth upon removing the indenter, and re-rounded up to 88% upon pressurization to 65% SMYS.
- For unconstrained smooth dents, the fatigue life was shorter for deeper dents.
- Minor stress concentrators, such as girth welds, reduced the fatigue life somewhat.
- Partially overlapping smooth dents exhibited shorter fatigue lives than individual dents.
- Hydrostatic testing had a beneficial effect on fatigue life due to re-rounding of the dent.
- Smooth dents failed by leaks in all cases; the dents were oriented longitudinally, and initiated on the D_o surface. In most cases the cracks were located on the sloping transition on the pipe-dent interface region. For constrained dents, the leaks were oriented transversely to the pipe's axis, and had initiated on the pipe internal surfaces. All failures were ductile in nature.

Alexander and Connelly (1998) performed a coherent body of experimental and analytical work on dented pipes. The tests were carried out on X52 steel grade pipes. The denting process for all cases was achieved under zero internal pressure. The author used two types of indenters to generate denting; a dome cap and a long bar. The maximum depth of the dent to the pipe diameter was 18%. Forty-four different dent configurations were

used during the course of testing. While the primary thrust of the work was experimental, numerical efforts were expended to examine dent mechanics, using first-order quadrilateral shell elements. Soil stiffness was modelled using spring elements with a trial-and-error approach. Alexander (1999) also reviewed the existing experimental and numerical data on dented pipes. The principal aim was to assess defect severity in terms of future behavior involving both static and cyclic pressure conditions. In his review, the consideration of a maximum allowable dent size of 10% of the outer diameter was proposed for pipelines under cyclic internal pressure.

Battelle Memorial Institute reported on the results of the first year of a Pipeline Research Council International (PRCI) sponsored project (Leis and Francini, 2000), looking at developing an improved criterion to assist in serviceability decisions for pipelines with dents and/or gouges. The intent was to extend the concepts of the ductile flaw growth model that was shown to accurately predict the behavior of axial flaws in pipelines. The project included experimental examination and validation of influence of the following parameters: pipeline support conditions, indenter considerations, pressure stiffening of the pipeline, re-rounding, residual dent size, pipeline grade and the effect of time and cycle dependent deformation.

A parametric study was carried out by Rinehart and Keating (2002) to quantify the influence of dents that fall into the transition region between short and long dents. Their analysis was based on the existing full-scale experimental data and finite element analysis results. The study showed that the unrestrained longer dents experienced center cracking, re-rounding, and relatively short fatigue lives. The shorter dents experienced cracking, little

re-rounding, and relatively short fatigue lives. Similar finding was also reported by Beller et al. (1991), who incorporated 3D finite element analysis in their investigation.

Gaz de France investigated damage to pipelines using both experimental and numerical means (Hertz, 2006). One finite element model was constructed to consider static denting, and another one was used to address dynamic puncture, and they considered non-linearities, including large displacements and strains, elastic-plastic material properties, contact between indenter and pipe, and the rupture process. Details were provided describing the mesh size selection and failure models, with failure models describing ductile rupture mechanisms such as softening and cavity growth.

2.3 Straight Pipe Response to Cyclic Axial and Bending Loads

2.3.1 Fatigue Ratcheting

In materials or structures subjected to cyclic stressing with non-zero mean stress, a cyclic accumulation of the inelastic deformation would occur, if the peak applied stress exceeds the material's yield limit. This phenomenon is referred to as ratcheting. Fatigue ratcheting is a phenomenon that leads to reduction in fatigue life of a structural component by loss of ductility due to cycle-by-cycle accumulation of plastic strain. One real-life example of a situation with fatigue ratcheting possibility is piping of power plants subjected to internal pressure (primary load) and cyclic bending (secondary load).

Ratcheting phenomenon can be categorized either as material ratcheting or as structural ratcheting. Material ratcheting occurs only in some materials and occurs in the absence of structural effects, only if the stress is distributed homogeneously in a structure. Material ratcheting depends on several factors such as the mean stress, stress amplitude, loading frequency, loading history and micro-structural characteristics (Blanchard et al., 2011). On

the other hand, structural ratcheting, coined by Hübel (1996), could occur in any metal. This type of ratcheting is produced by the inhomogeneity of the state of stress in a structure.

Pressurized pipelines, which constitute the main structures in the oil, gas, nuclear and petrochemical industries, are frequently subjected to variable mechanical and thermal loads over the course of their service lives. The variation in these loads is often cyclic in nature. In 1990s, it was found that the ratcheting behavior of a pressurized straight pipe subjected to seismic excitation could result in the reduction of the fatigue life of the piping components.

Consider a simple straight pipe that is under constant and uniform pressure. Such a pipe is subjected to a primary load in the axial and circumferential directions. A secondary cyclic axial stress could then be exerted on the pipe as a result of start-up and shut-down cycles over the pipe's lifespan. If the resulting cyclic loads are effectively large, such to cause the material to yield, the resulting plastic deformation may accumulate, cycle by cycle, until the plastic collapse of the structure occurs.

Similar to other common damage mechanisms (e.g., those due to fatigue and creep), ratcheting is considered as a governing criterion by many codes of practice when designing engineering components and structures. The ratcheting criterion requires structures to remain below the defined ratcheting limit, where the elastic or plastic shakedown would occur (Abdel-Karim, 2005). The ASME Boiler and Pressure Vessel Code, Section III incorporated provisions for reversed dynamic loading and ratcheting in the Code. The allowable primary stress in the piping components, subjected to level D service loads recommended in this code is three times S_m, where value of S_m is the minimum of 2/3 of yield strength or 1/3 of ultimate strength of the material.

However, the current methods that establish ratcheting limits are either too conservative or non-conservative. It is thus crucial to investigate the ratcheting response of pipelines in order to predict their response in a reasonably accurate manner.

The ratcheting behaviors of various pressurized piping structures of different materials have been extensively studied in the last several decades. These structures include straight and elbow pipes as the typical ones, as well as other geometries such as tees and lateral nozzles. Internal pressure has been the common constant load considered in design of these structures. Cyclic loadings in two control modes, that is, displacement-controlled and load-controlled have been incorporated in the related experimental studies.

The experimental set-ups to apply cyclic loads to pressurized straight pipes have mainly been done by axial loading (Jiao and Kyriakides, 2011), four-point bending (Gao et al., 2006), and pure bending (Rahman, 2006). Three commonly-used setups for these modes are shown in Figure 2.4.

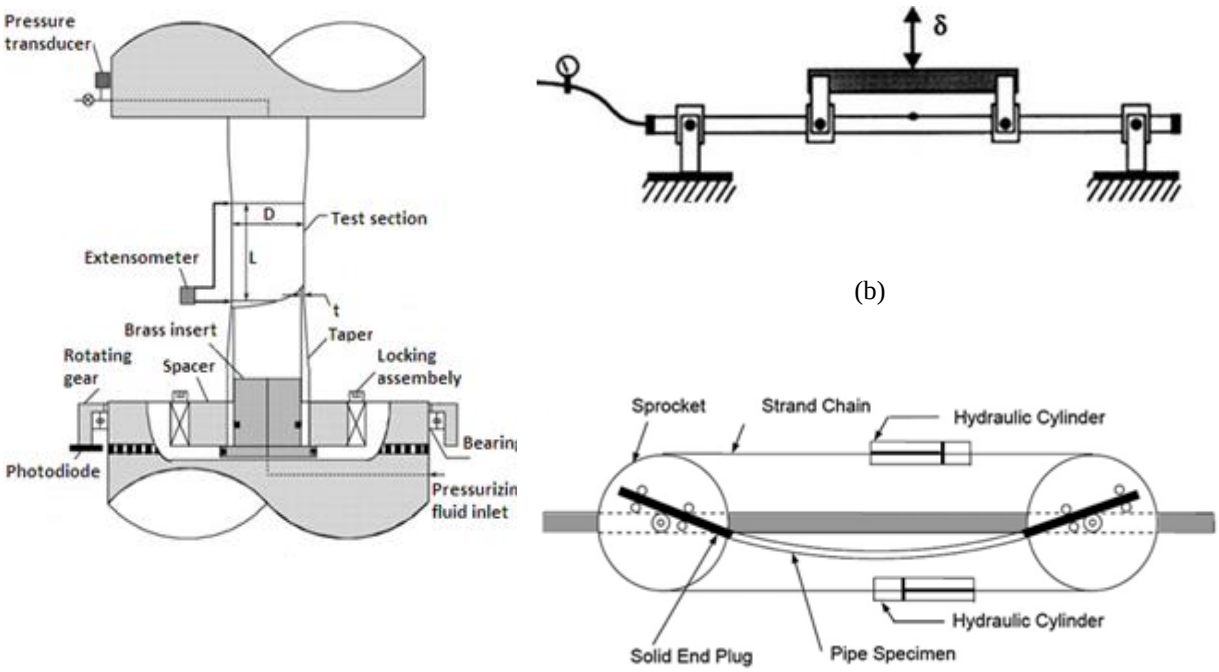

Figure 2.4 Sketch of the apparatus for testing of straight pipe subject to: (a) Axial loading (Jiao and Kyriakides, 2011); (b) Four-point bending (Gao et al., 2006); (c) Pure bending (Rahman, 2006).

In searching for the relevant literature regarding types of pipelines undergoing cyclic loads, three different groups of cyclic loading apparatus were found to have been studied. It was also noted that the subject of pipelines ratcheting response to cyclic pressure was comprehensively studied and well-treated in codes of practice. However, a scarcity of research works was observed when the problem of a dented pipe subjected to cyclic axial and bending loads was of interest. The purpose of the following subsections is, therefore, to provide a clear view of the available experimental and numerical methodologies in reference to straight pipes subjected to such loadings.

2.3.2 Experimental Investigations - Cyclic Axial Loads

Yoshida et al. (1984) performed one of the earliest investigations regarding ratcheting response of pipes subjected to cyclic axial loads. They studied mechanical ratcheting in a carbon steel pipe under combined cyclic axial load and constant internal pressure. The results showed that the biaxial strain accumulation in the pipe was influenced by maximum effective stress, stress ratio and steady stress.

Steel pipes that undergo axial compression loading beyond their yield limit often experience small amplitude wrinkles. If the pipe is subsequently loaded cyclically with a non-zero mean stress, the structure may collapse due to accumulation of compressive strain (Klever et al., 1994; DiVito et al., 2010). Pipelines are usually considered as axially restrained structures. Because of this inherent condition, a pipeline resting on the seabed can undergo plastic deformation due to a temperature change caused by the passage of hot hydrocarbons. In some cases, initiation of axial wrinkling becomes inevitable (Paquette and Kyriakides, 2006).

Jiao and Kyriakides (2009) analyzed inelastic buckling of pipelines that were subject to axial cyclic loading, which subsequently yielded to the accumulation of plastic strain and their final collapse. The problem was investigated experimentally using SAF 2507 super-duplex steel tubes with D/t of 28.5. The pipes were first compressed to strain levels high enough to cause mild wrinkles to form; then they were cycled axially under stress-controlled state about a compressive mean stress. It was reported that the pipe average strain initially grew nearly linearly with respect to the number of cycles, but as a critical value of wrinkle amplitude was approached, wrinkling localized, and then the rate of ratcheting grew exponentially, and the tube collapsed.

Jiao and Kyriakides (2011) extended their previous study to also consider the effect of internal pressure. Their results showed that the rate of ratcheting and the number of cycles to collapse depended on magnitudes of the initial compressive pre-strain, the internal pressure, and the stress cycle parameters, all of which were varied sufficiently to generate an adequate database. Moreover, in all cases, collapse was found to occur when the accumulated average strain reached the value at which the tube would develop wrinkles under a monotonic compressive load.

2.3.3 Experimental Investigations - Cyclic Bending Loads

The ovalization of a pipe's cross-section (i.e., change in the outside diameter to the original outside diameter, $\Delta D_o/D_o$, after application of loading), could occur due to bending loads. Reversal cycles (i.e., tension-compression) of bending loads result in a gradual increase in the ovalization. The increase in ovalization would in turn degrade the bending rigidity of the pipe. Once a critical magnitude of ovalization is reached, the pipe would then locally buckle. Therefore, understanding the variation in ovalization of pipes subjected to cyclic bending load is critical and of paramount importance in most industrial applications.

The response of pipes under monotonic or cyclic bending loads (with or without external pressure) have been extensively investigated by Kyriakides and coworkers. For instance, Kyriakides and Shaw (1982) studied the response and stability of elastoplastic pipes under combined bending and external pressure conditions. They reported the maximum moment capacity and curvature as a function of the material parameters, geometric features, and applied external pressure.

The inelastic behavior of pipes with respect to cyclic bending was studied by Shaw and Kyriakides (1985). They reported that reverse bending and any repeated cyclic bending

would result in a gradual growth of ovalization of the cross-section. Further, they extended their analysis to characterize the stability of circular tubes under cyclic bending (Kyriakides and Shaw, 1987). They observed that a tube would progressively ovalize to a critical value when subjected to a curvature-symmetrical loading, and would finally buckle. The critical ovalization value of a pipe was observed to be approximately equal to the value of ovalization observed just prior to the onset of buckling in the pipe under monotonic bending loading state.

Corona and Kyriakides (1988) analyzed the stability of circular tubes under combined bending and external pressure. In their study, the curvature-pressure interaction collapse scenarios were generated for two different loading paths involving bending, followed by application of external pressure and subsequent bending. Also, the specimens' response was observed to be strongly affected by the loading path. Corona and Kyriakides (1991) also investigated the degradation and buckling of circular tubes subjected to cyclic bending and external pressure. In that study, the effects of the cyclic bending and external pressure on the rate of accumulation of ovalization and the onset of instability were investigated.

According to the reported experimental studies, some engineering materials, such as 304 stainless steel, 316 stainless steel and high-strength titanium alloys are classified as rate dependent. As a result, the response and failure modes of tubes made of such materials would be different when subjected to cyclic bending at different curvature rates. Pan and co-workers analyzed the influence of curvature-rate on the response and failure mode of tubes made of different alloys subjected to cycling bending loads. In their studies, tubes made of 304 stainless steel (Pan and Her, 1998), titanium alloy (Lee and Pan, 2001) and 316L stainless steel (Chang et al., 2005) were considered. The effects of the curvature rate

at the preloading stage on the subsequent creep (i.e. while pipes were subjected to a constant bending moment for a period of time) and curvature's relaxation were investigated by Pan and Fan (1998). They used thin-walled 304 stainless steel tubes, and found that under the application of pure bending, the curvature rate at the preloading stage strongly influenced the subsequent creep or relaxation behavior. Moreover, the response and stability of 304 stainless steel tubes subjected to cyclic bending with different curvature rates was also studied by Pan and Her (1998). They found that the degree of hardening of the metal tubes increased when the applied loading rate increased. Moreover, they observed that by increasing the applied curvature rate, the ovalization of cross-section increased accordingly.

A series of tests using mild and stainless-steel pipe specimens was conducted by Moreton et al. (1994). These specimens were pressurized and subjected to fully reverse cyclic bending moments at a frequency of approximately 5 Hz. It was observed that ratcheting strain of the mild steel specimens was larger than that of the stainless-steel specimens.

The influence of diameter-to-thickness ratio D/t on the response and stability of circular tubes subjected to cyclic bending was studied by Lee et al. (2001). Having maintained the inside diameter of their SUS 304 stainless steel tubes constant, they machined the outside surface of the tubes to obtain the required D/t ratio in order to highlight the influence of D/t ratio on their pipes' response. Their work was therefore restricted to investigating varying D/t ratios (i.e. 30, 40, 50, and 60) with a fixed inside diameter. They observed that the specimens with smaller outside diameters endured less number of cycles before the onset of buckling than those with larger outside diameters.

Vishnuvardhan et al. (2010) conducted an experimental investigation on the fatigue ratcheting response of TP304 LN stainless steel straight pipes, subjected to a constant internal pressure and four-point cyclic bending. The load, load-line displacement, and deflections at three locations along the pipe were continually monitored during each test; as well, the number of cycles corresponding to development of through-thickness cracks and final failure of the components were recorded. Pipes' ratcheting response included local bulging (by 13% to 19% with respect to the original diameter along the gauge length portion), which caused thickness thinning of 8% to 16%, as well as ovalization of the pipe cross-section. While continuous ratcheting was observed on pipes' mid-section, no shakedown was evident during the experiments.

To evaluate the low cycle fatigue life of pipes with local wall thinning subjected to cyclic bending loads, Miyazaki et al. (2002) conducted low cycle fatigue tests on 100A carbon steel pipes that had local wall thinning. Ratcheting deformation was observed on these pipes under load-controlled tests, and the fatigue endurance became less than that observed for cracked pipes. The investigated pipes had a 100 mm long eroded section along the axial direction, and 0.5 mm in-depth eroded section. Under the displacement-controlled tests, the fatigue strength of these pipes was almost equal to that obtained by the design fatigue curves in ASME B&PV Code (2007) Sec. III. It was concluded that the low cycle fatigue curves can be used to conservatively estimate the low cycle fatigue life of an eroded pipe, and that the validity of estimated results could be confirmed experimentally.

Wang et al. (2014) studied the quasi-static three-point cyclic bending of pressurized straight pipes under load-controlled and displacement-controlled states. The experiment results showed that the ratcheting strain occurred mainly in the hoop direction, while there

was less ratcheting strain in the axial direction. The characteristics of the bending ratcheting behavior of the pipes were derived and compared under load-controlled and displacement-controlled states. It was reported that combined cyclic bending loads and the internal pressure affected the ratcheting behavior of the pressurized straight pipe significantly when tested under load-controlled state. In the meantime, the ratcheting characteristics were also highly associated with the cyclic displacement and the internal pressure under displacement-controlled condition. Not only did all these factors affect the saturation of the ratcheting strain, but the ratcheting strain rate was also affected.

2.3.4 Finite Element Simulation

As discussed in aforementioned section, the ratcheting behavior of pressurized pipes has been investigated experimentally by several investigators, and valuable results have been obtained to assist us to understand the general rules of ratcheting deformation and fatigue. However, it is noted that the structural dimensions and their type, and the loading conditions that had been considered in these studies are somewhat limited. To overcome the shortfalls, one can utilize the finite element approach. The approach can be used to predict the ratcheting response of pressurized pipes using appropriate constitutive models under various loading conditions. One can also examine the effect of geometric parameters (e.g., D/t) on the response in an effective and efficient manner. However, it has been demonstrated that the choice of the constitutive material model can significantly influence the outcome of such computational simulations. Therefore, in the following subsections, the progresses made in the development of constitutive material models for simulation and prediction of ratcheting in straight pipelines are reviewed.

2.3.4.1 Material Model Tuning Efforts

Ohno (1990, 1997) reviewed the investigations that had considered strain accumulation, and the related constitutive models developed up to 1997. After 1997, the focus appears to have been in tuning the models, so that the influence of the ratcheting phenomenon could be modeled more accurately. Since then, new features of ratcheting have been observed and many cyclic constitutive models have been proposed.

The first and foremost important kinematic hardening rule was presented by Prager. Prager's model, which assumes a linear relation between the back-stress tensor and the plastic strain increment, was inspired by Hooke's law, applicable to linear isotropic material. However, since the shape of the yield surface under this hardening rule has been assumed to remain unchanged under forward and reverse loadings, the use of this model would produce a closed-loop hysteresis, and thus, cannot model the ratcheting phenomenon. To account for this drawback, Armstrong and Frederick (1966) proposed a nonlinear kinematic hardening rule, which resulted in overestimation of the ratcheting strain. Due to this drawback, a number of studies have since been carried out to modify the Armstrong-Frederick hardening rule, so to establish a better estimation of the ratcheting strain. For instance, Chaboche (1989) modified the Armstrong-Frederick hardening rule to improve its capability to predict the ratcheting strain. Another modification to the Armstrong-Frederick hardening rule was presented by Bower and Johnson (1989), who introduced a new kinematic variable to decrease the overestimated prediction of the ratcheting strain by Armstrong-Frederick model.

Later, Ohno and Wang (1993) introduced a kinematic hardening rule by decomposing the backstress components. To activate the dynamic recovery terms, these components

require meeting a critical state. Bari and Hassan (2002) reported that when a sufficient number of decomposed components are used in the Ohno-Wang model, the model could provide a closer agreement between the predicted ratcheting strains and those obtained experimentally. To further improve accuracy in predicting the ratcheting strains, McDowell (1994) and Jiang and Sehitoglu (1996) modified exponents of the Ohno-Wang's model. Similar approach to Bari and Hassan's was also later adopted by Chen et al. (2005) in the framework of the Ohno-Wang model. The aim of the modification was to include shakedown and over-prediction in ratcheting strains within a larger number of stress cycles.

Over the past two decades, several scholars have investigated the parameters that influence ratcheting of materials and structures. For a comprehensive review of literature related to material tuning with respect to ratcheting, the reader is referred to the work of Abdel-Karim (2005). The review includes assessment of various approaches regarding shakedown problems in various structures, including beams, rotating discs, thin infinite plates, infinite plates with a central hole, and pipes under internal pressure and variable temperature.

There are currently several hardening models available in some of the commercially available finite element programs for simulating the ratcheting behavior of structures. The bilinear kinematic hardening (BKH), the multi-linear kinematic hardening (MKIN), the nonlinear kinematic hardening model and combined nonlinear kinematic/isotropic models are some of the commonly used available models.

Gau (1990) verified the integrity of the modified BKH model in ANSYS and the unmodified version of the model available in ANSYS and ABAQUS codes, against three sets of experimental results obtained on a straight pipe. The modified BKH model of

ANSYS produced results with significant improvement over those obtained based on the unmodified BKH of ANSYS and ABAQUS codes. It was found that the unmodified BKH models generated lower elastic-plastic modulus, which in turn, over-predicted the ratcheting strain rate significantly.

2.3.4.2 FE Models of Straight Pipelines

Another notable study is that conducted by Rahman et al. (2008) who investigated the experimental ratcheting response of straight pipes subjected to cyclic bending and constant internal pressure. In their study, the response of the pipes was also simulated numerically using ANSYS finite element code, incorporating several well-known cyclic plasticity models. However, none of the models could simultaneously simulate the variations in the moment-rotation, diameter change ratcheting, and circumferential strain ratcheting responses accurately. They then incorporated some of the more sophisticated cyclic plasticity models (i.e., the modified Chaboche, Ohno and Wang, Abdel Karim and Ohno, and modified Ohno–Wang models). Nonetheless, they discovered that even these sophisticated models could not produce results with acceptable accuracy.

In another study, Zakavi and Nourbakhsh (2014) investigated the ratcheting behavior of four pairs of stainless steel elbows using the finite element method in which Armstrong and Frederick's nonlinear kinematic hardening model was considered. To calibrate the model and obtain the hardening coefficients, they conducted uniaxial plasticity tests on several cylindrical bars (up to the necking stage), under a symmetric strain-controlled scheme with different strains. They compared their numerical results with the experimental results reported by Yahiaoui et al. (1996). Their FE models included the same loading conditions investigated experimentally (i.e., subjecting the elbows to two different constant

internal pressures, followed by dynamic conditions that induced out-of-plane external moments applied at typical seismic excitation frequencies). The ratcheting rate in their study was observed to depend significantly on the magnitude of the internal pressure, the dynamic bending moment and the constant parameters used in their nonlinear kinematic hardening model. Although the strain ratcheting rates obtained by their FE model agreed well with the experimental results, their FE model overestimated the other ratcheting results.

Kulkarni et al. (2003; 2004) predicted the ratcheting strain of a straight pipe under three-point and four-point bending modes with the use of Chaboche model in ANSYS. The results showed that the ratcheting strain only occurred in the circumferential direction, and no strain accumulation was observed in the longitudinal direction.

Zakavi et al. (2010) studied the ratcheting behavior of pressurized carbon steel (BS4360-43A) and stainless steel (304L) straight pipes subjected to the seismic bending moment with the combined nonlinear hardening model available in ABAQUS finite element code. The finite element results were compared with those obtained from the experiments to evaluate the capability of the proposed modified AF model, which was used within an isotropic/kinematic hardening rule to predict the cyclic loading behavior of a straight pipe. The results showed that the hoop-ratcheting strain predicted by their FE analysis was close to that found experimentally in all cases with $M/M_{P0.2} \leq 1$, where $M_{P0.2}$ is the 0.2% curvature offset plastic moment; otherwise, their FE analysis overestimated the experimental values.

Chapter 3

An Experimental Study on the Response of Dented Pipes undergoing Pure Monotonic and Quasi-Static Cyclic Axial Loading

3.1 Summary

When long cylindrical tubes and pipes undergo axial compression loading, they behave as beam-columns, and usually deform with a curvature and may even buckle. Shell-type localized buckling occurs mainly when the structure is restrained from lateral movement. This, for example, is the case for a pipeline buried in a trench or resting on a deformable foundation. Such a pipe may experience compressive loading due to passage of hot hydrocarbons carried from the well to a central gathering point by buried flowlines in offshore operations. Support motion caused by fault movement, landslides, ground subsidence, permafrost melting, or soil liquefication can also result in development of significant compressive load in such pipes. Both loading scenarios can impose large compressive strains, resulting in shell-type buckling of the system. Temperature also changes and repetitive start-up/shutdown in offshore pipelines generate cycles of axial compression and relaxation. Under the application of repeated loading, pipes can undergo ratcheting. Pipelines can also be subject to damage in the form of dents. This form of damage has a profound effect on a pipe's ratcheting response when it undergoes cyclic loading.

Previous studies investigating the topic of cyclically loaded pipes have shown that in the absence of a pre-existing damage in a structure, the governing parameters that control the response of pipes are the initial strain, the mean stress and the stress amplitude. In this

chapter, the influence of a mechanical damage in the form of a dent, stress amplitude and mean stress in pipes subjected to monotonic and cyclic axial loads is investigated.

3.2 Features of Axial Plastic Buckling

Unlike elastic shell buckling in which collapse is sudden and catastrophic, plastic buckling failure is preceded by a cascade of events, where the first instability (wrinkle) and collapse can be separated by average strains of 1-5%. The behavior is summarized by the axial stress-shortening response of a long pipe shown in Figure 3.1.

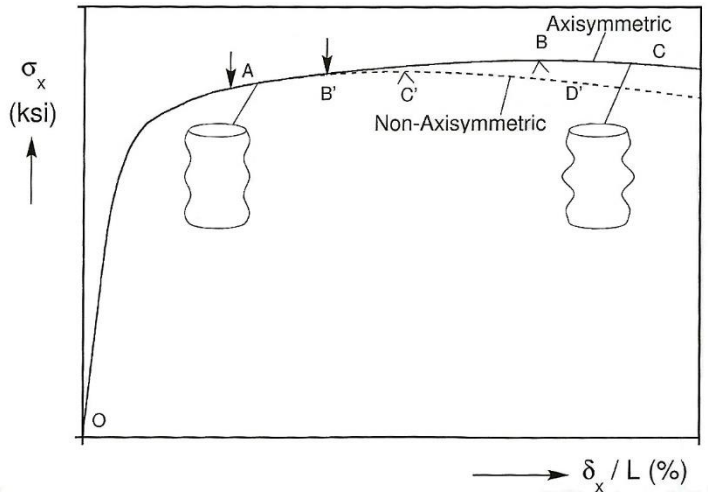

Figure 3.1 Stress-shortening responses expected in a compression test of a pipe. Shown are the onset of wrinkling (A) (Kyriakides and Corona, 2007)

Initially, the tube deforms uniformly (OA). At some strain level indicated by "↓" on the response, axisymmetric wrinkling takes over. The wrinkles, initially small in amplitude, gradually grow to visible levels as load increases (AB). During the process, the axial rigidity of the tube is reduced. For thicker shells, this eventually leads to a limit load instability (indicated by "^") that can be considered the ultimate limit state of the structure. Under displacement-controlled loading, deformation localizes with a decrease in load

carrying capacity (BC) in Figure 3.1. The localized deformation can be in the form of an axisymmetric lobe that keeps growing until its folded walls come into contact. The process can subsequently be repeated, resulting in concertina folding, as illustrated in Figure 3.2.

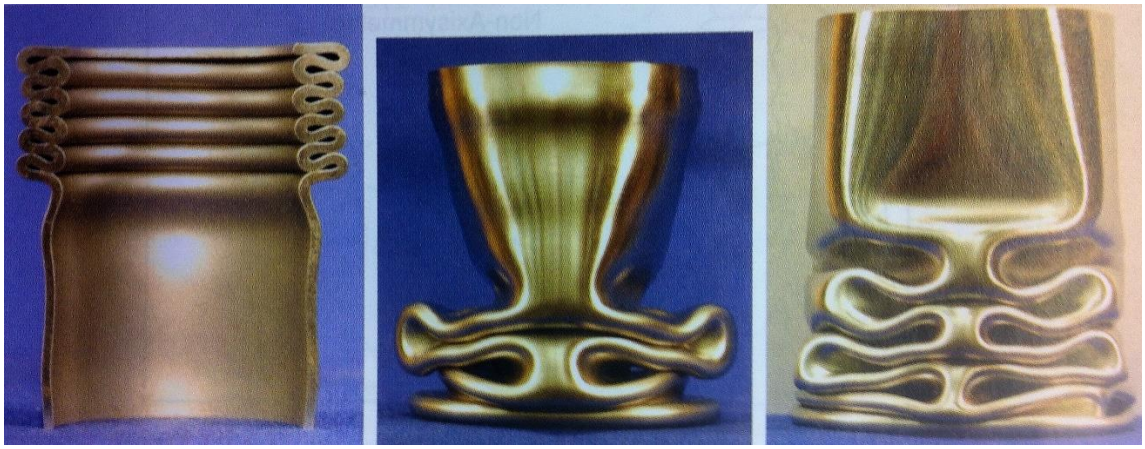

(a) (b) (c)

Figure 3.2 (a) Carbon steel tube that developed axisymmetric concertina folding; (b) mode 2 folding (c) mode 3 folding, taken from (Kyriakides and Corona, 2007)

Alternatively, a non-axisymmetric mode with two, three or more circumferential waves could develop in the zone of localization. In thinner shells, the non-axisymmetric mode develops before reaching the limit load that is associated with the purely axisymmetric deformation. This results in an earlier softening of the response, causing a lower limit load. For intact pipes, the material stress-strain response and D/t determine which of the two paths a given cylinder would undergo.

Axial plastic buckling is influenced by geometric imperfections, as well as by stress concentration such as those generated by clamped or other end constraints. In addition, a full development of the progression of events described above requires that the specimen be of sufficient length. For example, in the experiment of Lee, conducted on a soft

aluminum pipe (AL-3003-0), clamped edges resulted in the early development of edge bulges. Such bulging masked the onset of axisymmetric wrinkling (Lee, 1962).

Particular care was taken when designing the following experiment, so as to limit the influence of both edge effect and pipe size on response of the pipe specimens. As a result, the investigation could focus on examination of the effect of a dent (as a form of surface imperfection) on the response of pipes undergoing axial cyclic loads. The results would therefore be representative of the actual behavior of in-service pipelines.

3.3 Experiment Layout and Procedures

The pipes were laterally indented with a cylindrical indenter to three initial dent depths. The depths were 10%, 12% and 14% of the outer pipe diameter. Subsequently, the dented pipes were subjected to monotonic axial compression displacement in order to initiate small amplitude wrinkles in the gauge section. Finally, the tests were concluded by performing axial cyclic tests.

3.3.1 Specimen Specifications

The dimensions of the specimens were chosen similar to those utilized in the cyclic tests conducted by Limam et al. (2010) and Jiao and Kyriakides (2009). The specimens were machined from API-5L grade B carbon steel seamless tube stock (with 60.3 mm OD and 3.91 mm wall thickness). A typical specimen and its dimensions are shown in Figure 3.3.

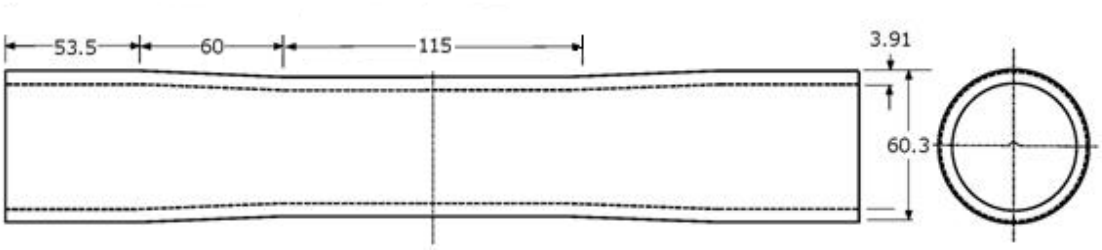

Figure 3.3 Geometry of a typical specimen (Not to scale – all dimensions in mm)

The overall specimen length was 342 mm, with some variations in the thickness as follows. Pipes' ends had thicker wall-thickness to accept the Ringfeders that connected the pipes to the test fixture. These sections were connected to the gauge section, located in the middle of the specimen, by two linearly tapering regions. The length of the tapered sections was established by utilizing the finite element method in such a way to facilitate a reasonably uniform transfer of stress from the thicker section to the gauge section. The established overall geometry facilitated the growth of wrinkling in the presence of the dent, thereby mimicking the stress variation of actual long dented pipes. The overall length of the test specimens was 342 mm.

The experimental investigation was conducted on low carbon steel pipes (API 5L grade B) with $D/\mathrm{t} > 35$ indented by a cylindrical indenter. Table 3.1 provides a summary of the material properties.

Table 3.1
Material properties obtained by standard tensile tests

Material type	Yield stress (MPa)	Ultimate stress (MPa)	Strain at failure
API 5L-B	290	415	3.8%

3.3.2 Indentation Procedure

During the indentation process, each pipe was supported by a structural steel flat plate with length of 114 mm and thickness of 10 mm, forming the denting bed. To indent the pipe, a solid cylindrical indenter, with a diameter of 9.47 mm, made from mild steel was positioned at the middle of the gauge section, perpendicular to pipe's longitudinal axis. To hold both ends of the pipe without fully restraining the ends, a fixture shown in Figure 3.4 was used. The indenter was then forced into the pipe at a constant speed of 0.1 mm/min to generate a quasi-static deformation. The indenter was removed after reaching the prescribed depth of dent, so to leave an unconstrained dent impression.

Figure 3.4 Test set up used for generating the indention

3.3.3 The cyclic and monotonic test set-up and procedures

In the next stage of the experiment, each dented pipe underwent both monotonic and cyclic axial loadings. A 200 kN servo-hydraulic Instron testing machine controlled by 8500+ electronics was utilized that could be operated in displacement- or load-control manner. The test set up is shown in Figure 3.5.

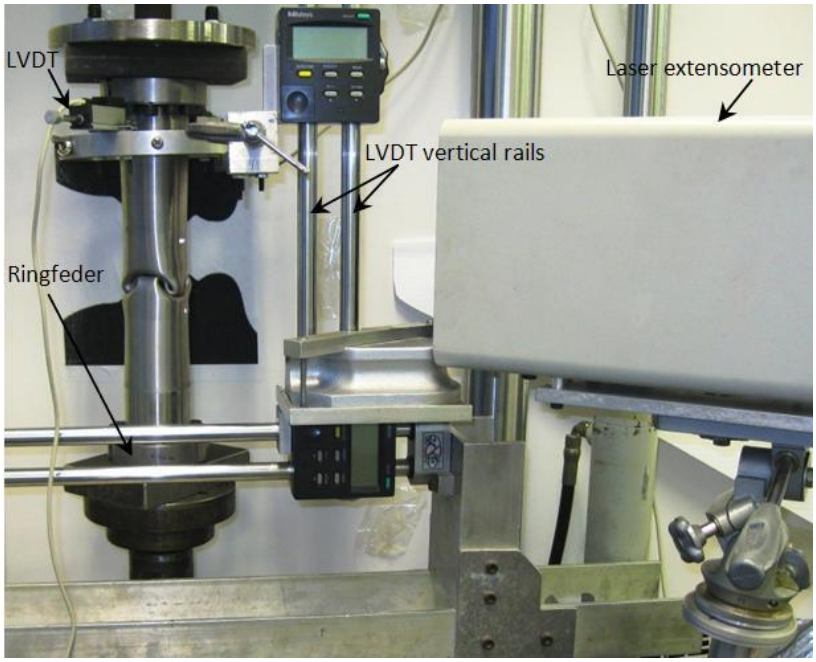

Figure 3.5 The monotonic and cyclic loading test set up

To fix the horizontal movement of the pipe and assure the concentricity of pipe's ends, each thicker end portion of the pipe was gripped by applying circumferential pressure using a Ringfeder locking assembly, attached to the testing machine. Solid inserts were placed inside the thicker ends of the specimens to support the applied pressure exerted by the Ringfeder. A laser extensometer that could scan the gauge section was used to measure the change within the gauge length. A linear variable differential transformer (LVDT), attached to a special rail that allowed the axial movement of the LVDT, was used to scan the dented section and to accurately measure the variation in its shape. During the cyclic experiments, the tests were periodically interrupted for a few seconds in order to perform an axial scan. The pipe was scanned in three stages: (i) at the zero-load; (ii) after applying the initial strain; (iii) and, during the cyclic loading, at every 50 cycles.

The initial monotonic loading was conducted at a strain rate of approximately $2x10^{-5}$ (s^{-1}), while the subsequent cycles had a period of 2 min (Jiao and Kyriakides, 2009). The

tests data, including those from the signals generated by the laser extensometer, the load cell and the displacement transducer were all captured through a computer operated data acquisition (DAQ) system that recorded the data concurrently.

3.4 Results and Discussion

The results from three monotonic loading experiments and ten cyclic loading experiments are reported and discussed in this section. The detailed cyclic experiments' results are reported in Table 3.2. In this table, δ_x^p is the average peak axial strain and N_f is the number of cycles at failure.

In the reported results, CL and ML stands for the cyclically loaded and monotonically loaded test specimens, respectively. The first number, refers to the initial dent depth. The number after the dash denotes the experiment number identifier at each dent depth ratio.

Table 3.2
Summary of results from cyclic loading experiments

Identifier	$\sigma_{x.max}$ (MPa)	σ_m (MPa)	σ_a (MPa)	δ_x^p (%)	N_f
CL10-1	294.40	143.61	150.79	3.21	1108
CL10-2	290.73	154.45	136.28	3.69	1089
CL10-3	279.52	148.95	130.56	4.07	2740
CL12-1	292.55	155.42	137.13	3.66	452
CL12-2	290.73	154.45	136.28	3.52	542
CL12-3	283.52	145.39	138.12	3.84	456
CL14-1	289.94	153.50	136.44	3.62	251
CL14-2	278.26	145.33	132.93	3.57	456
CL14-3	279.09	149.02	130.07	3.72	607
CL14-4	277.92	142.62	135.30	3.41	552

Essentially two parameters determine the choice of the initial strain that should be used to initiate the simulation of the actual load that pipelines experience in service. These are the critical strain, ε_C, at which the wrinkling initiates, and the limit strain, ε_L. Figure 3.6a pictorially shows these two critical average strain values measured for specimen ML-14. As observed in the experiments performed in this study, the wrinkling initiated at a strain of about 0.95%, followed by the pipe collapsing at an average strain of approximately 3.05% (the exact value is influenced by the small geometric imperfections, as well as the inherent anisotropy of the material).

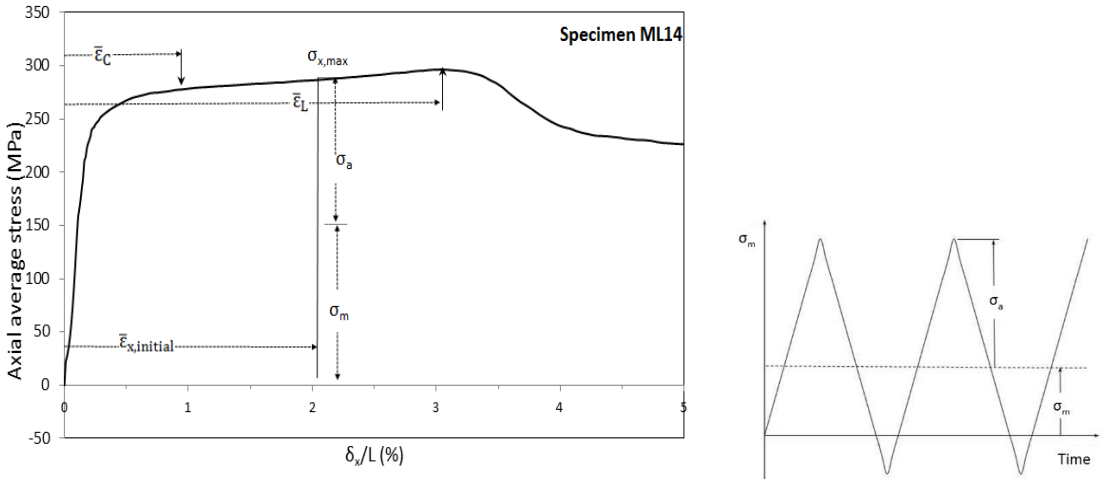

(a) (b)

Figure 3.6 (a) The stress-strain response of a 14% indented pipe tested under monotonic loading condition; (b) Typical stress-history used in cyclic testing

In the cyclic tests, the specimens were initially loaded to a compressive strain of $\varepsilon_C < \varepsilon_{x,initial} < \varepsilon_L$ (see Figure 3.6a), so that small wrinkles would be generated on their surface; subsequently, the pipes were cyclically loaded. The axial stress history shown in Figure 3.6b was applied with an amplitude of σ_a measured with respect to a compressive mean

stress of σ_m. The previous investigations have shown that the stress amplitude and mean stress govern the rate of material's ratcheting. However, to the best of our knowledge, the effect of denting on structural ratcheting has not been previously investigated.

3.4.1 Representative Indentation

As presented in Table 3.3, the unpressurized pipes were initially dented to three amplitudes, equivalent to 10%, 12%, and 14% of the outer diameter. It should be noted that δ is the initial dent depth and $\delta_{residual}$ is dent's depth after rebound. After attaining the prescribed dent depth, the indenter was slowly removed. Due to the elastic rebound of the dented area after removing the indenter, the residual dent depth to the outer diameter ratio decreased to actual amplitudes of 6.7%, 8.2% and, 9.8% of the outer diameter.

Table 3.3
Summary of specimens' geometry and indentation results

Exp. No.	D (mm)	t (mm)	D/t	t_{max}/t_{min}	δ/D (%)	$\delta_{residual}/D$ (%)	F_{max} (kN)
CL10-1	56.05	1.63	34.39	1.66/1.57	10	6.8	6.58
CL10-2	56.04	1.61	34.81	1.63/1.54	10	6.7	6.39
CL10-3	56.05	1.59	35.25	1.62/1.52	10	6.9	6.66
CL12-1	56.03	1.6	35.02	1.63/1.56	12	8	7.68
CL12-2	56.04	1.61	34.81	1.67/1.55	12	8.3	7.46
CL12-3	56.03	1.61	34.80	1.61/1.53	12	8.2	7.34
CL14-1	56.05	1.62	34.60	1.64/1.57	14	9.6	8.03
CL14-2	56.03	1.59	35.24	1.63/1.52	14	9.9	7.91
CL14-3	56.04	1.63	34.38	1.68/1.56	14	9.8	8.22
CL14-4	56.03	1.6	35.02	1.61/1.54	14	9.9	8.11
ML10	56.05	1.62	34.60	1.65/1.57	10	6.7	6.31
ML12	56.03	1.59	35.24	1.63/1.55	12	8.3	7.53
ML14	56.04	1.6	35.03	1.64/1.57	14	9.8	8.17

Typical plots of denting-force versus depth of indentation for the three dent amplitudes are shown in Figure 3.7 for pipes CL10-1, CL12-1, and CL14-1. As mentioned in chapter two, the load-deflection history of the indentation process of an unpressurized pipe can be characterized by six segments. Figure 3.7 clearly shows that for all three dent depths, the curves follow the same route as the indenter moves forward. The load-deflection curves for the investigated dent depths pass segments I, II, III, and IV through the same route (see Figure 2.2). As can be seen in the figure, during unloading, the three curves associated with CL10-1, CL12-1, and CL14-1 follow the same slope. However, pipes with deeper dents show a higher elastic rebound as characterized by segment VI (see Figure 2.2).

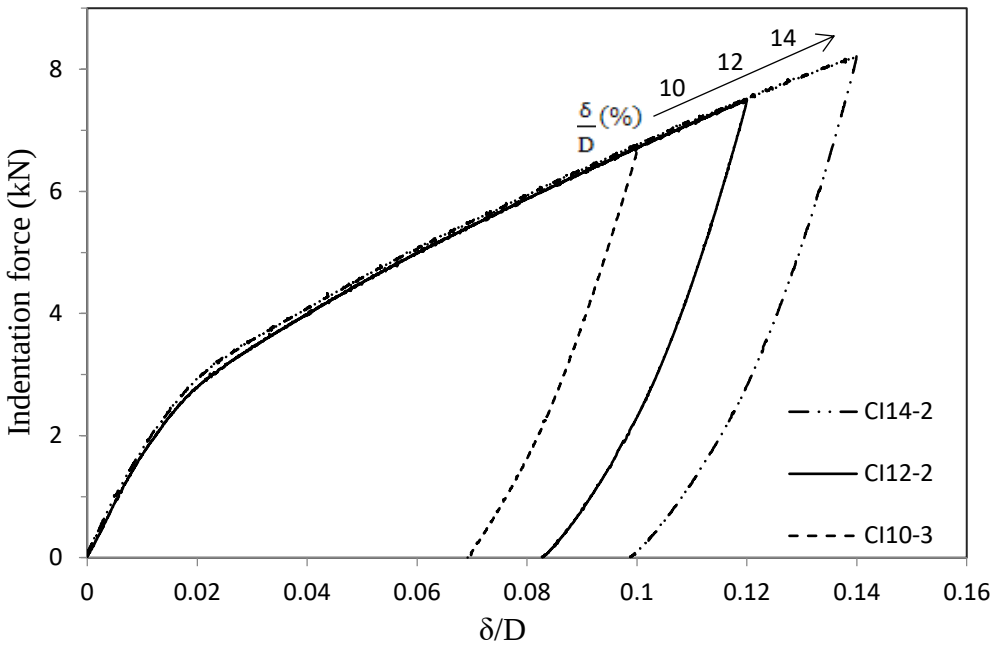

Figure 3.7 Denting force versus depth of the dent

3.4.2 Representative Monotonic Loading

Figure 3.8 shows representative average stress-strain responses of specimens with the three indentation depths subjected to monotonic loading. Instability at a limit load corresponding to strain of $\delta_x/L = 3.05\%$ could be seen in all tested specimens. The main influence of the dent depth in specimens subject to the monotonic loading is observable by considering the curves segment between the limit and final failure loads. Moreover, higher dent depth caused a significant decrease in the load-bearing capacity of the components.

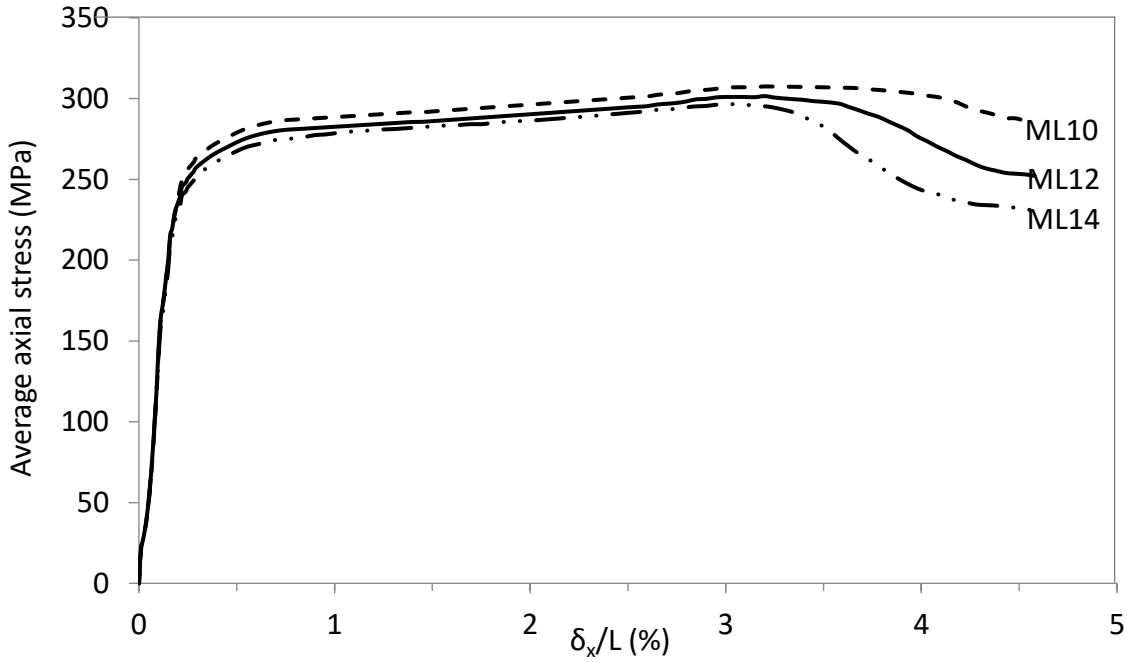

Figure 3.8 Average stress-strain response of the specimens having three different indentation depths, tested under monotonic loading

At an average strain of $\delta_x/L = 4.6\%$, the load capacity of the dented pipes at denting depths of 10%, 12% and 14% are 286 MPa, 254 MPa, and 231 MPa, respectively. In other words, at the mentioned strain, the load-bearing capacity of the component decreased from 21.9% to 12% when the denting depth changed from 10% to 14%. The other effect of dent depth, though relatively much less insignificant, is the minute decrease of approximately 1 MPa in the axial load-bearing capacity of the pipe corresponding to every 2% increases in the denting depth.

3.4.3 Representative Cyclic Loading

The pipe was initially compressed to a strain ($\bar{\varepsilon}_{x,initial}$) of 2.04% (causing an axial stress of, $\sigma_{x,max}$ = 289.94 MPa), and was subsequently unloaded. Upon reaching this initial strain, five wrinkles developed in the gauge section upon. Two pairs of wrinkles were located

symmetrically about the middle of the gauge length, near pipes' ends. An asymmetric wrinkle was also observed in the midsection, opposite to the indented region. The pipe was then loaded cyclically under an axial compressive load with a mean stress of σ_m = 136.44 MPa and an amplitude σ_a = 153.50 MPa. In this way, the maximum stress in each cycle was similar to that applied under the monotonic loading. Under the loading, the specimen immediately started to ratchet axially, as can be observed through the response illustrated in Figures 3.9 and 3.10. The ratcheting eventually grew exponentially in the neighborhood of 189th cycle (corresponds to an average strain of about 2.34%).

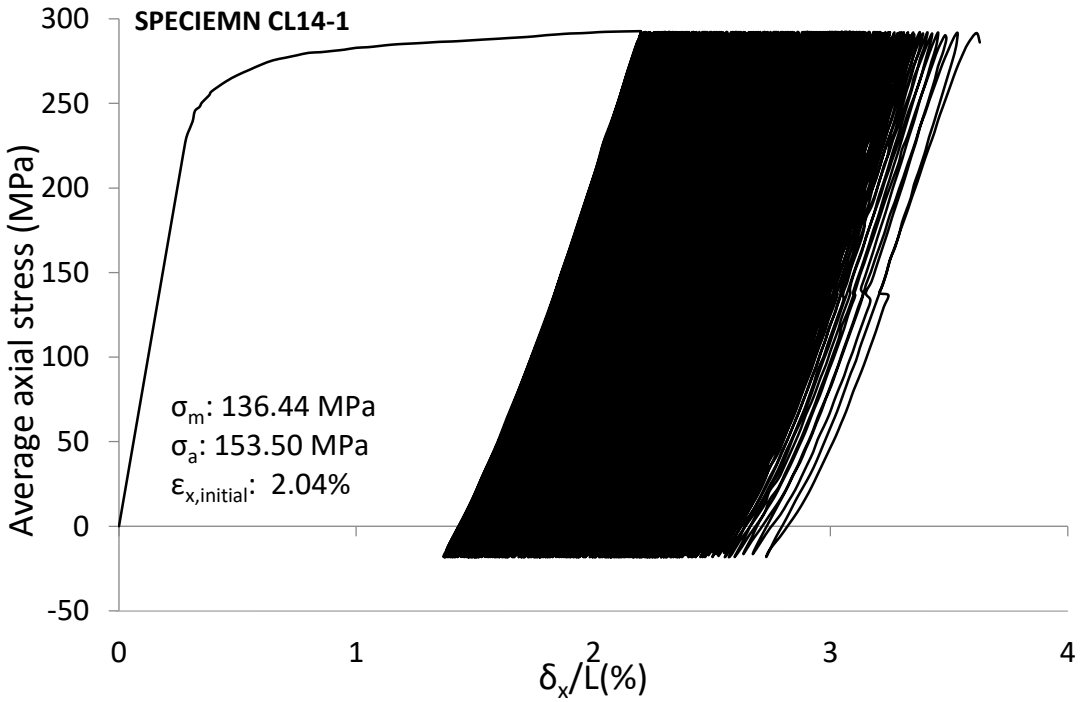

Figure 3.9 Average stress–strain response of specimen CL14-1

Figure 3.9 shows the variation in the average stress–strain response of specimen CL14-1 that was tested under the cyclic loading. An axial scan of the pipe was carried out prior to the application of the initial strain (see Figure 3.11). Three observations can be made by

examining Figure 3.9. Firstly, as one approaches the failure cycle, the width of the stress loops increases progressively. In the meantime, the peaks of the cycles become rounder. Finally, the failure occurs after the stress reaches to its cyclic peak in the 251st cycle.

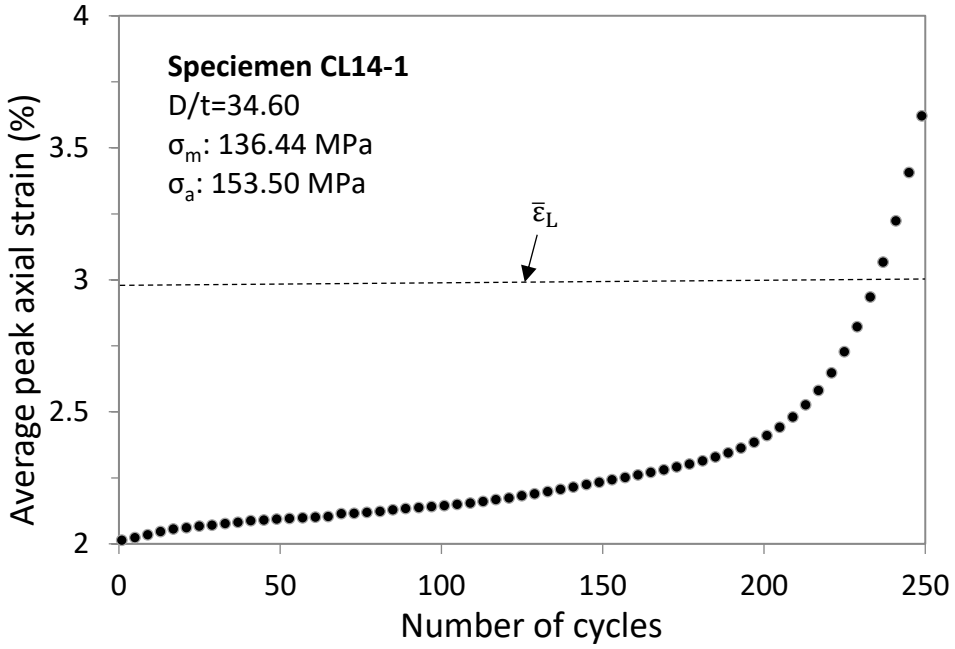

Figure 3.10 Peak average axial strain versus number of cycles for specimen CL14-1

Due to the structural damage caused firstly by the indentation and then by the resulting shortening of the dented section due to the growth of the amplitudes of the symmetric and axisymmetric wrinkles, the observed ratcheting (in δ_x^P) is believed to have been originated from both material and geometric responses. In other words, no local deformation in the gauge length was observed during the first 30 cycles (which can be viewed as the transient part of the cyclic history); therefore, it is postulated that material induced ratcheting was the main contributor in this regime. On the other hand, during the exponential growth of δ_x^P, the wrinkles amplitude grew and the indentation section deepened; thus, one could conclude that geometric induced ratcheting governs in this regime of the loading.

Figure 3.11 shows the variation in the indentation depth within half gauge-length obtained by scanning the region after application of various numbers of loading cycles (noted by "N" in the graph) of specimen CL14-1. As can be seen, and as noted earlier, the maximum residual dented depth with respect to the outer diameter at the beginning of the tests is 9.6%.

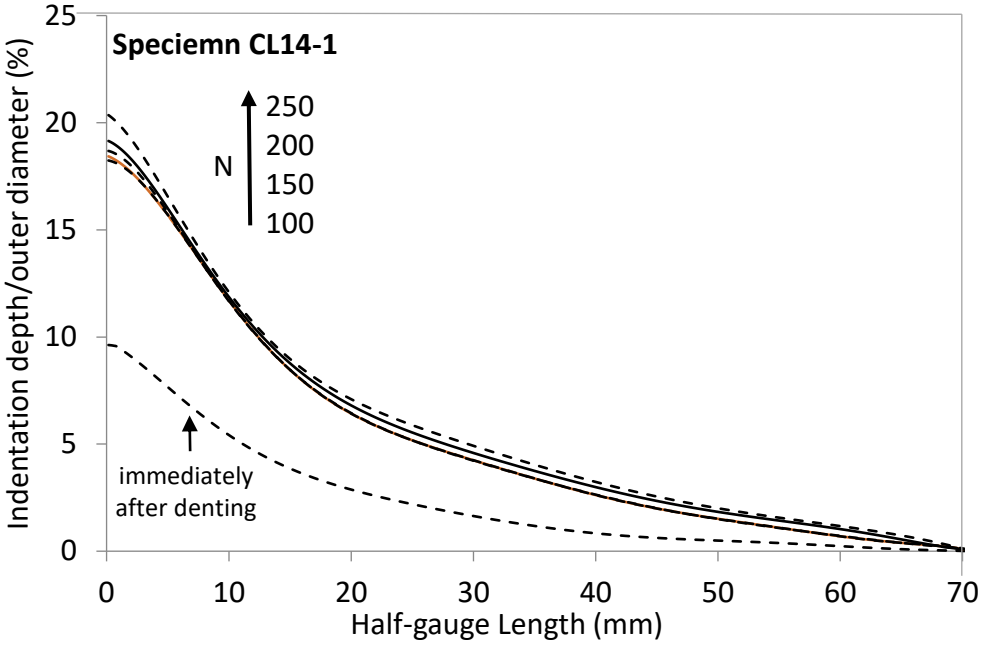

Figure 3.11 Variation in the half gauge-length profile of specimen CL14-1

After initially compressing the pipe, this value increased suddenly to 18.2%. As seen in the figure, an increase of 2% in the value of the normalized dented depth was generated after the application of the last loading cycle. As it is also evident, the effect of initial compression on increasing the dent depth is considerably more than that caused by cyclic loading. At some stage in the process, possibly before approaching the limit load, the deformation in the neighborhood of the dent completely reverted to a non-axisymmetric

buckling mode. Continued loading led to progressive concertina folding, with two faces of the dent contacting each other. Figure 3.12 illustrate the geometry of the specimen at various loading stages.

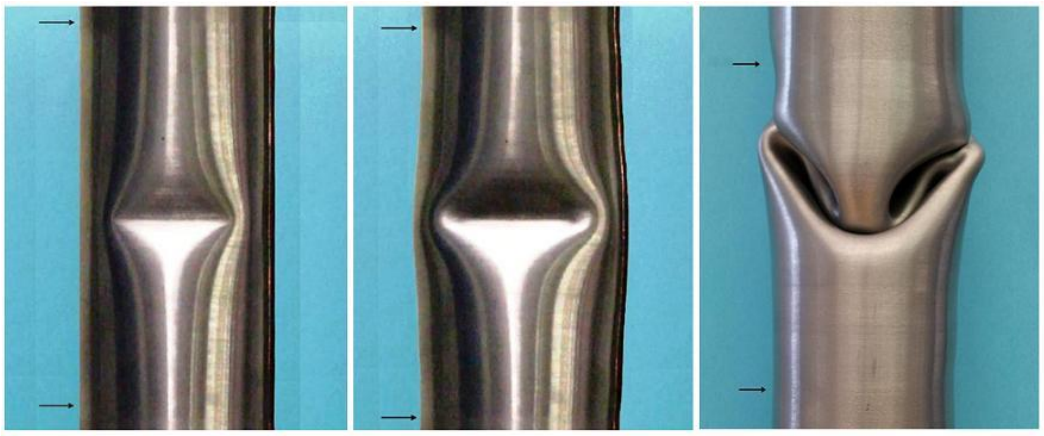

(a) (b) (c)

Figure 3.12 Gauge length's profile (a) immediately after denting (b) after the application of the initial strain (c) at the collapsed stage

The comparison of the ratcheting responses obtained through the tests conducted of specimens (CL14-1, CL12-1, and CL10-2) with three different indentation depths are illustrated in Figure 3.13.

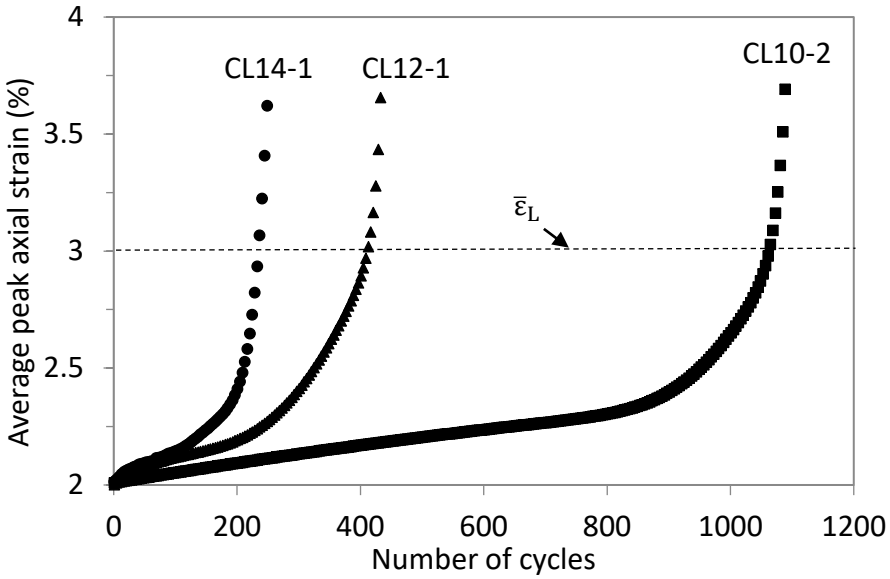

Figure 3.13 Variation of the peak average axial strain as a function of applied loading cycles for specimens with three different indentation depths

The results are extracted from the experiments having similar stress amplitudes and the same initial axial strain. All three specimens exhibited similar creep-like response (i.e. a transient response during the first few cycles, followed by a linear response, and finally an exponential response).

The main observation is that the specimens with lower dent depth exhibited elongated linear response with a lower variation (i.e., slope). The total number of cycles to failure decreased dramatically when the indentation depth changes from 10% to 14%. For instance, specimen CL10-2 collapsed after 1,089 cycles while CL14-1 reached the critical state after only 251 cycles.

The second important observation is that the rate of ratcheting is seen to accelerate when the accumulated deformation approaches the strain limit. This trend is observed again in Figure 3.14. The figure shows the ratcheting of pipes that had the same dent depth, but were subject to different stress amplitudes. The observed trend is in concert with

Kyriakides and Shaw's observation (1987), regardless of the existence of a dent. They observed that under cyclic loading, tubular specimens tend to collapse at an average strain level similar to the collapse strain experienced under monotonic loading.

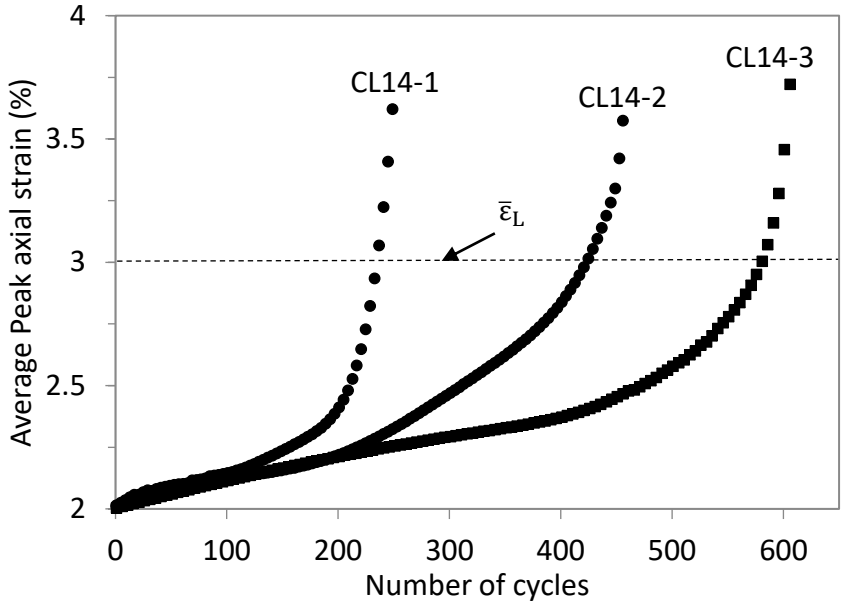

Figure 3.14 Influence of the applied load amplitude (σ_a) on the peak axial strain as a function of applied loading cycles for the specimens with 14% indentation depth (CL14)

The influence of the stress amplitude, σ_a, that also affects the rate of ratcheting, was further evaluated. The rate of ratcheting recorded as represented by the average peak axial strain per cycle is reported and compared in Figure 3.14. In this figure, the ratcheting results obtained from tests conducted on three specimens, having 14% depth of indentation, are compared. These specimens were subjected to approximately the same initial compressive strain ($\bar{\varepsilon}_{x,initial}$) of 2%, but then subjected to different cyclic stress amplitudes (σ_a). As expected, all responses present a creep-like characteristic. The effect of σ_a on the rate of ratcheting, which is represented by the slope of the nearly linear part of the curves is quite

significant. Furthermore, in all cases, at some point, the rate of growth of the plastic strain, δ_x^P/L, starts to accelerate exponentially. All specimens were cycled up to collapse.

3.5 Conclusions

In consideration of cyclically loaded pipes, previous studies have shown that, in the absence of a pre-existing damage in the given pipe, the parameters that govern the collapse of such a pipe are the initial strain, the mean stress and the stress amplitude. However, limited information is available regarding the ratcheting response of dented pipes. In this chapter, the effect a mechanical damage (in the form of a dent) on the ratcheting response and collapse of axially loaded pipes was investigated. The work also included the investigation of the applied stress amplitude. The following results and observations were obtained from the experimental investigation:

(i) Significant variation in pipes response was observed for the investigated dent depth. The numbers of cycles prior to collapse dramatically decreased by as much as 75% when the indentation depth was increased by only 4%.

(ii) Comparison of the average strain at the onset of collapse in pipes loaded monotonically or cyclically indicated that collapse would essentially occur at the same strain level, regardless of the nature of the applied loads.

(iii) The effect of cyclic load on increasing the dent depth was observed to be marginal as compared with that observed after the initial compressive load was applied. Prior to collapse, the cyclic axial load generated a maximum increase of 2% in the value of the normalized dented depth in all the performed tests.

(iv) In the case of monotonic loaded pipes, the presence of a dent reduced the load-bearing capacity (i.e., the load corresponding to the limit strain) of the pipes. For the specimens investigated in this study, the observed reductions were from 21.9% to 12% corresponding to the normalized indentation depth of 10% and 14%, respectively.

(v) The results of cyclic tests indicated that as the number of cycles increased, the increase in the dent depth shortened the linear portion of the average peak axial strain response curve. The outcome was significant in the total number of cycles to failure.

Chapter 4

Numerical Analysis of the Response of Dented Pipes Undergoing Pure Monotonic and Quasi-Static Cyclic Axial Loading

4.1 Summary

To expand understanding of the ratcheting behavior of dented pipes, the details of a 3D finite element (FE) modeling framework, developed using the commercial software ABAQUS, are presented in this chapter. The numerical results are verified against the experimental results presented in chapter 3. The FE model considered in this study is capable of capturing several nonlinear phenomena associated with the problem, including the plastic deformation of the steel, large deformation, contact stresses, and material non-linearity.

The dented pipes were initially subjected to a monotonic axial compression load, which causes the initiation of small amplitude wrinkles, and were subsequently subjected to an axial cyclic loading regime. A non-linear material model, using a combined hardening model, was adopted to model the response of the material during the entire loading regime. The parameters required by the material model were obtained from cyclic tests conducted on representative coupon specimens.

The developed FE framework was subsequently used to perform a parametric study to assess the effect of each influencing parameter on the dented pipe's response. The influence of the loading condition including initial strain level, stress amplitude, mean stress, and loading regime were investigated. As well, the influence of material hardening properties of the material model were considered.

4.2 Material Model

4.2.1 Theoretical Framework of Cyclic Plasticity

Basic elements of cyclic plasticity incorporate the yield criterion, elastic constitutive rule (i.e., Hook's law), and the plastic constitutive rule called flow rule which relates the incremental plastic strain to the stress increment. The strain increment consists of the elastic and plastic strain components, represented by:

$$d\boldsymbol{\epsilon} = d\boldsymbol{\epsilon}^{\mathbf{e}} + d\boldsymbol{\epsilon}^{\mathbf{p}} \tag{4.1}$$

The elastic strain incremental component $d\varepsilon_{ij}^{e}$ is obtained through Hook's constitutive law as:

$$d\epsilon_{ij}^{e} = \frac{1}{2\mu} d\sigma_{ij}^{e} - \frac{\lambda}{2\mu(2\mu + 3\lambda)} d\sigma_{kk}^{e} \tag{4.2}$$

in which $\lambda = \nu E/(1+\nu)(1-2\nu)$ and $\mu = E/2(1+\nu)$ are the two Lamè constants for an isotropic linear elastic solid expressed in terms of the Young's modulus (E) and the Poisson's ratio (ν), and i, j, k are the Levi-Civita tensor indices, taking values of 1 and 2 for plane stress case. The plastic strain $d\boldsymbol{\epsilon}^{\mathbf{p}}$ is obtained from the flow rule as:

$$d\boldsymbol{\epsilon}^{\mathbf{p}} = \frac{1}{H}(d\boldsymbol{\sigma}_{dev}.\mathbf{n})\mathbf{n} \tag{4.3}$$

where H is the plastic modulus and **n** denotes the normal to the yield surface.

$$\mathbf{n} = \frac{\boldsymbol{\sigma}_{dev} - \mathbf{a}}{|\boldsymbol{\sigma}_{dev} - \mathbf{a}|} \tag{4.4}$$

in which $d\boldsymbol{\sigma}_{\mathbf{dev}}$ is the incremental deviatoric stress tensor and **a** is the back-stress tensor. The yield surface translates without any change in its orientation, meaning that such surface

does not have rotation. As a basic assumption, the shape of the yield surface does not change during the cyclic plastic loading. Further, among the various yield criteria, the von-Mises yield criterion is expressed by:

$$\left(\sigma_{ij}^{dev} - \mathbf{a}\right) \cdot \left(\sigma_{ij}^{dev} - \mathbf{a}\right) = \frac{2}{3} Y^2 \tag{4.5}$$

in which $\boldsymbol{\sigma}^{\mathbf{dev}}$ denotes the deviatoric stress tensor and is obtained by

$$\sigma_{ij}^{dev} = \sigma_{ij} - \frac{1}{3}\sigma_{kk}\delta_{ij} \tag{4.6}$$

While the elastic-plastic deformation is happening, the consistency condition of the yield surface must be satisfied. Such condition stipulates that the projection of the back-stress tensor a on the unit normal n, and that of the increment of the deviatoric stress tensor $\boldsymbol{\sigma}^{\mathbf{dev}}$ increments on the unit normal n remains the same during the loading. In other words,

$$d\mathbf{a} \cdot \mathbf{n} = d\boldsymbol{\sigma}^{dev} \cdot \mathbf{n} \tag{4.7}$$

The plastic modulus H can be derived using the flow rule (Equation 4.6), the consistency condition of the yield surface (Equation 4.7), and a kinematic hardening rule. The hardening rule defines the motion of the yield surface in the stress space and its possible expansion during the inelastic deformation (Jiang, 1993).

To simulate the inelastic response of materials under cyclic loading, one may use the isotropic and kinematic hardening model. However, materials modeled by plasticity material models that include isotropic hardening, continue to harden under the application of cyclic loading. Thus, the isotropic hardening model is generally not recommended for modeling cyclic plasticity, unless the aim is to predict the shakedown behavior.

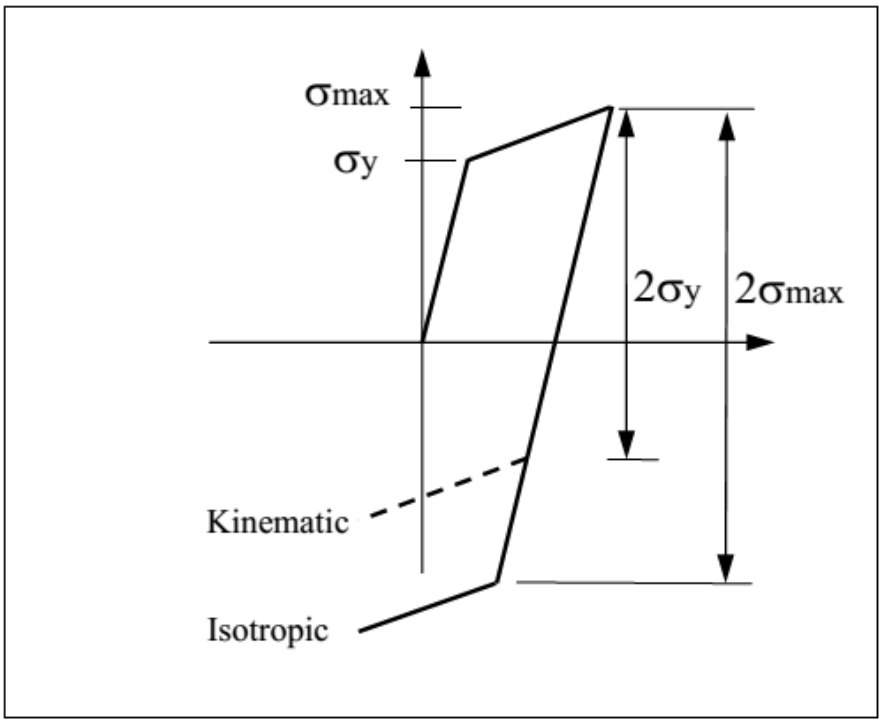

Figure 4.1 Kinematic versus isotropic hardening model

A nonlinear kinematic hardening model or a combined nonlinear kinematic/isotropic hardening model can also be used to simulate the response of materials to cyclic loading (Zakavi et al., 2010). However, Zeinoddini and Peykanu (2011) showed that the nonlinear kinematic hardening model falls short of predicting the inelastic behavior of a plain dent that is subjected to axial cyclic loading. Therefore, the nonlinear kinematic/isotropic hardening model was recommended to be used to simulate the hardening response of materials that have undergone ratcheting.

4.2.2 Nonlinear Kinematic Hardening Model

The kinematic hardening model describes the translation of the center of the yield surface in the stress space. The nonlinear kinematic hardening model was first proposed by Armstrong and Fredric (1966) by adding a "recall" term to the Prager model. The recall

term assumes different hardening moduli for loading and unloading stages, so that the transformation of stress would be different during loading and unloading.

Lemaitre and Chaboche (1994) expressed the yield function for time independent plasticity by employing the von Mises yield criterion, as:

$$f = J_2(\boldsymbol{\sigma} - \mathbf{X}) - k \tag{4.8}$$

where $\boldsymbol{\sigma}$ and $\mathbf{X}$ are stress and back stress tensors, respectively, k is the initial size of the yield surface, and J_2 is the von Mises distance in the deviatoric stress space, which can be mathematically expressed by:

$$J_2(\boldsymbol{\sigma} - \mathbf{X}) = [\frac{3}{2}(\boldsymbol{\sigma}' - \mathbf{X}'):(\boldsymbol{\sigma}' - \mathbf{X}')]^{1/2} \tag{4.9}$$

In which $\boldsymbol{\sigma}'$ and $\mathbf{X}'$ are the stress and back stress deviatoric tensors in the stress space, respectively.

Armstrong and Frederick also introduced nonlinearities to the Prager model by adding a recall term, as shown below:

$$d\mathbf{X} = \frac{2}{3}C d\boldsymbol{\varepsilon}^{\mathbf{p}} - \gamma \mathbf{X} d\boldsymbol{\varepsilon}^{\mathbf{p}} \tag{4.10}$$

where $d\boldsymbol{\varepsilon}^{\mathbf{p}}$ is the equivalent plastic strain rate, and C and γ are material-dependent coefficients. The linear kinematic law is reached when γ is set to zero.

The normality hypothesis and the consistency condition, $df = 0$, provide an expression for the plastic strain rate, as follows (Lemaitre and Chaboche, 1994):

$$d\boldsymbol{\varepsilon}^{\mathbf{p}} = d\lambda \frac{\partial f}{\partial \sigma} = \frac{H(f)}{h} \langle \frac{\partial f}{\partial \sigma} : d\boldsymbol{\sigma} \rangle \frac{\partial f}{\partial \sigma} \tag{4.11}$$

where H is the Heaviside step function: $H(f)$ will be zero if $f < 0$, and $H(f)$ will becomes equal to 1 if $f \geq 0$. The symbol $\langle\rangle$ is the MacCauley bracket, such that $\langle v \rangle = (v + |v|)/2$.

The hardening modulus h can be evaluated by the following equation:

$$h = C - \frac{3}{2}\gamma \mathbf{X} : \frac{\boldsymbol{\sigma}' - \mathbf{X}'}{k} \tag{4.12}$$

In tension-compression loading scenarios, the flow and hardening can be expressed in the following forms:

$$f = |\boldsymbol{\sigma} - \mathbf{X}| - k = 0 \tag{4.13}$$

$$d\boldsymbol{\varepsilon}^{\mathbf{p}} = \frac{1}{h} \langle \frac{\boldsymbol{\sigma} - \mathbf{X}}{k} d\boldsymbol{\sigma} \rangle \frac{\boldsymbol{\sigma} - \mathbf{X}}{k} = \frac{d\boldsymbol{\sigma}}{h} \tag{4.14}$$

$$d\mathbf{X} = C d\boldsymbol{\varepsilon}_{\mathbf{p}} - \gamma \mathbf{X} \left| d\boldsymbol{\varepsilon}_{\mathbf{p}} \right| \tag{4.15}$$

$$h = C - \gamma \mathbf{X}\, \mathrm{Sgn}(\boldsymbol{\sigma} - \mathbf{X}) \tag{4.16}$$

Lemaitre and Chaboche (1994) analytically derived the equation of hardening and presented it as:

$$X = \upsilon \frac{C}{\gamma} + \left(X_0 - \upsilon \frac{C}{\gamma} \right) \exp\left[-\upsilon\gamma(\varepsilon_p - \varepsilon_{p_0}) \right] \tag{4.17}$$

where $\upsilon = \pm 1$ accounts for the direction of flow, and ε_{p_0} and X_0 are the initial values of the plastic strain and back stress, respectively. Moreover, C is the initial kinematic

hardening modulus and γ defines the rate of kinematic hardening decrease as the plastic strain develops.

4.2.3 Isotropic Hardening Model

As the plastic strain grows, the yield surface grows in size uniformly in all directions. The isotropic hardening model predicts this behavior. The yield surface for isothermal plastic deformation and time independent plasticity can be expressed as:

$$f = f(\sigma, R) \tag{4.18}$$

where R is a scalar variable that governs the evolution of the loading surface and is expressed as a function of the equivalent plastic strain ε_p by:

$$R = R(\varepsilon_p) \tag{4.19}$$

in which ε_p is defined by:

$$d\varepsilon_p = \sqrt{\frac{2}{3} d\varepsilon^p : d\varepsilon^p} \tag{4.20}$$

Using the von Mises criterion, the above equation can be expressed as:

$$f = J_2(\sigma) - R - k \tag{4.21}$$

where k is the initial size of the yield surface and J_2 is the von Mises yield surface distance from the origin of axes (i.e., from location where ($\sigma_1 = \sigma_2 = \sigma_3$) in the deviatoric stress space:

$$J_2(\sigma) = \sqrt{\frac{3}{2}\sigma' : \sigma'} \tag{4.22}$$

The general form of the flow rule can be expressed as follows:

$$d\varepsilon^p = d\lambda \frac{\partial f}{\partial \sigma} = \frac{3}{2} d\lambda \frac{\sigma'}{R + k} \tag{4.23}$$

where the constant $d\lambda$ is defined as $d\lambda = d\varepsilon_p$.

Chaboche (1989) used the evolution of the size of the yield surface to express the isotropic hardening:

$$dR = b(Q - R)d\varepsilon_p \tag{4.24}$$

By considering Equation (4.21), with the initial value of $R = 0$, and integrating the above equation one would obtain:

$$R = k + Q[1 - \exp(-b\varepsilon_p)] \tag{4.25}$$

where Q and b are the material parameters. Here, Q controls the maximum change that the yield surface can attain, and b controls the rate of the yield surface changes as the plastic strain grows.

4.2.4 Nonlinear Kinematic/Isotropic Hardening Model

The nonlinear kinematic/isotropic hardening model consists of two components: a nonlinear kinematic component that defines the translation of the yield surface in stress space, and an isotropic hardening component that defines the size of yield surface as a function of the plastic strain.

To accurately obtain the nonlinear kinematic/isotropic hardening parameters, it has been recommended that the hardening model be calibrated against experimental data within a loading regime and a strain close to those that are expected to occur in the actual application (Zakavi et al., 2010).

The calibration procedure, therefore, consisted of testing of five bars. In one test, the material was subjected to monotonic tensile load until necking occurred, which led to evaluation of the isotropic hardening component. In the other tests, the test coupons were subjected to a set of symmetric strain-controlled loading cycles with different strain levels, to establish the values of kinematic hardening's components. During these calibration tests, the stress state remained essentially uniaxial. There are three different ways to provide data for the kinematic hardening component of the plasticity model used in this study: (i) by using a half-cycle test data; (ii) by using a single stabilized cycle data; and (iii) by using the test data obtained from several stabilized cycles. The stress–strain data can be readily obtained from several stabilized cycles of test specimens that are subjected to symmetric strain cycles. The third approach has been commonly used during recent years; therefore, it was utilized in this study.

When conducting symmetric strain-controlled experiments, the equivalent plastic strain equals the summation of the absolute value of the change in the longitudinal strains; that is:

$$\bar{\varepsilon}_p = \sum \left|\Delta\varepsilon_p(i)\right| = \sum_i \left|\Delta\varepsilon_i - \Delta\bar{\sigma}_{exp}/E\right| \tag{4.26}$$

where ε_i is the total strain, $\bar{\sigma}_{exp}$ is the measured stress and E is the elastic moduli. The equivalent back stress, $\bar{X}$, equals one-half of the difference in the yield stress obtained at

the end of tensile loading and the first yield occurring at the subsequent compressive loading.

The resulting data pairs $(\overline{X}, \overline{\varepsilon}_p)$, are plotted in Figure 4.2b. The kinematic hardening parameters, C and γ, could now be estimated by correlating Equation (4.17) to the coupon test data as illustrated in Figure 4.2b.

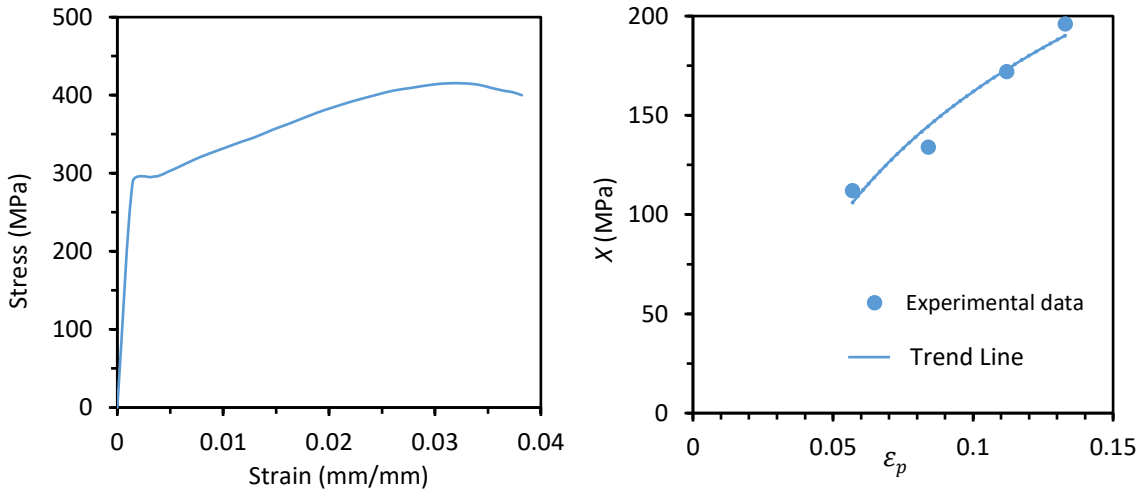

(a) Stress-strain curve

(b) Curve fit data from cyclic tests

Figure 4.2 Material properties of API 5L-B to calibrate the hardening parameters

As briefly stated, the data for the equivalent stress versus equivalent plastic strains up to the point of necking was extracted from the monotonic tension tests. An empirical equation was obtained by fitting a nonlinear least-square curve to the data to establish the equivalent stress at arbitrarily high values of equivalent strains. Using the experimental data corresponding to one-half of the necking strain shown in Figure 4.2a, and fitting a

nonlinear least-squares regression curve to the monotonic hardening data-set led the following relationship:

$$\bar{\sigma} = \sigma_y \left(1 + \frac{\bar{\varepsilon}_p}{m}\right)^n \tag{4.27}$$

where $\bar{\sigma}$ is the equivalent stress, σ_y is the initial uniaxial yield stress, and m and n are material constants. Upon fitting Equations (4.17) and (4.27) to the experimental data, σ and $\bar{X}$ can be readily estimated at any increment of the equivalent plastic strain. The isotropic component of the hardening, σ_0 , is then defined as a function of equivalent plastic strain by:

$$\sigma_0(\bar{\varepsilon_p}) = \sigma(\bar{\varepsilon_p}) - \bar{X}(\bar{\varepsilon_p}) \tag{4.28}$$

The isotropic material parameters, Q and b, can also be determined by fitting Equation (4.28) to the results obtained by Equation (4.25), using the nonlinear least-squares regression method.

Briefly, the calibration procedure consisted of testing of five bars. In one test, the bar was subjected to monotonic tensile load until necking occurred, which led to evaluation of the isotropic hardening component. In the other tests, the bars were subjected to symmetric strain-controlled loading cycles with different strain levels, to establish the kinematic hardening parameters. The material parameters for the kinematic hardening model were determined to be: C= 1544 MPa, and $\gamma = 10$, and for the isotropic material model have been evaluated as b = 16.8 and Q = 85 MPa.

The general material properties of the low-carbon steel pipes (API 5L grade B) presented in Table 4.1.

Table 4.1
Material properties obtained by standard tensile tests

Material type	Module of elasticity (GPa)	Yield stress (MPa)	Ultimate stress (MPa)	Strain at failure
API 5L-B	198	290	415	3.8%

4.3 Finite Element Modeling Framework

In this phase of the study, the commercial software ABAQUS was used to develop a FE framework to simulate the ratcheting response of dented steel pipes under cyclic loadings. To verify the validity of the framework, firstly, the developed FE model reproduced the three stages of the experimental test procedure described in previous chapter, including indentation, monotonic and cyclic loading. The obtained results were then compared against the results of the experimental study.

Eight-node, solid elements type C3D8R, with hourglass control and reduced integration options were used to model the specimens. To reproduce the specimens' boundary conditions imposed during the experiments, the two lateral translational degrees of freedom of the external nodes of the numerical model (at both ends) that fall within the Ringfeders were constrained. The longitudinal degree of freedom at the bottom end nodes was constrained but let free on the nodes located on the opposite end of the pipe. Moreover, a finer mesh was used to model the region along the mid-region of the pipe. Mesh configuration and orientation of model's parts are presented in Figure 4.2.

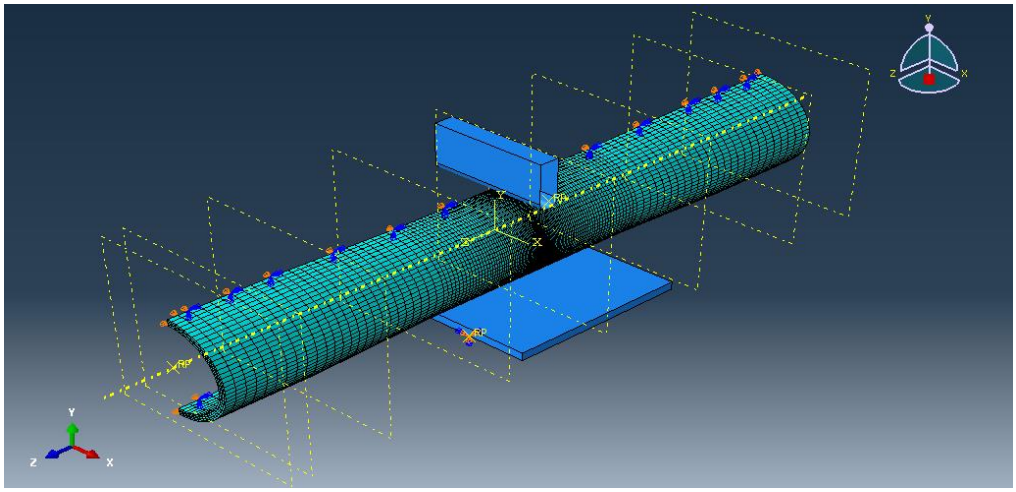

Figure 4.3 Parts' orientation and mesh configuration of the 3D finite element model

The modeling trials' results indicated that to simulate the response of the material within the indentation region with a reasonable accuracy, one should model the region with at least three layers of elements (through the pipe's thickness direction). Although increasing the number of layers of elements through-the-thickness within the indentation zone would produce more accurate results; however, it would require considerably longer running time in simulating the cyclic loading effect. As a result, a compromise was made to adopt a mesh with three layers of elements through the thickness, which produced a set of reasonably accurate results within a practical time frame.

The element size and mesh refinement were established following Jiao and Kyriakides's experimental results (2009). They reported formation of approximately seven wrinkles along the mid-region of their specimens, with an average wave length of approximately 10 mm. With this in mind, that portion of the specimen was modeled by discretizing the region by 100 rows of elements (along the axial direction of the specimen), ensuring that the formation of wrinkles could be captured in the simulation.

As was done in the experiment, the cylindrical indenter was first pressed into the pipe at the mid-span of the pipe, perpendicular to the pipe's longitudinal axis. Then, the axial loading was introduced to the model in two stages. First, to attain the desired axial strain (developed in the gauge section), the model was axially compressed by applying prescribed displacement to the nodes forming the end portions of the model. The resulting strain value was comparable to the actual initial non-linear strain measured during the experiments. The second loading stage involved application of pressure loading to the end portions of the.

4.3.1 Simulation of the Indention

Appropriate boundary conditions were applied to mimic the indention process. The computational results indicated that it was sufficient to use three layers of 3D brick elements through the wall thickness.

The indenter and the saddle were both surface hardened in the experimental phase of the study. This allowed the indenter to be modelled as a 3D analytical rigid surface, which comes into contact with the pipe outer surface. The coefficient of friction between contacting surfaces was assumed to be 0.3 (Blachut and Iflefel, 2008). An analytical rigid flat surface simulated the saddle which in contact with the lower end of the pipe reacted the indentation force. The contact between the pipe and two rigid surfaces (indenter and flat surface) was modeled by using the master-slave approach as described in ABAQUS user's manual. The advantage of using the analytical rigid surface option in ABAQUS is the lower required computational effort in comparison to using rigid elements. More details of the FE modeling procedure of pipes with defects can be found in (Blachut and Iflefel, 2008). Similar to the experiment, the dents were perpendicular to the pipe longitudinal axis and located at the mid-span of the pipe.

Table 4.2, presents specimens' geometric properties and the resulting indentation produced by the FE simulation. It was tried to select test samples from the experimental study that share similar geometry. This will help to focus the comparative study, experiment versus simulation, only on the effect of the dent depth.

Table 4.2
Summary of specimens' geometry and indentation results

Model No.	D (mm)	t (mm)	D/t	t_{max}/t_{min}*	δ/D (%)	$\delta_{residual}/D$ (%)	F_{max}** (kN)
CL10-2	56.04	1.61	34.81	1.63/1.54	10	6.7	6.39
CL12-2	56.04	1.61	34.81	1.67/1.55	12	8.3	7.46
CL14-1	56.05	1.62	34.60	1.64/1.57	14	9.6	8.03

* Maximum and minimum thickness through the pipe length
** Maximum indentation force

Figure 4.3 depicts a closer view of the model of specimen CL12-2 at various stages of indentation.

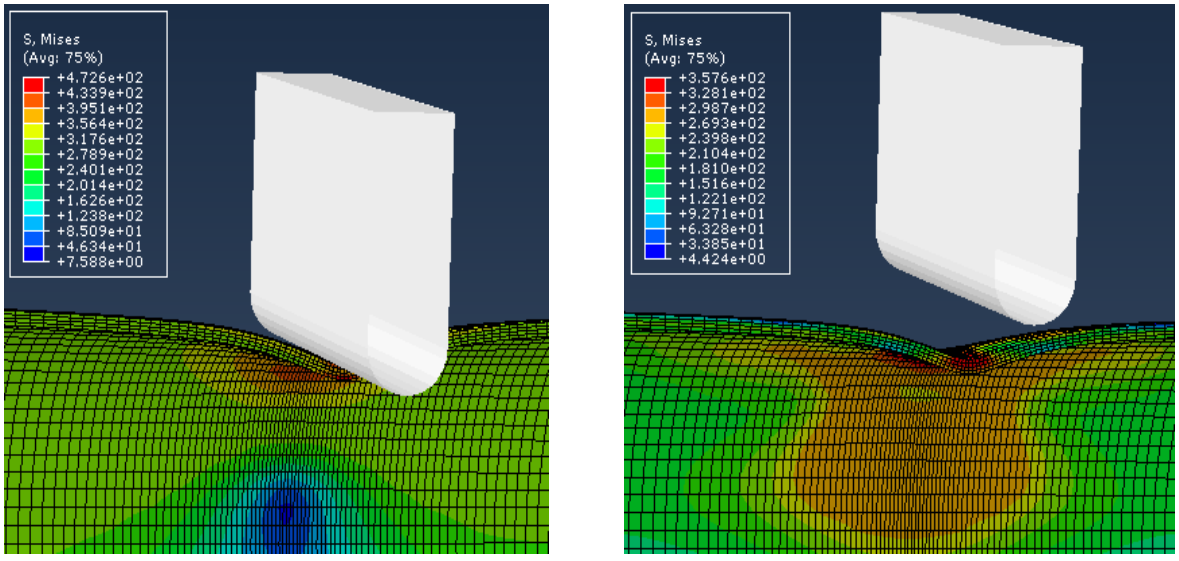

(a) At the maximum depth (b) At the residual depth

Figure 4.4 FE simulation of the indentation process (a) during, and (b) after indenter removed

Denting was achieved by applying incremental vertical displacement to the rigid indenter, as it was done during the experiment. The calculated indentation force is plotted against the indentation depth ratio for both simulation and experiment in Figure 4.4. The results are seen to follow the corresponding measured response very closely. The pipe was unloaded incrementally essentially at the same point as in the experiment. Interestingly, the unloading part of the response was also reproduced with less than 23% error.

However, there are two visible discrepancies apparent in the results. Firstly, the maximum indentation load for simulation is slightly higher than the experimental value (by 0.51 kN). Secondly, the residual dent depth in the simulation is 11.4% of the pipe's outer diameter while the recorded value for the experiment is at 9.6%.

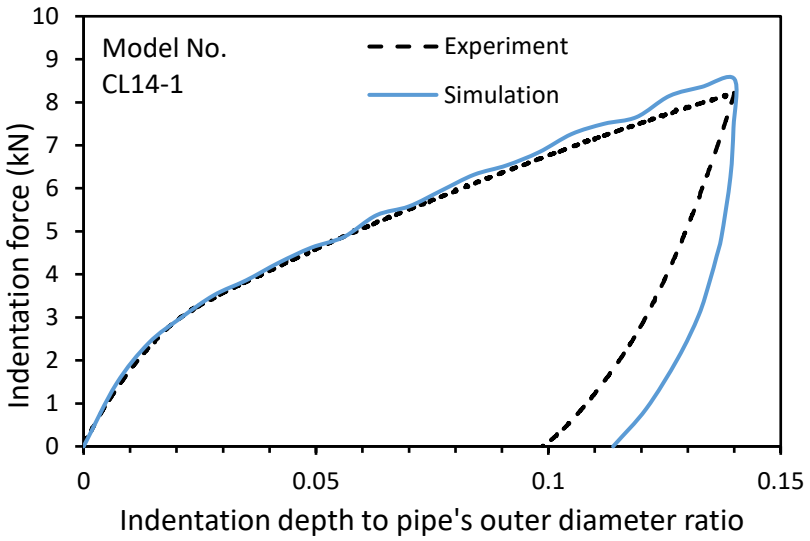

Figure 4.5 Variation of the denting force versus depth of dent

It should be emphasized that in order to accurately simulate the contact interaction between indenter and pipe, several layers (at least 10 layers) of elements should be used to model the pipe through the thickness (Blachut and Iflefel, 2008). The numerical trials that

were carried out in this study validated the suggestion as well. For instance, one trial results revealed that the residual dent depth could be reduced from 11.4% to 11% by incorporating four layers of elements through pipe's thickness (instead of three layers of elements). However, this increase in the number of elements increased the run-time significantly, especially when simulating a material's response during a cyclic loading. Consequently, it was concluded that the selected mesh produces reasonably accurate results. The reminder of the numerical investigation was carried with the original mesh configuration. Table 4.3 compares results for dent depths of 10%, 12% and 14%.

Table 4.3

Indentation force and residual dent depth, experiment versus simulation

Model No.	δ/D (%)	$\delta_{residual}$/D (%)		F_{max} (KN)	
		Experiment	Simulation	Experiment	Simulation
CL10-2	10	6.7	8.6	6.39	7.08
CL12-2	12	8.3	10.1	7.46	7.68
CL14-1	14	9.6	11.4	8.03	8.54

4.3.2 Simulation of the Monotonic Loading

Figure 4.5 illustrates the numerical and experimental axial stress-strain results obtained for a dented pipe subject to a monotonic axial loading condition. These results comprise the second FE model's verification. These results show a reasonable agreement between the experimental and the numerical stress-strain results.

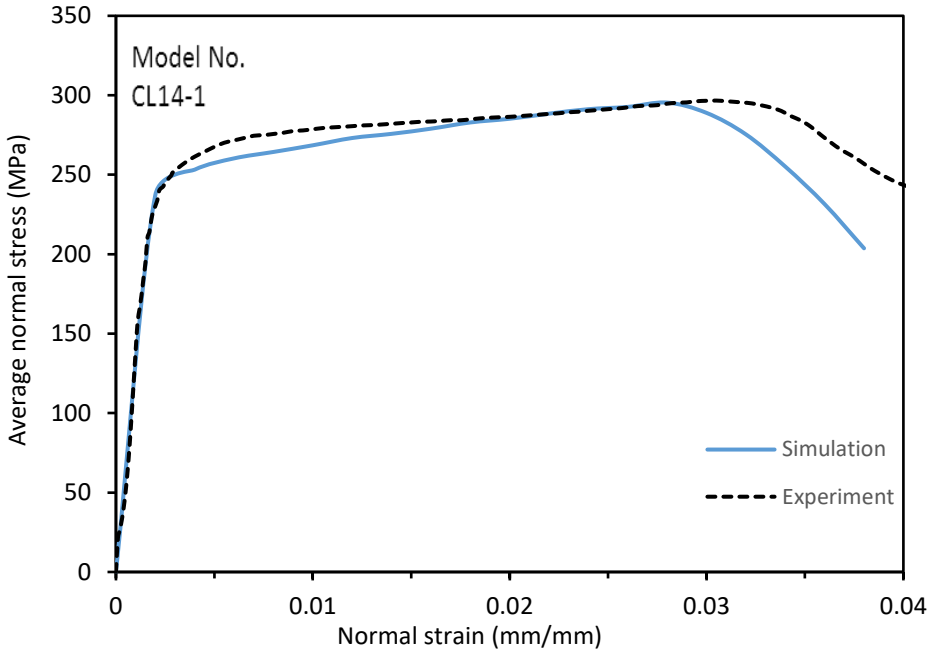

Figure 4.6 Comparison of the simulation and experiment results for the monotonic loading

The deformed geometry of a representative dented pipe tested experimentally, and that obtained through the numerical analysis are shown in Figure 4.6. As can be seen, an axisymmetric wrinkle has been generated in the middle portion of the model, which matches the shape and location of that in the actual article. It should be noted that, whereas the wrinkle has a small and constant amplitude in the radial direction in the beginning stage of loading, a further increase in the axial load causes the wrinkle's amplitude to grow. The radial amplification of the wrinkles, in turn lead to the degradation of the axial rigidity. As in the actual case, the first wrinkle was observed to initiate in the dented region and then the other wrinkles were subsequently developed and gradually propagated in the gauge section along the pipe.

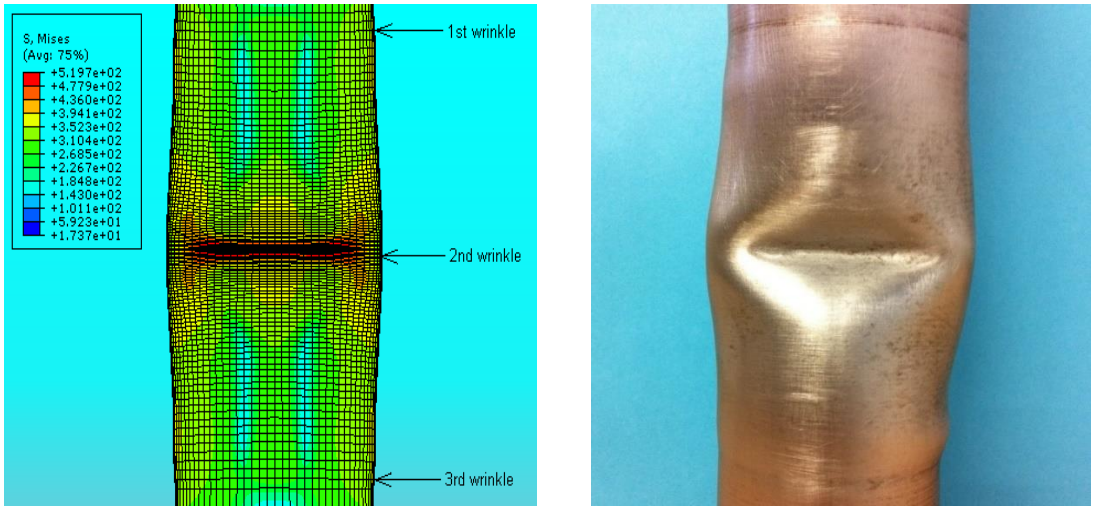

Figure 4.7 Deformed shapes of a typical indented pipe subjected to monotonic axial load at specific axial strain values (left) the numerical simulation results at 4% strain; (right) experiment at 3.8% strain

4.3.3 Simulation of the Cyclic Loading

Accurate simulation of the ratcheting behavior of specimens subjected to cyclic loadings requires the selection of a suitable isotropic/kinematic hardening model and an evaluation of the associated parameters. For this phase of the simulation, the values of the required parameters were obtained through testing coupons of the same steel alloy used in the experiments. The same loading regime used in the experiments (i.e., the same initial axial non-linear strains, stress cycle amplitude and mean stress), was adopted in the numerical model. It should be noted that in simulating the response of the material to cyclic load, the failure cycle is assumed to be the cycle at which an element experiences a critical equivalent plastic strain of 3.7%.

Results of the third and final FE model's verification is presented in Figure 4.7 and Table 4.4. The numerical predictions and experimental results for a dented specimen subjected to axial cyclic loading are shown in Figure 4.7. The figure presents the variation

of axial strain against the mean axial stress over the middle section of the pipe. The cyclic load was initiated at an initial gross axial strain of 2%. The numerical and experimental results for dented pipes under different cyclic loadings are also summarized in Table 4.4.

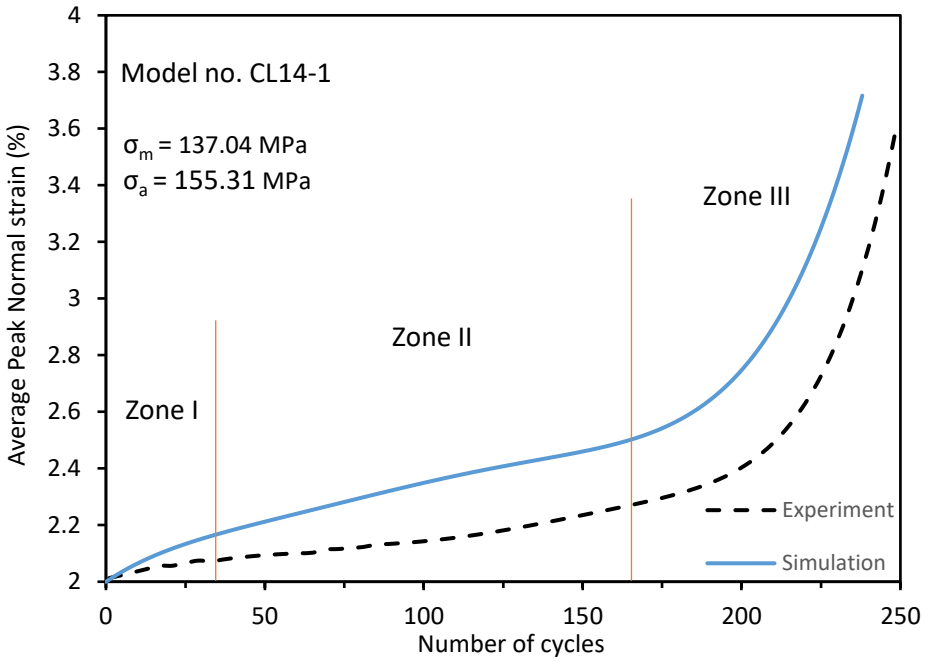

Figure 4.8 Plot of the average peak axial strain versus number of cycles

In Figure 4.8, three subdivisions can be noted for the ratcheting behavior of the dented pipe. In the first zone, the peak axial strain follows a non-linear decelerating trend (zone I) and then shows a nearly linear response (zone II). At the final stage, the ratcheting strain path again changes to be non-linear, following an exponential path (zone III). These three zones are reported throughout the literature as being the three subdivisions of territory ratcheting behavior (Zhang, 2005).

Table 4.4

Ratcheting strain data for intact tubes under cyclic loading

Model no.	Number of loading cycles		Initial axial strain	Peak strain before failure	
	Simulation	Experiment		Simulation	Experiment
CL12-2	552	542	2%	3.58	3.52
CL14-1	226	251	2%	3.67	3.62

In comparing the results shown in Figure 4.8 with the results of the available studies on the ratcheting response of intact pipes under pure axial loading (Jiao and Kyriakides, 2009), one can see that the main difference lies within the transition region from zone-II to zone-III. The curves' slopes are very similar until the end of stage-II. However, a dented pipe shows greater acceleration in ratcheting within the third stage. One reason for this phenomenon is the formation of a so-called "hinge" around the dent when the ratcheting path is approaching failure. The more cycles applied to the pipe, the more the semi-wrinkle around the dent works as a hinge, and the more rapidly the average strain grows.

At this juncture, it should also be noted that the available discrepancy between the experimental and actual results seen in Figure 4.7 is believed to be associated with the followings:

- Discrepancy in simulation of the actual restrains.
- The imposed limitation on selecting fewer layers of elements through the thickness of the pipe in the FE model.
- Untraceable misalignments of the experimental dents.
- The actual variation in pipe thickness along the test gauge of the pipe, which could not be incorporated in the simulation.

To elaborate on the role of the first factor, it should be noted that although the pipe is perceived to be simply supported, the supports (i.e., the Ringfeders) apply a state of restrain that is somewhat complex for actual and exact modeling. The simulation results are extremely sensitive to the way the restraints are implemented in the FE models. This becomes even more critical in the case of slender components undergoing an axial impact event (i.e., a pulse-buckling event). It suffices to state that if one applies a simply supported condition to the nodes forming the end of the pipes consider in this study, one would then obtain a discrepancy with much larger value than the one seen in Figure 4.7. On the other hand, the application of an appropriate contact algorithm in modeling the restraints provided by the Ringfeders, one could further improve the accuracy of the simulation result, but in the expense of extremely length run-times. Similar argument can be made for selecting more number of layers through the pipes thickness in order to obtain more accurate results. Since the main objective of the numerical investigation is to gain a better understanding of the influence of the parameters that affect the ratcheting response of dented pipes, it was concluded that the selected mesh and modeling technique could produce results with accurate results.

4.4 Parametric Studies

The numerical model, as reported in the previous section, provided acceptable simulations on the response of steel pipes under indentation, monotonic and cyclic axial loads. The model was subsequently used for a parametric study on the behavior of the dented pipes. The geometrical and material properties for the parametric study remained the same to sample No. CL14-1. Effects of the following parameters were examined:

- Indentation depth
- Cyclic loading regime
- Cyclic mean stress and stress amplitude
- Hardening model parameters

The utilized model in the following sessions underwent a certain indentation depth, after which it was subjected to an initial axial strain, and finally a cyclic load was applied.

4.4.1 Influence of Indentation Depth

In this section, the effect of dent depth on the ratcheting response of pipes was investigated. For this, four initial dent depths were applied to steel pipes preceded by initial axial monotonic compression to attain an initial axial strain of $\bar{\varepsilon}_{x,initial} \approx 2\%$. The models were then subjected to cyclic loads with $\sigma_m = 137.04$ MPa and $\sigma_a = 155.31$ MPa.

Figure 4.9 depicts the effects of indentation depth on a pipe's tertiary ratcheting response with respect to the zones depicted in Figure 4.8. The trend exhibits a similar trend for Zone-I ratcheting for all indentation depth ratios. However, the increasing indentation depth ratio had two effects on the linear part (or Zone-II) of ratcheting response: (i) the slope of zone II increased, and (ii) it took fewer number of cycles to reach the third stage of ratcheting. Comparatively, the indentation depth has a more profound effect on zone-III; in other words, the slope of this region significantly increases, and its length elongated as the indentation depth ratio increases.

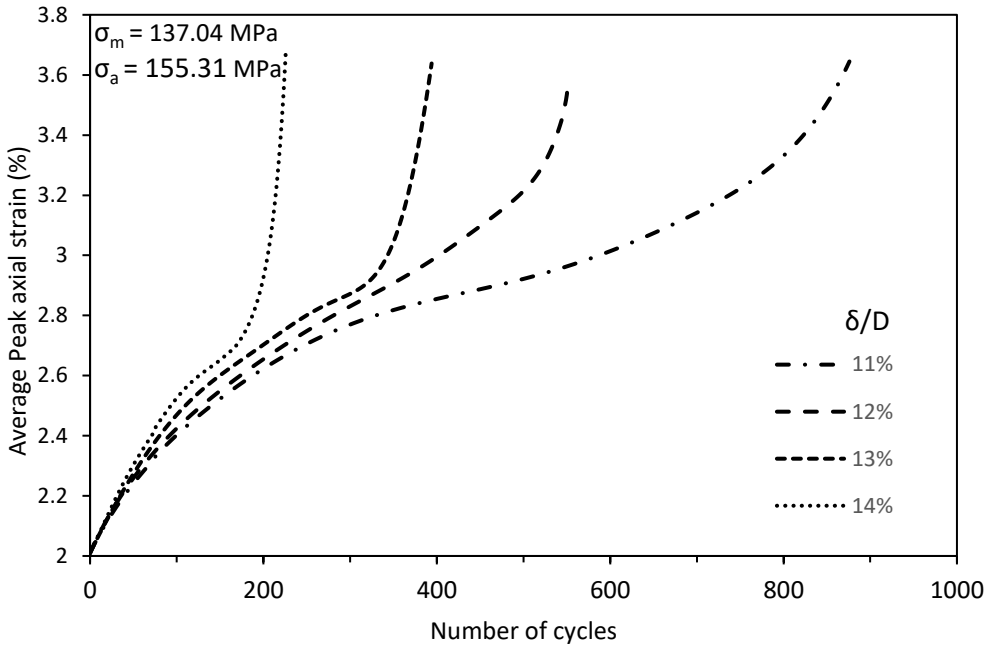

Figure 4.9 Effect of indentation depth on ratcheting response of dented pipes

In summary, as can be seen in Figure 4.9, increasing the indentation depth ratio from 11% to 14% decreases the number of cycles from 867 to 226.

4.4.2 Influence of the Cyclic Load Regime

In this part of the parametric study, the effect of the cyclic load regime on the ratcheting behavior of 12% dented pipes was investigated. The three studied load regimes were: i) compression-compression, ii) compression-zero, and iii) compression-tension. To better study the effect of each load regime, the peak compressive stress in all models was kept constant, slightly above the material's yield strength (i.e., at 296 MPa). Table 4.5 shows the applied stresses and the number of cycles to failure in the models.

Table 4.5

Cyclic load regime effect for specimen CL12

Loading regime	Mean stress (MPa)	Stress amplitude (MPa)	Maximum stress (MPa)	Number of cycles to failure
Compression-compression I	155.31	140.69	296	258
Compression-compression II	151.65	144.35	296	190
Compression-zero	148	148	296	148
Compression-tension II	144.35	151.65	296	122
Compression-tension I	140.69	155.31	296	102

Figure 4.10 depicts the average peak axial strains against the number of cycles. As can be seen, the load regime has substantially shortened the length of the linear trajectory and increased the slope of zone III of the pipe's tertiary ratcheting response by changing from compression-tension to compression-zero and then to compression-compression conditions.

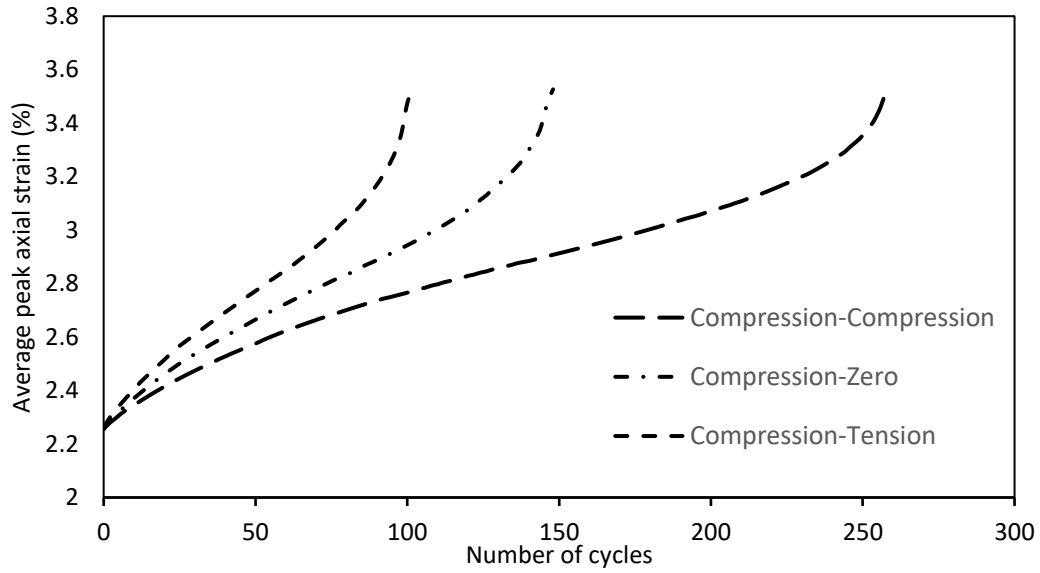

Figure 4.10 Effect of loading regime on ratcheting response of dented pipes

4.4.3 Influence of the Mean Stress and Stress Amplitude

To investigate the effect of axial mean stress and stress amplitude on the ratcheting response dented pipes, a total of five scenarios is investigated. All the models were initially indented up to 12% the pipe's outer diameter. Then, they were subjected to monotonic axial compression to attain an initial axial strain of $\bar{\varepsilon}_{x,initial} \approx 2\%$. To study the stress amplitude effect, the subsequent cyclic axial loads oscillated around a constant mean value for models No. 2 and 3. Whereas, the stress amplitude remained constant and the mean stress was changed to investigate the mean stress amplitude in models No. 4 and 5.

Table 4.6 provides a summary of the applied stresses and results. The number of cycles to failure decrease considerably by increasing the axial mean stress and stress amplitude. Another observation that can be made from this table is the greater impact of stress amplitude over mean stress. Comparison of scenarios 2 and 4 or 3 and 5 shows that when the maximum stress is kept constant, the pipe subjected to higher stress amplitude fails sooner than one under higher mean stress. The maximum stress for scenarios 2 and 4 is 294.17 MPa. As stated earlier, due to the higher stress amplitude, pipe of scenario 4 failed after 404 cycles, whereas the number of cycles to failure for scenario 2 was 508.

Table 4.6

Influence of the cyclic axial mean stress and stress amplitude, specimen CL12

	Model no.	Mean stress (MPa)	Stress amplitude (MPa)	Maximum stress (MPa)	Number of cycles to failure
	1	137.04	155.31	292.35	552
Stress amplitude effect	2	137.04	157.13	294.17	404
	3	137.04	158.96	296	86
Mean stress effect	4	138.86	155.31	294.17	508
	5	140.69	155.31	296	102

4.4.4 Influence of the Hardening Model Parameters

To evaluate the sensitivity of the numerical models to the material hardening rule, the effects of hardening parameters were investigated for a pipe with a 14% indentation depth. Nine models of indented pipes were considered. The applied mean stress and stress amplitude of 137.04 MPa and 155.31 MPa, respectively, formed the applied compression-tension load regime on the models. In models 2 to 9, the kinematic hardening parameters, C and Y, as well as the isotropic hardening parameters, Q and b, varied by approximately 3% with respect to those in model 1. The effects of variation of these parameters on the number of cycles to failure and maximum peak strain are given in Table 4.7. The results show that the ratcheting response is extremely sensitive to small variations of C, Y, and Q. Increasing the value of these parameters by 3% pushed the number of cycles to failure

beyond 1,000 cycles. Furthermore, decreasing the values of these three parameters did not change the number of cycles to failure markedly.

Table 4.7.

Effect of different material hardening parameters, specimen CL14-1

Model no.	Mean Stress (MPa)	Stress amplitude (MPa)	C (MPa)	Y	Q (MPa)	b	Number of cycles to failure	Max peak strain (%)
1	137.04	155.31	1544	10	85	16.8	226	3.67
2			1544	9.7	85	16.8	310	3.68
3			1544	10.3	85	16.8	226	3.62
4			1498	10	85	16.8	84	3.50
5			1590	10	85	16.8	>1000	3.14
6			1544	10	82.5	16.8	72	3.48
7			1544	10	87.5	16.8	>1000	3.57
8			1544	10	85	16.3	106	3.54
9			1544	10	85	17.3	>1000	3.53

Decreasing the values of C, Y, and Q by the same amount lowered the number of cycles to failure to 84, 72 and 106, respectively. On the other hand, the results show that the ratcheting response is less sensitive to changes in parameter b. With a variation of around ±3% in the value of b, the number of cycles to failure changed from 226 (model no. 1) to a maximum of 310 (model no. 2) and remain the same 226 cycles, but with a lower peak strain in model no. 3.

4.5 Concluding Remarks

In this chapter, the low cycle fatigue response of dented pipes undergoing monotonic and cyclic axial loads was numerically simulated. A combined non-linear isotropic/kinematic hardening material model was utilized to capture the cyclic response of the dented pipes. Moreover, the results were compared with the experimental tests data carried in the previous chapter. The experimental and numerical results showed a reasonable degree of agreement. The effects of loading conditions and hardening model parameters were also investigated. The following contribution and observations were obtained from this phase of the study investigation:

(i) The pipe indentation, monotonic and cyclic loading were simulated using solid finite element models. Similar to the experiment, it was observed that the indentation depth significantly shortened the ratcheting life-cycles of dented pipes compared to their life-cycles observed under monotonic loading condition.

(ii) It was shown that the ratcheting response of dented pipes was governed by the maximum stress, stress amplitude and mean stress. The results reported in Table 4.6 indicated that the ratcheting response of the pipes was mainly controlled by the magnitude of the maximum applied stress, i.e. $\sigma_m + \sigma_a$, in each cycle. However, by maintaining the same maximum stress, higher stress amplitude contributed to the ratcheting response more than the mean stress. This agrees with the empirical findings of the previous chapter which addressed the axial ratcheting behavior of dented pipes.

(iii) It was shown that necessary requirements for success of the model are correct modeling of material hardening parameters. The applied stress, σ_{max}, caused the pipe to fail after a certain number of cycles for the calibrated hardening parameters used in the material model. However, it was observed that a minor change in the value of each of the variables resulted in a noticeable change in the relative difference between the maximum applied stress, $\sigma_{x,max}$, and the ultimate stress used in defining the material model; this, in turn, affected the ratcheting response in a dramatic fashion. It was concluded that the simulation of the ratcheting response of dented pipes was extremely sensitive to the parameters used to define the non-linear isotropic/kinematic hardening material parameters. Thus, choosing accurate values for these parameters is essential for obtaining a proper simulation of the strain ratcheting response of dented pipes.

Chapter 5

Life Estimation of Dented Pipes undergoing Low Cycles of Large Reverse Bending Moments

5.1 Summary

As noted, the response of dented pipes undergoing pure cyclic axial loads was investigated experimentally and numerically as presented in chapters 3 and 4, respectively. In this part of the thesis, the attention is shifted towards the influence of pure cyclic bending loads on the flexural rigidity of the dented pipes.

Bending of pipes leads to ovalization of the pipe cross-section (change of the outside diameter/original outside diameter, $\Delta D_o/D_o$). Reverse bending and subsequent repeated cyclic bending may cause a gradual growth of ovalization. The increasing ovalization causes a progressive reduction in the bending rigidity of the pipe. In the presence of a dent, the final stage of local instability of the pipe cross-section is accompanied by initiation of fatigue cracks. Under cyclic loads, the cycle at which fatigue cracks initiate is considered as the failure cycle.

In this phase of the study, the influence of dent depth in the flexural rigidity of pipes and evolution of ovalization under low cycles of curvature-controlled symmetric cyclic bending is investigated. Moreover, two empirical formulas are proposed to estimate the remaining in-service life of dented pipes. The first formula estimates the number of cycles until local instability of pipe's cross-section and consequently, initiation of fatigue cracks. The second equation predicts the variation of ovalization as a function of the applied loading cycles.

5.2 Experiment Layout and Procedures

The pipes are laterally indented using a spherical indenter to four initial dent depth-to-outer diameter ratios of 12.5%, 15%, 17.5% and 20%. The indenter was removed to form an unconstrained dent for the next phases of the experiment. The pipes were subsequently subjected to symmetric bending cycles under a curvature-controlled scheme until fatigue cracking was observed within the dented region.

5.3 Experimental Set-up

To carry out the quasi-static cyclic bending tests on the dented pipes, the specimens were first dented using a 10-mm diameter spherical indenter[1]. Each pipe was supported by a 114 mm x 60 mm flat steel plate during the denting procedure. A solid spherical indenter made of high-strength steel with a diameter of 10 mm, was used throughout.

Four different initial indentation depth ratios (δ/D_o) of 12.5%, 15%, 17.5%, and 20% were considered to study the effect of cyclic symmetric bending loads of different magnitudes. The rate of applied displacement used to create the dents was kept at 0.1 mm/min. The indenter was removed once the prescribed depth of dent was obtained. The final recorded (after rebound) depths of indentation of the pipes were 5.33%, 7.21%, 8.4%, and 10.03%.

The pipes were subsequently subjected to symmetric tension-compression bending cycles under a curvature-controlled scheme until fatigue cracking was observed within the dented region.

[1] To avoid any minor misalignment of a cylindrical indenter on pipe, as experienced in chapter 3, a spherical indenter is utilized in this phase.

A four-point bending fixture was used for conducting the experiments. The test set up, as shown in Figure 5.1, is composed of six main components, including a cross head, a lower section, roller bearings, extension limbs, an ovalization measurement device, and a digital inclinometer.

(a) Opening bending moment

(b) Closing bending moment

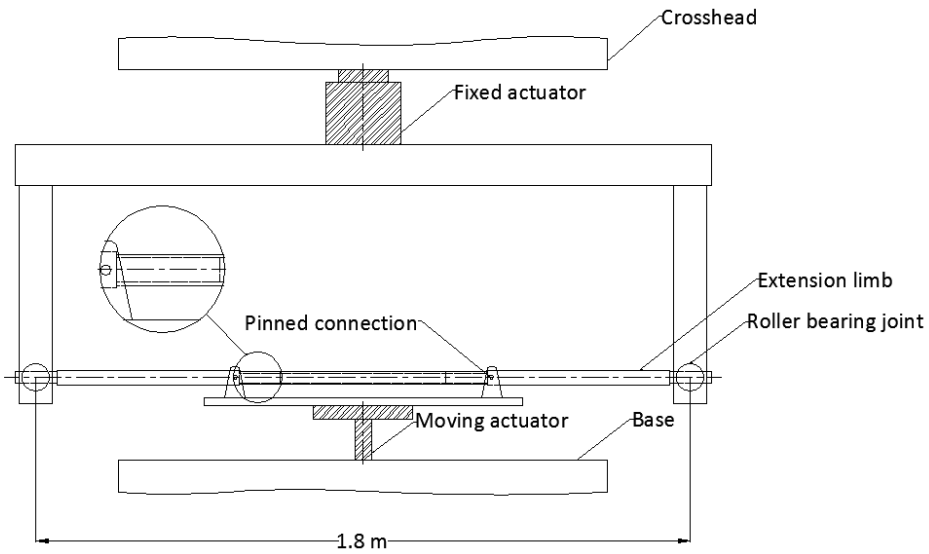

(c) Schematic design of the set up

Figure 5.1 Test set up for ovalization measurement under cyclic four-point bending load – the dent is located on the upper surface

In the arrangement shown in Figure 5.1, the test specimen, with the dent side up, is mounted within roller bearing supports through the extension limbs, within an Instron servo hydraulic testing machine model 8500+, equipped with digital controller. Within the Instron, the cross-head remains stationary, to which a 250 kN load cell is bolted on. The movement of the actuator in the lower portion of the machine applies curvature onto the specimens. The actual magnitudes of the curvature, and bending moment are then extrapolated (Chang and Pan, 2009).

The moment, curvature, and ovalization data were normalized with respect to $M_0 (= \sigma_o D_o{}^2 t)$, $\kappa_o (= t/D_o{}^2)$ and D_o, respectively, where σ_o is the 0.2% strain offset yield stress.

Each specimen is hinged to two stiff tubular rods (the extension limbs), with surface hardened steel pins. The length and the diameter of these extensions are 25" (635 mm) and 1.25" (31.75 mm), respectively. Furthermore, the material is high-strength steel, with the measured yield strength of 735 MPa. The two ends of the extension limbs are connected to the crosshead vertical beam through the roller bearings, thus subjecting the specimen to a four-point bending loading scheme. Once the lower actuator moves, the reaction forces are developed at the limbs' ends, thereby subjecting the specimen to a pure bending state. It should be noted that with this arrangement, the localized strains developed at the contact region between the limbs and the inner pipe wall would not be generating any local deformation in the pipe.

An ovalization measuring apparatus, similar to the one designed and reported by Kyriakides and Shaw (1987), was used to record the pipe's cross-section deformation. The device consists of an LVDT displacement transducer that is mounted on the dented cross-

section of the pipe, which monitors the change in the diameter of pipe's cross section during cyclic loading.

The curvature measuring device is an inclinometer (TURCK Co., B2N45H-Q20L60-2LU3-H1151). The inclinometer is bonded to the top end surface of the pipe (see Figure 5.2), to monitor the tilt angle during loading.

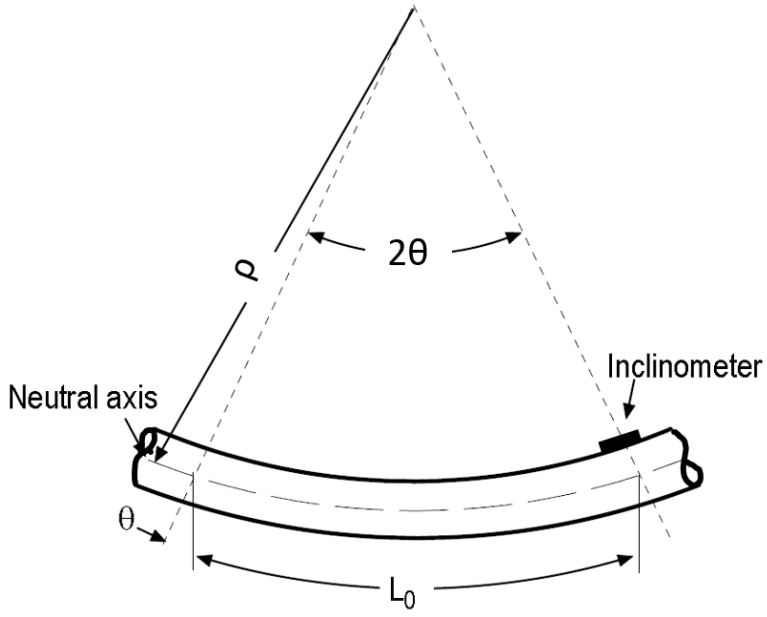

Figure 5.2 Longitudinal deformation developed between the two ends of the pipe under pure bending

In Figure 5.2, the change in angle detected by the inclinometer is denoted as θ. The value of L_o is determined by the following relationship:

$$L_0 = 2\rho\theta \tag{5.1}$$

where ρ is the radius of curvature. The curvature of the tube, κ_c, is then evaluated by the following equation.

$$\kappa_c = \frac{1}{\rho} = \frac{2\theta}{L_0} \tag{5.2}$$

The applied loadings were computer controlled, and the sensors were also controlled by a computer operated data-acquisition system. Therefore, the output signals from the ovalization measuring device, the inclinometer and the load cell are recorded simultaneously.

Each test specimen is 25" (635 mm) long with nominal diameter and thickness of 1.25" (31.75 mm) and 0.035" (0.889 mm), respectively. Material properties of TP316L stainless steel are provided in Table 5.1.

Table 5.1
Material properties obtained by standard tensile tests

Material type	Yield stress (MPa)	Ultimate stress (MPa)	Elongation
TP316L	201	558	38%

5.4 Experimental Results and Discussion

Due to the presence of the dent in the specimens, the application of a cycle of reverse symmetric bending to the pipe would not develop the same magnitude of ovalization under the compressive and tensile loading cycles. Typical variation in the cross-sectional ovalization as a function of the applied loading cycles for a pipe with δ/D_o= 20%, subjected to curvature controlled loading of κ_c/κ_o = 0.3088 is illustrated in Figure 5.3. The cross-section ovalization was defined as $\Delta D_0 - \Delta D_{o,initial}/D_o$, where D_o is the outside diameter, $\Delta D_{o,initial}$ is the change of D_o upon introduction of the indentation (before application of bending load), and ΔD_0 is the change of D_o during cyclic bending. Per the

illustrated results, the application of the so-called closing moment, by which the dented region becomes subjected to a compressive loading state, generated a larger ovalization growth than that developed under the opening moment (tensile loading cycle). Moreover, as the dented region became subjected to more tensile (opening) loading cycles, after a certain number of cycles, a crack developed in the dented region. The initiation and propagation of the resulting cracks in the dented region of the pipe were found to cause fatigue failure, augmented by the progressive accumulation of the cross-section ovalization during the cyclic loading.

Thus, the corresponding cycle at which the size of the ovalization region started to decrease in the opening moment was referred to as the fatigue failure cycle (N_f).

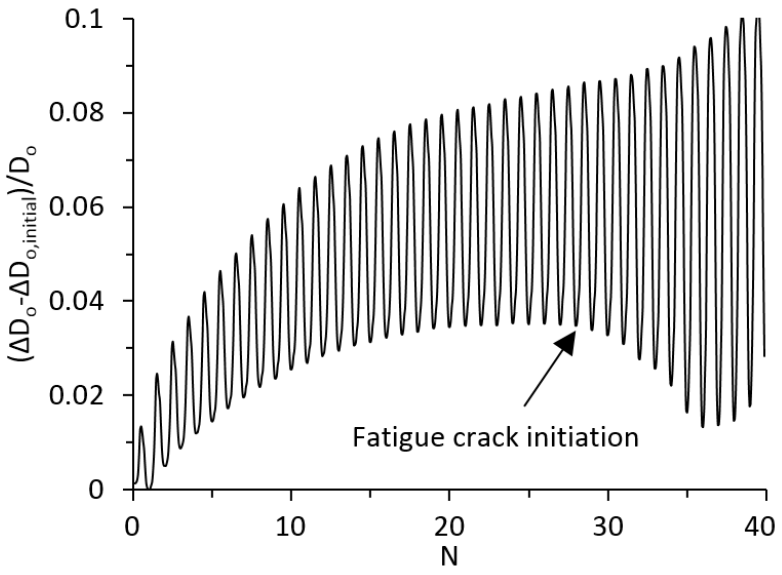

Figure 5.3 Variations in cross-section ovalization versus number of cycles of a pipe with $\delta/D_o = 20\%$ subjected to curvature controlled (κ_c/κ_o= 0.3088)

Figure 5.4 presents the experimental results in the form of moment–curvature hysteresis for TP316L stainless steel pipes with δ/D_o ratios of 12.5%, 15%, 17.5%, and

20%, respectively. As can be seen, the moment-curvature loops for all δ/D_o ratios became gradually steady after a few cycles. This would indicate that the TP316L stainless steel pipes indeed hardened upon the application of the symmetrical curvature cyclic loadings. It can, therefore, be expected that under such a loading condition, a relatively lower magnitude of bending moment would cause deformation of the pipe into the desired curvature, since a larger plastically deformed region would be developed in pipes with greater δ/D_o ratios. However, the process also resulted in an unnoticeable decrease in the recorded bending moments for pipes with larger δ/D_o ratios. In other words, when the width of the loops decreased (which occurs at higher δ/D_o ratios), the effect of δ/D_o ratio on the moment-curvature curves became greater.

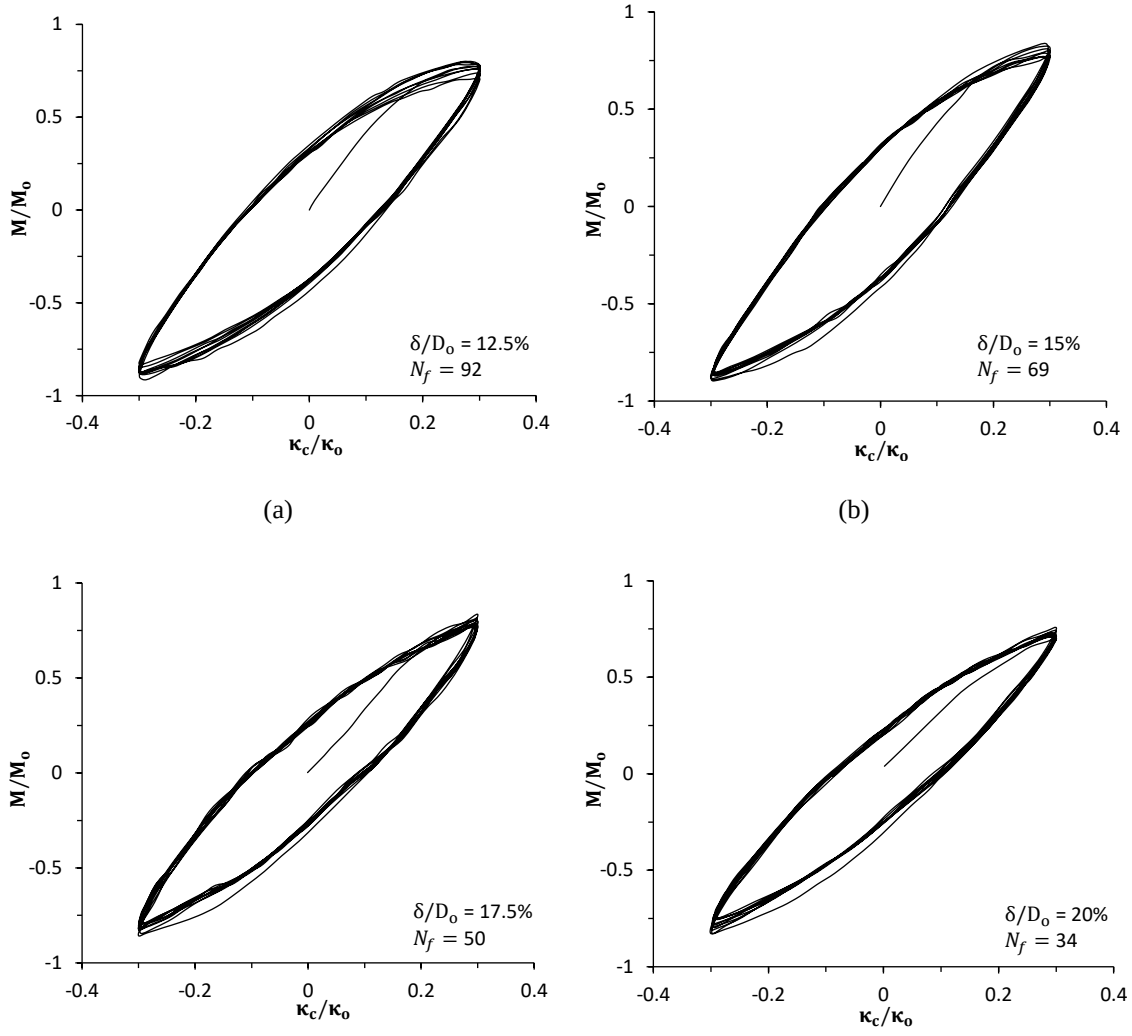

Figure 5.4 Moment-curvature hystereses of the curvature controlled κ_c/κ_o = 0.3005) experiments for pipes with δ/D_o of (a) 12.5%, (b) 15%, (c) 17.5%, and (d) 20%

The corresponding ovalization-curvature results of the above-mentioned pipes are shown in Figure 5.5. As can be seen, as the pipes underwent cyclic bending, their cross-section experienced a gradual accumulation of ovalization, which was the result of inelastic deformation of their dented region. Upon the application of the first loading cycle, the ovalization in each pipe attained its maximum value when the pipe attained its maximum curvature. Then, upon unloading to zero curvature, the pipe accumulated permanent

deformation in its cross-section. The ovalization subsequently further increased as the pipe underwent the reverse bending that forced the pipe to attain its minimum curvature. Cycle by cycle, the ovalization continued evolving to a point that it reached a certain critical value and a fatigue crack developed in the dented region. It was also observed that the ovalization grew in a faster rate when the applied δ/D_o ratio was higher.

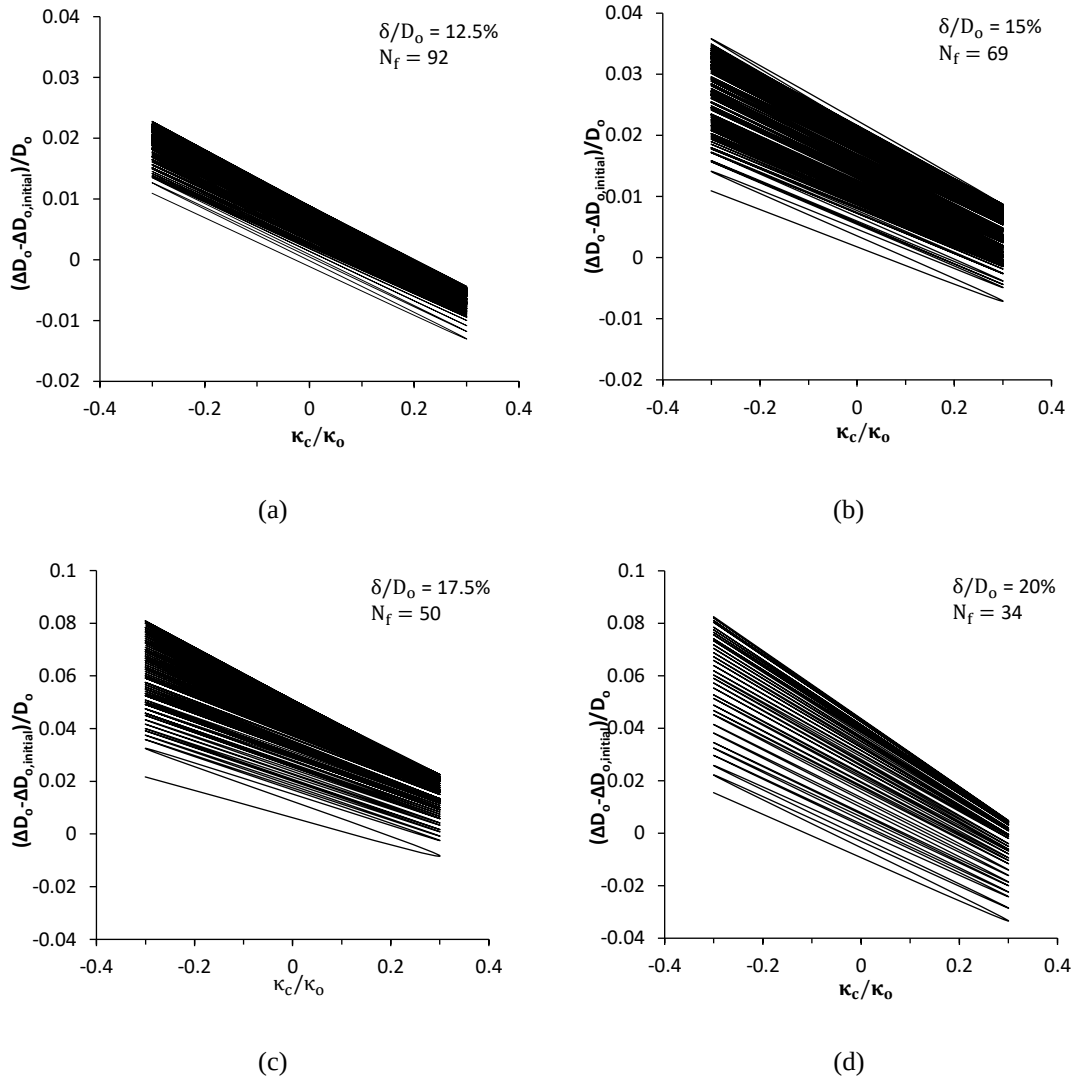

Figure 5.5 Variation in cross-section ovalization of pipes subjected to curvature controlled (κ_c/κ_o = 0.3005) loading scenario with δ/D_o of (a) 12.5%, (b) 15%, (c) 17.5%, and (d) 20%

Figure 5.6 illustrates the variation in the average ovalization per cycle as a function of the number of loading cycles (N), for pipes tested at a constant curvature. As seen from the above figures, the number of cycles causing fatigue failure became significantly low as the cross-section ovalization increases rapidly in pipes with larger dent ratios. It can also be stated that a higher curvature values caused greater ovalization growth rates (i.e., greater $\Delta D_0 - \Delta D_{0,initial}/D_0$).

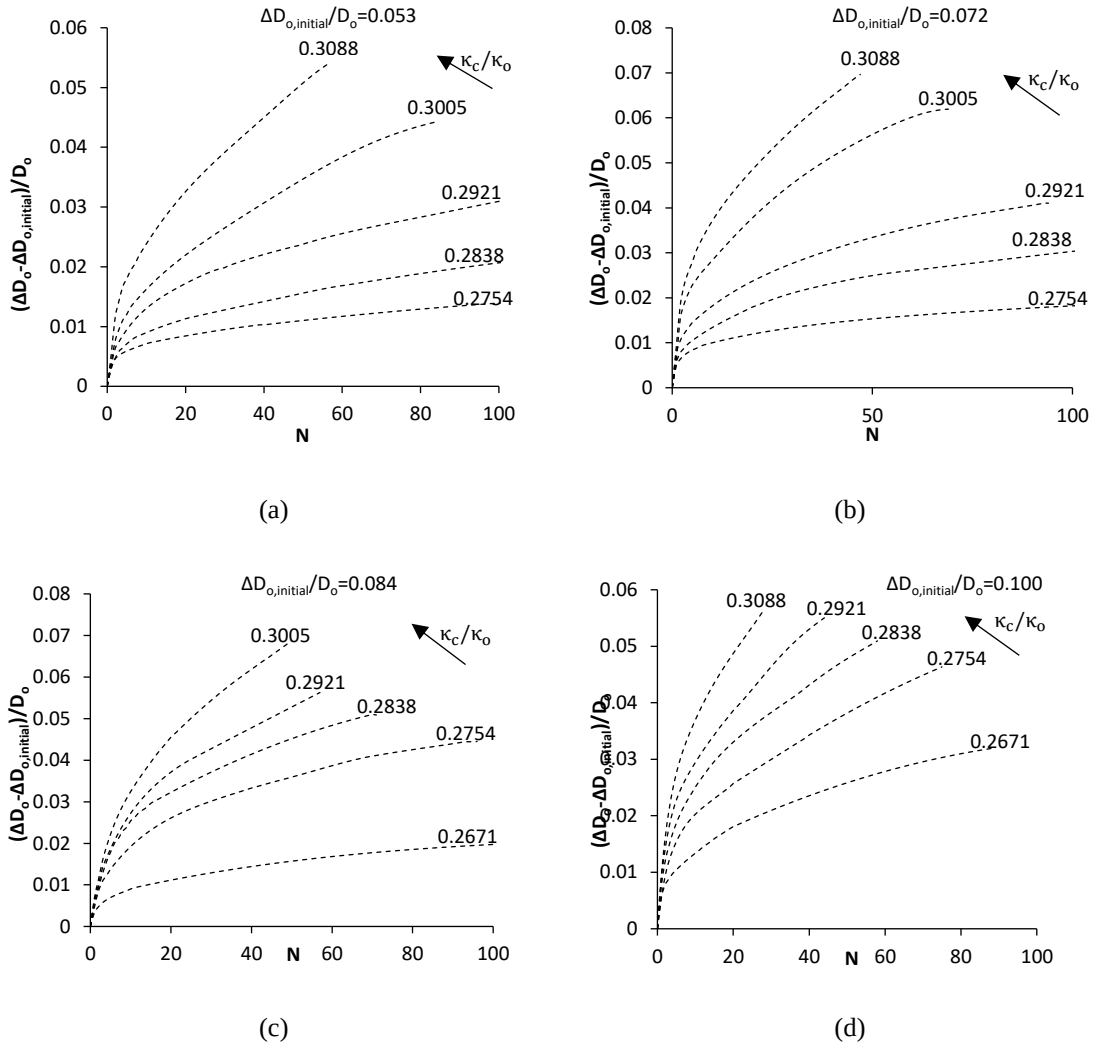

Figure 5.6 Plot of cross-section ovalization, $\Delta D_0 - \Delta D_{0,initial}/D_0$, versus number of loading cycles, N, for pipes with δ/D_o of (a) 12.5%, (b) 15%, (c) 17.5%, and (d) 20%

It should be noted that the onset of crack initiation in each pipe's dented region occurred at the cycle number that corresponds to the end of each curve shown in Figure 5.6. Moreover, the graphs show two relatively distinct response stages (the initial and secondary stages). In the initial stage, once cyclic bending is initiated, the magnitude of ovalization increases; it is, therefore, clear that a great portion of the ovalization occurs during the initial stage. The ovalization growth enters the secondary stage when the rate of ovalization gradually decreases; nevertheless, the ovalization increases steadily as a function of the applied loading cycles within this stage, finalized by the fatigue failure of the pipe.

5.5 Curvature versus Number of Cycles to Failure

Figure 5.7 illustrates variation in the curvature as a function of number of cycle to failure, N_f, for pipes with δ/D_o ratios of 12.5%, 15%, 17.5%, and 20%. As seen, at a given curvature, as the value of δ/D_o ratio increases, the value of ovalization increases as well, and the pipe fails at lower number of cycles. Similar trend was observed when 6061-T6 aluminum and 1018 steel pipes were tested by Kiriakides and Shaw (1987), and also by Lee et al. (2001), when they examined SUS 304 stainless steel pipes.

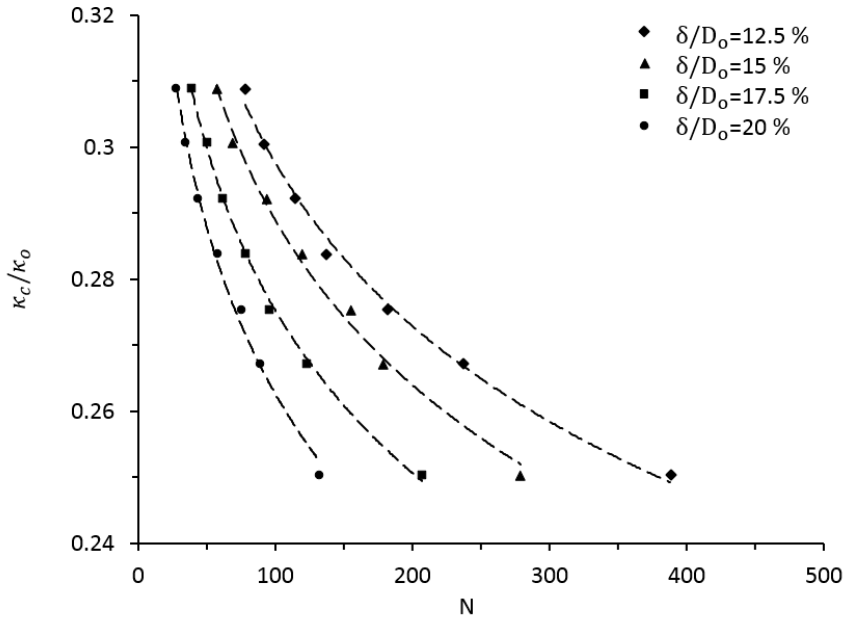

Figure 5.7 Variation of cross-section ovalization versus curvature for pipes tested under curvature controlled (κ_c/κ_o = 0.3005) loading

Kyriakides and Shaw (1987) proposed an empirical equation, relating κ_c/κ_o and N_f with the following mathematical form:

$$K_c/K_o = A(N_b)^{-\alpha} \tag{5.3}$$

where A and α are material related parameters. The parameter A corresponds to the controlled cyclic curvature magnitude at the first bending cycle (i.e., $N_b = 1$), and α is the slope of the line constructed by plotting the data illustrated in Figure 5.7 in a log-log scale. Equation (5.3) has been widely used for simulating curvature-controlled cyclic bending tests.

The log-log plot of the normalized curvature versus number of cycle to failure, N_f, of the data presented in Figure 5.7 is illustrated in Figure 5.8. The dashed lines are constructed by the least-square fitting of the data. As can be seen, the data corresponding to each tested

δ/D_o ratio pipe follows a linear trend. The values of parameter A for the pipes considered in this investigation (i.e., with δ/D_o of 12.5%, 15%, 17.5%, and 20%) were determined using Equation (5.3), as 0.5370, 0.5223, 0.4937, and 0.4784, respectively. The four dashed lines are essentially parallel to one another. The magnitude of α is evaluated to be 0.1287.

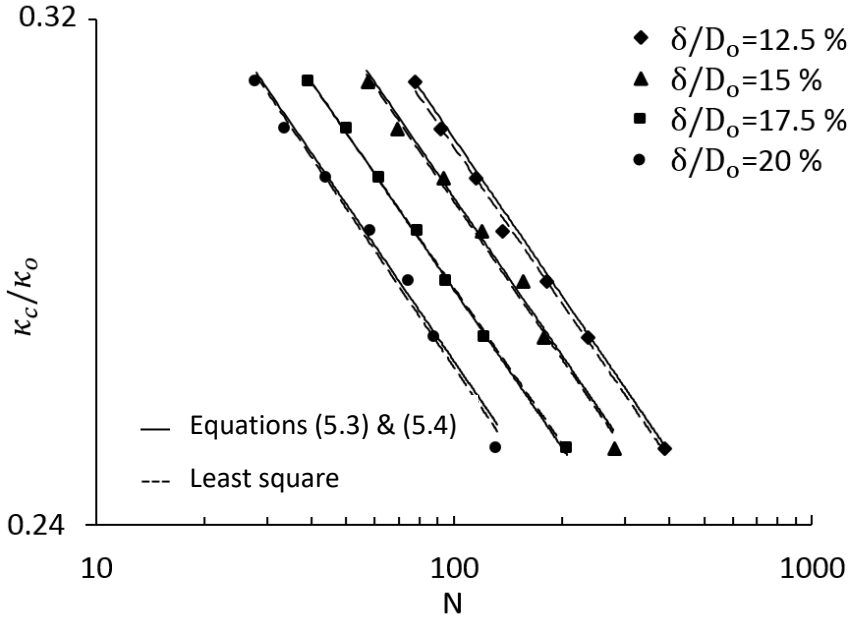

Figure 5.8 Variation of cross-section ovalization as a function of number of applied loading cycles for pipes tested under curvature controlled (κ_c/κ_o= 0.3005) loading.

Figure 5.9 shows the relationship between the material parameter A and δ/D_o ratio on a log-log scale. As can be seen, a least square fit straight line can capture the trend reasonably well. Based on the above results, the following equation was proposed, which enables one to account for the influence of δ/D_o ratio on the collapse of the dented pipes:

$$A = A_o(\delta/D_o)^{-\gamma} \tag{5.4}$$

where A_o and γ are material parameters. For the material considered in this study, the magnitude of A_o and γ are found to be 0.3107 and 0.1896, respectively. As can be seen,

the variation follows a linear trend, thus, the relationship can be represented by a linear least square fit, as illustrated. The final shape of the tested pipes are illustrated in Figure 5.10.

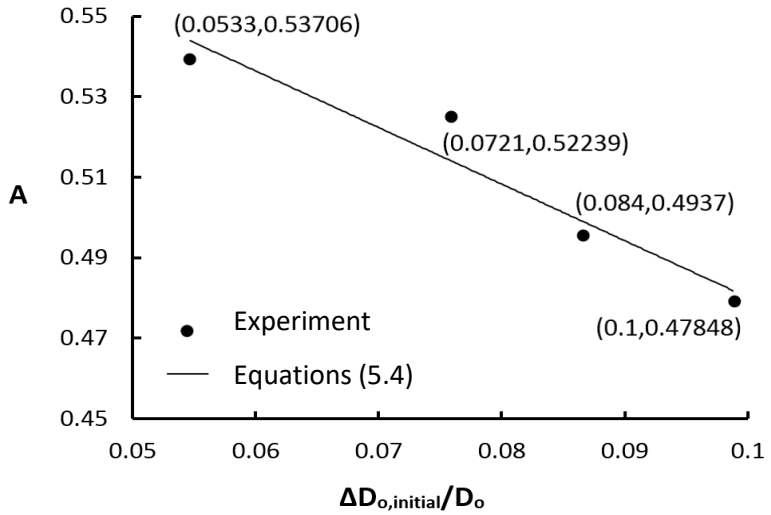

Figure 5.9 Variation of material parameter A as a function of (δ/D_o) ratio

Figure 5.10 Final shapes of the pipes tested under symmetric cyclic bending loads

5.6 Ovalization versus Number of Cycles to Failure

The variation of cross-section ovalization as a function of the applied loading cycles illustrated in Figure 5.6, closely resembles the creep response (strain–time curve) of a metallic alloy when subject to uniaxial loading (Chang and Pan, 2009).

At this juncture, therefore, the applicability of a modified version of the Bailey–Norton law, for characterization of the ovalization response in dented pipes, is considered.

The Bailey–Norton law, which was originally developed for characterizing uniaxial creep in metals is mathematically represented as follows:

$$\varepsilon_c = B(\sigma)^m(t)^n \tag{5.5}$$

Here, ε_c is the creep strain, σ is the hold uniaxial creep stress, t is the Newtonian time, and B, m and n are material related constants. Following a similar structure, the following mathematical relationship is proposed by the author to relate the ovalization to the rate of curvature and number of loading cycles by:

$$\Delta D_0 - \Delta D_{0,\text{initial}}/D_0 = B(\kappa_c/\kappa_o)^m N^n \tag{5.6}$$

where m and n are material constants and B is a function of the δ/D_o ratio. Following the above relationship, the magnitudes of m and n are determined to be 13.066 and 0.3753, respectively, for the steel alloy used in this study. Based on the experimental data, the values of parameter B are 5,270, 74,225, 111,528, and 151,783 for the pipes with (δ/D_o) ratios of 12.5%, 15%, 17.5%, and 20%, respectively. Furthermore, the following relationship is also proposed for establishing the value of parameter B.

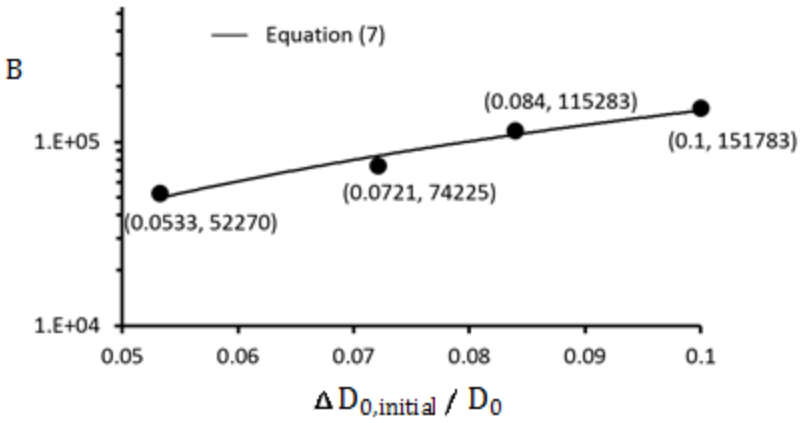

Figure 5.11 Variation of the material parameter B as a function of (δ/D_o)

$$B = B_o(\delta/D_o)^{-\gamma} \tag{5.7}$$

where B_o and γ are material constants. Based on the results presented in Figure 5.11, the magnitudes of B_o and γ are evaluated to be $8.1x10^6$ and 1.738, respectively. The comparison of the results obtained using Equation (5.6) and the experimental data are shown in Figure 5.12. As can be seen, the predicted results corroborate with the experimental data quite well, thereby validating the integrity of the proposed equation.

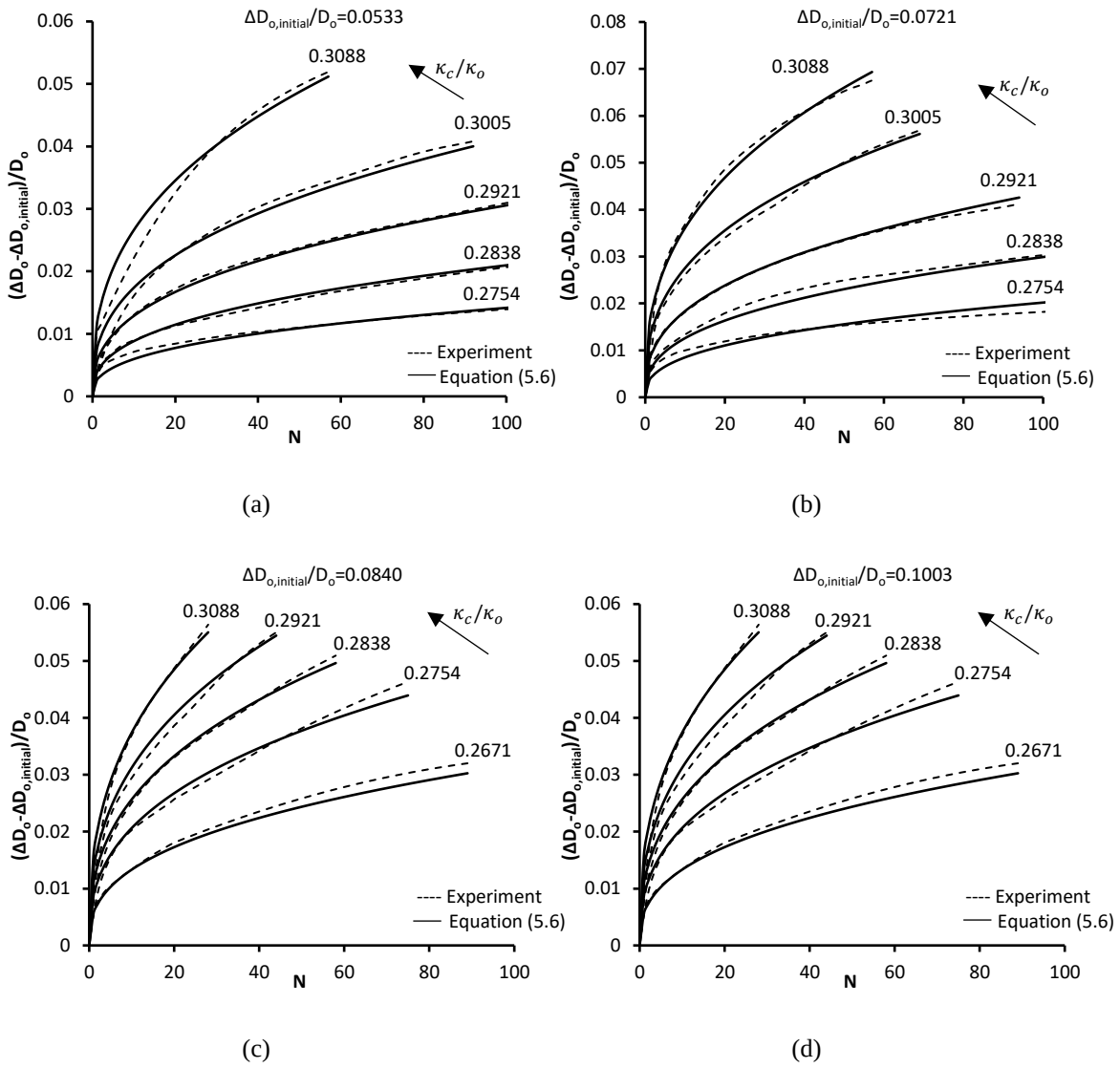

Figure 5.12 Comparison of the results obtained using the proposed equation and the experimental data for pipes with δ/D_o of (a) 12.5%, (b) 15%, (c) 17.5%, and (d) 20%

5.7 Concluding Remarks

Evaluation of the safe in-service life of a dented pipeline is an important and a critical task in a fitness-for-purpose assessment process. However, to the best of author' knowledge, no study has investigated the effect of cyclic bending load on the life-cycle of metallic dented pipes. The work presented in this chapter attempted to address the void in the literature

today. In doing so, the response of dented pipes made of TP316L stainless steel, in the form of growth in their cross-section ovalization, as a result of applied symmetric cyclic loads, was investigated experimentally. The experimental results provided a better understanding of the resultant crack initiation response of dented pipes when subject to low frequency cyclic bending. It is believed that the results presented in this study could be used as a preliminary guideline for developing a comprehensive criterion that could be used for assessing the response of dented pipes made of different materials, subject to cyclic loadings. The following conclusions were drawn based on the findings of this study:

1. Behavior of dented pipes under an applied bending moment becomes significantly influenced by the location of a dent (i.e., whether the dent is on the compression side or tension side of the pipe. Such dented pipes respond in a stronger manner when the dent is located on the surface that undergoes a tensile loading.
2. The number of loading cycles causing failure of the dented pipes was found to be inversely proportional to the indentation depth.
3. A linear trend could be observed when the graphs of pipe curvature versus the number of cycles causing failure were plotted on a log-log scale.
4. Observation of the change in the moment-curvature of the pipes as a function of the applied loading cycle revealed that such pipe exhibited a stiffer response as the number of cycles was increased. The response reached a steady state after a certain number of applied loading cycles.
5. An empirical relationship was developed for estimating the loading cycle corresponding to the onset of crack initiation in dented pipes. Comparison of

the results produced by the suggested equation and those obtained experimentally validated the accuracy of the proposed equation.

6. The variation in the pipes' cross-section ovalization followed a trend that could be described by the well-known Bailey–Norton model. The second proposed empirical equation was obtained by modifying the Baily-Norton's equation. This formula proved to be accurate in simulating the pipe's cross-section ovalization as a function of the applied loading cycles and curvature.

Chapter 6

Conclusion

6.1 Summary

In this thesis, the ratcheting and low cycle fatigue response of dented pipes undergoing quasi-static cyclic loads were investigated through a series of experiments conducted on small-scale pipe samples, and performing detailed nonlinear FE analysis. The investigation addressed the response, and in-service life estimation of dented pipes undergoing inelastic cycles of axial, and flexural loads. The research was carried out within three phases. The resulting collection forms a complimentary body of works, providing a better understanding of the response of dented pipes. The three-part investigation outlined in this thesis consisted of the following:

(i) Experimental investigation of strain-ratcheting response of dented pipes undergoing cyclic axial loading (outlined in Chapter 3).

(ii) Development and calibration of a robust FE framework for modeling the ratcheting response of dented pipes subjected to cyclic axial loading (outlined in Chapter 4). The chapter also outlined details of a parametric FE study, by which the influence of various parameters that affect the response of dented pipes was comprehensively examined.

(iii) Life cycle estimation of dented pipes undergoing low cycles of large reversing bending moments was outlined in Chapter 5. The chapter also introduced a practical empirical equation for estimating life-cycle of the pipes.

Parts (i) and (ii) complement one another in the sense that part (ii) provides an alternative robust and cost-effective FE approach for estimation of in-service life of dented pipes undergoing cyclic axial loading. The highlight of part (iii) is the development of an empirical equation by which practicing engineers can estimate the in-service life of dented pipes subjected to pure bending cyclic loads.

6.2 Conclusions

While the conclusions of each chapter have been given at the end of the respective chapter, only the most salient findings are outlined here:

- The contribution of dent depth in pipes subject to monotonic loading was observed to be insignificant up to the limit load, whereas it noticeably affected the failure load carrying capacity of the pipes. It was also observed that regardless of the nature of the applied loads, collapse of pipes loaded monotonically or cyclically would essentially occurs at the same average strain level. The experimental results revealed that larger dent depths shortened the linear portion of the respective strain versus the number of cycle curve and significantly affected the total number of cycles to failure; the number of cycles prior to collapse dramatically decreased by as much as 75% when the dent depth was increased by 2%.
- A FE model was developed as an alternative approach for estimation life cycle of dented pipes undergoing cyclic axial loading. The model was successfully calibrated by the results obtained from the experimental parts of the study. A set of parametric FE analyses was performed to investigate the influence of mean stress, stress amplitude, loading regime and hardening-related parameters. It was concluded that

the application of larger stress amplitudes (while maintaining the same maximum stress) contributed to pipes earlier failure in comparison to the condition when pipes were subjected to a higher mean stress. It was also observed that the combined non-linear kinematic/isotropic hardening model was extremely sensitive to the material parameters used in describing the model. It was therefore concluded that the lack of an established standardized procedure for establishing the parameters used in the model has limited the real-life applications of such computational approaches.

- An experimental framework was designed to investigate the ovalization growth of dented pipes undergoing quasi-static cyclic bending. Based on the results, two empirical formulas were developed and proposed to estimate the remaining in-service life of dented pipes. The first empirical formula predicts the number of loading cycles causing the local instability of a dented pipe's cross-section, which in turn would initiate a fatigue crack. The second empirical equation, derived based on modification of the Bailey–Norton creep relationship, can be used to establish the variation of cross-section ovalization as a function of the applied loading cycles.

6.3 Recommendations for Future Work

A stated, a comprehensive set of experimental and numerical investigations were carried to increase understanding of the performance of dented pipes subject to cyclic axial and bending loads. The objectives also included development of accurate and practical equations for estimating the life cycle of the dented pipes. While the goals of the study have been fulfilled, the following recommendations would complement the work presented herein, and will enhance understanding of the complex mechanisms associated with the performance of dented pipes subject to cyclic loads.

- The investigations undertaken in this thesis covered the influence of depth of a dent. It would be very useful to also investigate the influence of
    - shape of the dent (smooth or kinked)
    - size of the dent (i.e., width and length ratios)
    - whether the dent is on or near a girth weld
    - and whether the dent contains any other defects (a gouge or a crack).
- Due to the experimental limitations, the influence of internal pressure, which is considered as a primary load in pipelines, could not be included in the investigation. The next practical step would be enhancement of the experiments and FE model by including the internal pressure.
- The proposed empirical equations developed in this study presented interesting insights. The proposed equations are based on simple frameworks and require a fewer number of coefficients, thus are robust for use by practicing engineers. However, the limitations of the equations should be established by investigating the influence of various grades of steel and other materials.
- Less work-intensive (material properties intensive) hardening rule can be implemented in the numerical simulation (Ahmadzadeh, 2013).
- The established FE framework presented in Chapter 4 could simulated the pipes' performance satisfactorily. With further CPU power and parallel computation, it should be feasible to consider the influence of existence of a fatigue crack and its propagation (especially within the domain of the dent).

Bibliography

- Abdel-Karim, M. (2005). Shakedown of complex structures according to various hardening rules. *International Journal of Pressure Vessels and Piping*, *82*(6), 427-458.

- Abdel-Karim, M. (2005). Shakedown of complex structures according to various hardening rules. *International Journal of Pressure Vessels and Piping*, *82*(6), 427-458.

- Ahmadzadeh, G. R., & Varvani-Farahani, A. (2013). Ratcheting assessment of materials based on the modified Armstrong–Frederick hardening rule at various uniaxial stress levels. *Fatigue & Fracture of Engineering Materials & Structures*, 36(12), 1232-1245.

- Alexander, C. R. (1999). Review of experimental and analytical investigations of dented pipelines. *ASME publications-PVP*, 395, 197-210.

- Alexander, C. R., and Connelly, L. M. (1998). Analytical recreation of a dent profile considering varied soil, operating, and boundary conditions (No. CONF-980213-). American Society of Mechanical Engineers, New York, NY, USA.

- Alexander, C. R., and Kiefner, J. F. (1997). Effects of smooth and rock dents on liquid petroleum pipelines. In *1999 API Pipeline Conference*, Dallas, TX, USA.

- API. (2000). Recommended practice for fitness-for-service (API RP579). American Petroleum Institute: Washington, DC, USA.

- Armstrong, P. J., and Frederick, C. O. (1966). A mathematical representation of the multiaxial Bauschinger effect. Central Electricity Generating Board and Berkeley Nuclear Laboratories, Research and Development Department.

- ASME Boiler and Pressure Vessel Code (2007). Section VIII division I, appendix 2. American Society of Mechanical Engineers, New York, NY, USA.

- ASME. (2012). *Pipeline transportation systems for liquids and slurries* (B31.4). New York, United States: American Society of Mechanical Engineers.

- ASME. (2012). *Gas transmission and distribution piping system* (B31.8). New York, United States: American Society of Mechanical Engineers.

- Azadeh, M., and Taheri, F. (2016). On the response of dented stainless-steel pipes subject to cyclic bending moments and its prediction. *Thin-Walled Structures*, 99, 12-20.

- Azadeh, M., and Taheri, F. (2015). Computational simulation of ratcheting in dented pipes due to monotonic and cyclic axial loading. *The Journal of Strain Analysis for Engineering Design*, 50(3), 163-174.

- Azadeh, M., and Taheri, F. (2014). Ratcheting response of dented pipes under monotonic and cyclic axial loadings. *The Journal of Strain Analysis for Engineering Design*, 49(2), 122-132.

- Bari, S., and Hassan, T. (2002). An advancement in cyclic plasticity modeling for multiaxial ratcheting simulation. *International Journal of Plasticity*, 18(7), 873-894.

- Beller, M. et al. (1991). Stress concentrations in pipelines due to the presence of dents. *In proceedings of the 1st International Offshore and Polar Engineering Conference*. International Society of Offshore and Polar Engineers, Edinburgh, The United Kingdom.

- Błachut, J., and Iflefel, I. B. (2008). Experimental and numerical investigation of plain and gouged dents in steel pipes subjected to pressure and moment loading. *Journal of Pressure Vessel Technology*, 130(2), paper no. 021203, 1-9.

- Blanchard, J. P. et al. (2011). Ratcheting models for fusion component design. *Fusion Science and Technology*, 60(1), 313-317.

- Bood, R. et al. (1999). EPRG methods for assessing the tolerance and resistance of pipelines to external damage (Part2), *3RInternational*, 806-811.

- Bower, A. F., and Johnson, K. L. (1989). The influence of strain hardening on cumulative plastic deformation in rolling and sliding line contact. *Journal of the Mechanics and Physics of Solids*, 37(4), 471-493.

- Brooker D. C. (2004). Denting of pressurized pipeline under localized radial loading. *International Journal of Mechanical Science*, 46, 1783–1805.

- BS. (2005). *Guide to methods for assessing the acceptability of flaws in metallic structures*. (BS 7910) British Standards Institution: London, UK.

- Chaboche, J. L. (1989). Constitutive equations for cyclic plasticity and cyclic viscoplasticity. *International Journal of Plasticity*, 5(3), 247-302.

- Chang, K. H., and Pan, W. F. (2009). Buckling life estimation of circular tubes under cyclic bending. *International Journal of Solids and Structures*, 46(2), 254-270.

- Chang, K. H. et al. (2005). Viscoplastic response and collapse of 316L stainless steel tubes under cyclic bending. *Steel and Composite Structures*, 5(5), 359-374.

- Chen, X, et al. (2005). On the Ohno–Wang kinematic hardening rules for multiaxial ratcheting modeling of medium carbon steel. *International Journal of Plasticity*, 21(1), 161-184.

- Corona, E., and Kyriakides, S. (1988). On the collapse of inelastic tubes under combined bending and pressure. *International Journal of Solids and Structures*, 24(5), 505-535.

- Corona, E., and Kyriakides, S. (1991). An experimental investigation of the degradation and buckling of circular tubes under cyclic bending and external pressure. *Thin-Walled Structures*, 12(3), 229-263.

- Cosham, A., and Hopkins, P. (2002). The pipeline defect assessment manual. In the proceedings of 4th International Pipeline Conference (pp. 1565-1581). American Society of Mechanical Engineers, New York, NY, United States.

- Cosham, A. et al. (2004). An experimental and numerical study of the effect of pre-strain on the fracture toughness of line pipe steel. In *the proceedings of International Pipeline Conference* (pp. 1635-1652). American Society of Mechanical Engineers, New York, NY, United States.

- CSA. (2015). Oil and gas pipeline systems (CAN/CSA-Z662-15). *Canadian Standards Association*, Toronto, Canada.

- DiVito, L. et al. (2010). Ultra heavy wall line pipe X65: Ratcheting in severe cyclic straining. In the proceedings of *29th International Conference on Ocean, Offshore and Arctic Engineering* (pp. 899-910). American Society of Mechanical Engineers, New York, NY, United States.

- DNV-OS-F101 (2013). *Submarine pipeline systems*, Det Norkse Veritas.

- Eiber, R. J. (1979). Causes of pipeline failures probed. *Oil and Gas Journal*, *77*(52), 80-88.

- Fowler, J. R. et al. (1994). *Cyclic pressure fatigue life of pipelines with plain dents, dents with gouges, and dents with welds* (Report No. AGA--94015627). American Gas Association, Inc., Arlington, VA, United States.

- Fowler, J. R. et al. (1992). *Criteria for dent acceptability of offshore pipelines* (Report No. AGA-93007051). American Gas Association, Inc., Arlington, VA, United States. Pipeline Research Committee; Stress Engineering Services, Inc., Houston, TX, United States.

- Gao, B. et al. (2006). Ratchetting and ratchetting boundary study of pressurized straight low carbon steel pipe under reversed bending. *International Journal of Pressure Vessels and Piping*, *83*(2), 96-106

- Gau, J. S. (1990). *Elastic-plastic behavior of pressurized pipe*, Doctoral dissertation. University of Akron, OH, United States.

- Hertz-Clémens, S. (2006). Experimental and numerical modelling of pipeline denting. In *2006 International Pipeline Conference* (pp. 171-179). American Society of Mechanical Engineers, New York, NY, United States.

- Hill, R. T. (1991). *Pipeline Risk Analysis*, I ChemE Symposium Series No. 130.

- Hopkins, P., and Leis B. N. (2003). Mechanical damage gaps analysis. *Design, Materials and Construction Committee Final Report to PRCI, Report No PR-003-0277.*Columbus, OH, United States: Battelle Corp.

- Hübel, H. (1996). Basic conditions for material and structural ratcheting. *Nuclear Engineering and Design*, *162*(1), 55-65.

- Hyde, T. H. et al. (2009). Analysis of stresses in pipes indented by long external indentations and subsequent stress variations due to pressure fluctuations. *International Journal of Pressure Vessels and Piping*, *86*(7), 428-434.

- Jiang, Y. (1993). *Cyclic plasticity with an emphasis on ratcheting*, Doctoral dissertation. University of Illinois at Urbana-Champaign, IL, United States.

- Jiang, Y., and Sehitoglu, H. (1996). Modeling of cyclic ratchetting plasticity, part I: development of constitutive relations. *Journal of Applied Mechanics*, 63(3), 720-725.

- Jiang, Y., and Sehitoglu, H. (1996). Modeling of cyclic ratchetting plasticity, part II: comparison of model simulations with experiments. *Journal of Applied Mechanics*, *63*(3), 726-733.

- Jiao, R., and Kyriakides, S. (2009). Ratcheting, wrinkling and collapse of tubes under axial cycling. *International Journal of Solids and Structures*, *46*(14), 2856-2870.

- Jiao, R., and Kyriakides, S. (2011). Ratcheting and wrinkling of tubes due to axial cycling under internal pressure: Part I experiments. *International Journal of Solids and Structures*, *48*(20), 2814-2826.

- Jiao, R., and Kyriakides, S. (2011). Ratcheting and wrinkling of tubes due to axial cycling under internal pressure: Part I experiments. *International Journal of Solids and Structures*, *48*(20), 2814-2826.
- Jones, D. G. (1982). The significance of mechanical damage in pipelines. *3R International*, *21*(7), 347-354.
- Keating, P., and Hoffmann, R. (1997). Fatigue behavior of dented petroleum pipelines. *Texas AandM University Final Report to US Department of Transportation*.
- Kiefner, J. F. (1969). Fracture initiation. In the proceedings of the *4th Symposium on Line Pipe Research, Pipeline Research Committee of the American Gas Association*, Dallas, Texas, United States.
- Klever, F. J. et al. (1994). Limit-state design of high-temperature pipelines. American Society of Mechanical Engineers, New York, NY, United States.
- Kulkarni, S. C. et al. (2003). Uniaxial and biaxial ratchetting study of SA333 Gr. 6 steel at room temperature. *International Journal of Pressure Vessels and Piping*, *80*(3), 179-185.
- Kulkarni, S. C. et al. (2004). Uniaxial and biaxial ratchetting in piping materials—experiments and analysis. *International Journal of Pressure Vessels and Piping*, *81*(7), 609-617.
- Kyriakides, S., and Corona, E. (2007). *Mechanics of offshore pipelines: volume 1 buckling and collapse* (Vol. 1). Elsevier.
- Kyriakides, S., and Shaw, P. K. (1982). Response and stability of elastoplastic circular pipes under combined bending and external pressure. *International Journal of Solids and Structures*, *18*(11), 957-973.
- Kyriakides, S., and Shaw, P. K. (1987). Inelastic buckling of tubes under cyclic bending. *Journal of Pressure Vessel Technology*, 109(2), 169-178.
- Lancaster, E. R., and Palmer, S. C. (1996). Strain concentrations in pressurized dented pipes. *Proceedings of the Institution of Mechanical Engineers, Part E: Journal of Process Mechanical Engineering*, *210*(1), 29-38.
- Lee, K. L., and Pan, W. F. (2001). Viscoplastic collapse of titanium alloy tubes under cyclic bending. *Structural Engineering and Mechanics*, *11*(3), 315-324.
- Lee, K. L. et al. (2001). The influence of the diameter-to-thickness ratio on the stability of circular tubes under cyclic bending. *International Journal of Solids and Structures*, *38*(14), 2401-2413.
- Lee, L. H. (1962). Inelastic buckling of initially imperfect cylindrical shells subject to axial compression. *Journal of the Aerospace Sciences*, 29(2), 87-95.
- Leis, B. N., and Francini, R. B. (2000). Line pipe resistance to outside force–volume two: assessing serviceability of mechanical damage. *Battelle Final Report to PRCI, Report No PR-3-9305-Volume*, *2*. Battelle, Columbus, OH, United States.
- Leis, B. et al. (1998). Pressure-displacement behavior of transmission pipelines under outside forces: Towards a serviceability criterion for mechanical damage. In *the proceedings of the 8th International Offshore and Polar Engineering Conference* (Vol. 2, pp. 60-67). Mountain view, CA, United States: International Society of Offshore and Polar Engineers.
- Lemaitre, J., and Chaboche, J. L. (1994) *Mechanics of solid materials*. Cambridge, United Kingdom: Cambridge university press.

- Limam, A. et al. (2010). Inelastic wrinkling and collapse of tubes under combined bending and internal pressure. *International Journal of Mechanical Sciences*, *52*(5), 637-647.

- McDowell, D. L. (1994). Description of nonproportional cyclic ratchetting behavior. *European Journal of Mechanics. A. Solids*, *13*(5), 593-604.

- Miyazaki, K., et al. (2002). Fracture strength and behavior of carbon steel pipes with local wall thinning subjected to cyclic bending load. *Nuclear Engineering and Design*, *214*(1), 127-136.

- Moreton, D. N. et al. (1994). The behaviour of pressurised plain pipework subjected to simulated seismic loading. *Strain*, *30*(2), 63-72.

- Noronha, D. B. et al. (2010). Procedures for the strain based assessment of pipeline dents. *International Journal of Pressure Vessels and Piping*, *87*(5), 254-265.

- Ohno, N. (1990). Recent topics in constitutive modeling of cyclic plasticity and viscoplasticity. *Applied Mechanics Reviews, 43*(11), 283-295.

- Ohno, N. (1997). Recent progress in constitutive modeling for ratcheting. *Journal of Material Science International, 3,* 1–9.

- Ohno, N., and Wang, J. D. (1993). Kinematic hardening rules with critical state of dynamic recovery, part I: formulation and basic features for ratchetting behavior. *International Journal of Plasticity*, *9*(3), 375-390.

- Ohno, N., and Wang, J. D. (1993). Kinematic hardening rules with critical state of dynamic recovery. II: Application to experiments of ratchetting behavior. *International Journal of Plasticity*, *9*(3), 391-403.

- Pan, W. F., and Fan, C. H. (1998). An experimental study on the effect of curvature-rate at preloading stage on subsequent creep or relaxation of thin-walled tubes under pure bending. *Journal of Solid Mechanics and Material Engineering*, *41*(4), 525-531.

- Pan, W. F., and Her, Y. S. (1998). Viscoplastic collapse of thin-walled tubes under cyclic bending. *Journal of Engineering Materials and Technology*, *120*(4), 287-290.

- Paquette, J. A., and Kyriakides, S. (2006). Plastic buckling of tubes under axial compression and internal pressure. *International Journal of Mechanical Sciences*, *48*(8), 855-867.

- Rahman, S. M. (2006). Finite element analysis and related numerical schemes for ratcheting simulation (Doctoral dissertation). North Carolina State University, Raleigh, NC, USA.

- Rahman, S. M. et al. (2008). Evaluation of cyclic plasticity models in ratcheting simulation of straight pipes under cyclic bending and steady internal pressure. *International Journal of Plasticity*, *24*(10), 1756-1791.

- Rinehart, A. J. (2004). Effects of localized geometric imperfections on the stress behavior of pressurized cylindrical shells (Doctoral dissertation). Texas AandM University, College Station, TX, United States.

- Rinehart, A. J., and Keating, P. B. (2002, January). Length effects on fatigue behavior of longitudinal pipeline dents. In the proceedings of 4th *International Pipeline Conference* (pp. 1849-1858). American Society of Mechanical Engineers, New York, NY, United States.

- Roovers, P. et al., (2000). EPRG methods for assessing the tolerance and resistance of pipelines to external damage. *Pipeline Technology, 2*, 405-425.

- Rosenfeld, M. J. et al. (2002). Basis of the new criteria in ASME B31.8 for prioritization and repair of mechanical damage. Paper 27122 presented at 4th International Conference on Pipeline Technology, Calgary, Canada.

- Rosenfeld, M. J. (1997). Development of a model for fatigue rating shallow unrestrained dents. *AGA Catalog*, (L51741).

- Rosenfeld, M. J. et al. (1997). Toward an acceptance criterion for shallow dents affecting girth welds in gas transmission pipelines. *American Society of Mechanical Engineers, Pressure Vessels and Piping Division(Publication) PVP*, *353*, 373-383.

- Shaw, P. K., and Kyriakides, S. (1985). Inelastic analysis of thin-walled tubes 4under cyclic bending. *International Journal of Solids and Structures*, *21*(11), 1073-1100.

- ABAQUS. (2010). ABAQUS Theory Manual Version 6.10-1. *Simulia Corp., Providence, RI, United States*.

- Urednicek, M. (1986). Effects of dents on failures of gas transmission pipelines. *Report No 14032. Materials Engineering Services to Nova Corporation, Calgary, AB, Canada*.

- Vishnuvardhan, S. et al. (2010). Fatigue ratcheting studies on TP304 LN stainless steel straight pipes. *Procedia Engineering*, *2*(1), 2209-2218.

- Wang, K. C., and Smith, E. D. (1982). *The effect of mechanical damage on fracture initiation in line pipe, part i: dents*. Energy, Mines and Resources Canada, Canada Centre for Mineral and Energy Technology.

- Wang, L. et al. (2014). Bending ratcheting behavior of pressurized straight Z2CND18. 12N stainless steel pipe. *Structural Engineering Mechanics*, *52*, 1135-1156.

- Yahiaoui, K. et al. (1996). Response and cyclic strain accumulation of pressurized piping elbows under dynamic in-plane bending. The Journal of Strain Analysis for Engineering Design, 31(2), 135-151.

- Yoshida, F. et al. (1984). Mechanical ratcheting behaviors of a steel pipe under combined cyclic axial load and internal pressure. *Society of Materials Science Proc. of the 27 th Japan Congr. on Mater. Res. p 13-24 (SEE N 85-34180 23-23)*.

- Zakavi, S. J., and Nourbakhsh, M. (2014). The ratcheting behaviour of stainless steel pressurized piping elbows Subjected to dynamic out-of-plane Moments. *Modern Mechanical Engineering*, *2014*.

- Zakavi, S. J, et al. (2010). The ratchetting behavior of pressurized plain pipework subjected to cyclic bending moment with the combined hardening model. *Nuclear Engineering and Design*, *240*(4), 726-737.

- Zarea, M. F. et al. (1996). Numerical models for static denting and dynamic puncture of gas transmission line pipe and their validation. In the proceedings of *1st International Pipeline Conference* (pp. 777-784). American Society of Mechanical Engineers, New York, NY, United States.

- Zeinoddini, M., and Peykanu, M. (2011). Strain ratcheting of steel tubulars with a rectangular defect under axial cycling: a numerical modeling. *Journal of Constructional Steel Research*, *67*(12), 1872-1883.

- Zhang, G. K. Q. K. J. (2005). Experimental study on the uniaxial cyclic deformation of 25CDV4. 11 steel. *Journal of Materials Science and Technology*, 21(1), 5-9.